

Supplementary Information for

**Structural and electrochemical properties of mononuclear copper(II) complexes
with pentadentate ethylenediamine-based ligands with
pyridine/quinoline/isoquinoline/quinoxaline binding sites**

Yuji Mikata,^{a,b,c,d,*} Miyu Akedo,^b Erina Hamamoto,^c Shoko Yoshida,^c Sunao Shoji,^{a,b}
Yutaka Ohasedo,^b Takashi Matsuo,^e Tim Storr^f and Yasuhiro Funahashi^g

^a*Laboratory for Molecular & Functional Design, Department of Engineering, Nara Women's University, Nara 630-8506, Japan*

^b*Cooperative Major in Human Centered Engineering, Nara Women's University, Nara 630-8506, Japan*

^c*Department of Chemistry, Biology, and Environmental Science, Faculty of Science, Nara Women's University, Nara 630-8506, Japan*

^d*KYOUSEI Science Center, Nara Women's University, Nara 630-8506, Japan*

^e*Division of Materials Science, Graduate School of Science and Technology, Nara Institute of Science and Technology (NAIST), Takayama, Ikoma, Nara 630-0192, Japan*

^f*Department of Chemistry, Simon Fraser University, Burnaby, BC, V5A-1S6, Canada*

^g*Department of Chemistry, Graduate School of Science, Osaka University, Machikaneyama, Toyonaka, Osaka 560-0043, Japan*

INDEX

Preparation of copper(II) complexes.....S5-S10

X-ray crystallography.....S12-S20

Table S1. Crystallographic data for $[\text{Cu}(\text{Me-PPP})](\text{ClO}_4)_2 \cdot \text{CH}_3\text{CN}$ and $[\text{Cu}(\text{Me-QQQ})](\text{ClO}_4)_2 \cdot 1.75\text{CH}_3\text{CN}$

Table S2. Crystallographic data for $[\text{Cu}(\text{Me-333})](\text{ClO}_4)_2 \cdot \text{CH}_3\text{OH} \cdot 0.5\text{CH}_3\text{CN} \cdot 0.5\text{CHCl}_3$ and $[\text{Cu}(\text{Bn-PPP})](\text{ClO}_4)_2$

Table S3. Crystallographic data for $[\text{Cu}(\text{Bn-111})](\text{ClO}_4)_2 \cdot \text{DMF}$ and $[\text{Cu}(\text{Bn-333})](\text{ClO}_4)_2 \cdot \text{CH}_3\text{CN} \cdot 0.25\text{H}_2\text{O}$

Table S4. Crystallographic data for $[\text{Cu}(\text{Ph-PPP})(\text{ClO}_4)]\text{ClO}_4$ and $[\text{Cu}(\text{Ph-PPP})(\text{ClO}_4)]\text{PF}_6$

Table S5. Crystallographic data for $[\text{Cu}(\text{Ph-QQQ})](\text{ClO}_4)_2 \cdot \text{NaClO}_4 \cdot \text{CH}_3\text{CN}$ and $[\text{Cu}(\text{Ph-PQQ})](\text{ClO}_4)_2 \cdot \text{CH}_3\text{CN}$

Table S6. Crystallographic data for $[\text{Cu}(\text{Ph-QQP})](\text{ClO}_4)_2$ and $[\text{Cu}(\text{Ph-PPQ})](\text{ClO}_4)_2 \cdot 0.75\text{CH}_3\text{OH} \cdot 0.125\text{H}_2\text{O}$

Table S7. Selected Bond Angles ($^\circ$) for **Me-PPP-Cu**, **Me-QQQ-Cu**, **Me-333-Cu**, **Bn-PPP-Cu**, **Bn-111-Cu**, and **Bn-333-Cu**

Table S8. Selected Bond Angles ($^\circ$) for **Ph-PPP-Cu**, **Ph-PPP-Cu'**, **Ph-QQQ-Cu**, **Ph-PQQ-Cu**, and **Ph-QQP-Cu**

Table S9. Selected Bond Angles ($^\circ$) for **Ph-PPQ-Cu**

Fig. S1. Perspective view for **Ph-PPP-Cu'**.

Fig. S2. Perspective view for **Ph-PPQ-Cu**.

Cyclic voltammetry.....S23-S26

Fig. S3. Cyclic voltammogram of **R-ArArAr-Cu** in acetonitrile.

Fig. S4. Cyclic voltammogram of **Ph-Ar¹Ar²Ar³-Cu** in acetonitrile.

Fig. S5. Cyclic voltammogram of **Ph-PPP-Cu** and **Ph-QQQ-Cu** in acetonitrile at various scan rates.

Absorption spectrum.....S27-S33

Fig. S6. Absorption spectrum of **R-ArArAr-Cu** in acetonitrile.

Fig. S7. Absorption spectrum of **Ph-Ar¹Ar²Ar³-Cu** in acetonitrile.

Fig. S8. Absorption spectrum of **R-ArArAr-Cu** in methanol.

Fig. S9. Absorption spectrum of **Ph-Ar¹Ar²Ar³-Cu** in methanol.

Fig. S10. Plot for maximum wavelengths of copper complexes with τ values.

¹H/¹³C NMR spectrum.....S34-S52

- Fig. S11.** ¹H/¹³C NMR spectrum of **Me-111** in CDCl₃.
Fig. S12. ¹H/¹³C NMR spectrum of **Me-333** in CDCl₃.
Fig. S13. ¹H/¹³C NMR spectrum of **Me-XXX** in CDCl₃.
Fig. S14. ¹H/¹³C NMR spectrum of **Bn-QQQ** in CDCl₃.
Fig. S15. ¹H/¹³C NMR spectrum of **Bn-111** in CDCl₃.
Fig. S16. ¹H/¹³C NMR spectrum of **Bn-333** in CDCl₃.
Fig. S17. ¹H/¹³C NMR spectrum of **Bn-XXX** in CDCl₃.
Fig. S18. ¹H/¹³C NMR spectrum of **Ph-QQQ** in CDCl₃.
Fig. S19. ¹H/¹³C NMR spectrum of **Ph-111** in CDCl₃.
Fig. S20. ¹H/¹³C NMR spectrum of **Ph-333** in CDCl₃.
Fig. S21. ¹H/¹³C NMR spectrum of **Ph-XXX** in CDCl₃.
Fig. S22. ¹H NMR spectrum of **Ph-PPH** in CDCl₃.
Fig. S23. ¹H/¹³C NMR spectrum of **Ph-PPQ** in CDCl₃.
Fig. S24. ¹H/¹³C NMR spectrum of **Ph-QHH** in CDCl₃.
Fig. S25. ¹H/¹³C NMR spectrum of **Ph-PQP** in CDCl₃.
Fig. S26. ¹H NMR spectrum of **Ph-PHH** in CDCl₃.
Fig. S27. ¹H/¹³C NMR spectrum of **Ph-PQQ** in CDCl₃.
Fig. S28. ¹H/¹³C NMR spectrum of **Ph-QQH** in CDCl₃.
Fig. S29. ¹H/¹³C NMR spectrum of **Ph-QQP** in CDCl₃.

IR spectrum.....S53-S71

- Fig. S30.** IR spectrum of **Me-PPP**.
Fig. S31. IR spectrum of **Me-QQQ**.
Fig. S32. IR spectrum of **Me-111**.
Fig. S33. IR spectrum of **Me-333**.
Fig. S34. IR spectrum of **Me-XXX**.
Fig. S35. IR spectrum of **Bn-PPP**.
Fig. S36. IR spectrum of **Bn-QQQ**.
Fig. S37. IR spectrum of **Bn-111**.
Fig. S38. IR spectrum of **Bn-333**.
Fig. S39. IR spectrum of **Bn-XXX**.
Fig. S40. IR spectrum of **Ph-PPP**.
Fig. S41. IR spectrum of **Ph-QQQ**.
Fig. S42. IR spectrum of **Ph-111**.
Fig. S43. IR spectrum of **Ph-333**.

Fig. S44.	IR spectrum of Ph-XXX
Fig. S45.	IR spectrum of Ph-PPQ .
Fig. S46.	IR spectrum of Ph-PQP .
Fig. S47.	IR spectrum of Ph-PQQ .
Fig. S48.	IR spectrum of Ph-QQP .
Fig. S49.	IR spectrum of Me-PPP-Cu .
Fig. S50.	IR spectrum of Me-QQQ-Cu .
Fig. S51.	IR spectrum of Me-111-Cu .
Fig. S52.	IR spectrum of Me-333-Cu .
Fig. S53.	IR spectrum of Me-XXX-Cu .
Fig. S54.	IR spectrum of Bn-PPP-Cu .
Fig. S55.	IR spectrum of Bn-QQQ-Cu .
Fig. S56.	IR spectrum of Bn-111-Cu .
Fig. S57.	IR spectrum of Bn-333-Cu .
Fig. S58.	IR spectrum of Bn-XXX-Cu .
Fig. S59.	IR spectrum of Ph-PPP-Cu .
Fig. S60.	IR spectrum of Ph-QQQ-Cu .
Fig. S61.	IR spectrum of Ph-111-Cu .
Fig. S62.	IR spectrum of Ph-333-Cu .
Fig. S63.	IR spectrum of Ph-XXX-Cu .
Fig. S64.	IR spectrum of Ph-PPQ-Cu .
Fig. S65.	IR spectrum of Ph-PQP-Cu .
Fig. S66.	IR spectrum of Ph-PQQ-Cu .
Fig. S67.	IR spectrum of Ph-QQP-Cu .

References S72

Preparation of copper(II) complexes

Me-PPP-Cu ([Cu(Me-PPP)](ClO₄)₂)¹

To a solution of **Me-PPP** (8.7 mg, 25 μmol) in ethanol (0.5 mL) was added Cu(ClO₄)₂·6H₂O (9.8 mg, 26 μmol) in ethanol (0.5 mL). After stirring for 5 min, resulting precipitate was collected by filtration and washed with ethanol to afford **Me-PPP-Cu** as a blue powder (13.0 mg, 21.3 μmol, 85%). Single crystals suitable for X-ray crystallography were obtained by recrystallization from acetonitrile and chloroform.

λ_{max}: 678 nm (CH₃CN), 672 nm (CH₃OH).

Anal Calcd. for C₂₂H_{26.5}Cl₂CuN_{5.5}O₈ (**Me-PPP-Cu**·0.5CH₃CN): C, 41.91; H, 4.24; N, 12.22.

Found: C, 41.52; H, 4.26; N, 12.63.

Me-QQQ-Cu ([Cu(Me-QQQ)](ClO₄)₂)²

To a solution of **Me-QQQ** (14.9 mg, 30.0 μmol) in ethanol (0.5 mL) was added Cu(ClO₄)₂·6H₂O (12.0 mg, 32.4 μmol) in ethanol (0.5 mL). After stirring for 5 min, resulting precipitate was collected by filtration and washed with ethanol to afford **Me-QQQ-Cu** as blue powder (18.1 mg, 23.8 μmol, 79%). Single crystals suitable for X-ray crystallography were obtained by recrystallization from acetonitrile.

λ_{max}: 655 nm (CH₃CN), 659 nm (CH₃OH).

Anal Calcd. for C₃₃H₃₃Cl₂CuN₅O₉ (**Me-QQQ-Cu**·H₂O): C, 50.94; H, 4.27; N, 9.00.

Found: C, 50.68; H, 4.34; N, 9.25.

Me-111-Cu

To a solution of **Me-111** (12.5 mg, 25.1 μmol) in ethanol (0.5 mL) was added Cu(ClO₄)₂·6H₂O (10.1 mg, 27.3 μmol) in ethanol (0.5 mL). After stirring for 5 min, resulting precipitate was collected by filtration and washed with ethanol to afford **Me-111-Cu** as a blue powder (14.4 mg, 18.9 μmol, 76%).

λ_{max}: 694 nm (CH₃CN), 687 nm (CH₃OH).

HRMS (ESI) *m/z*: [Me-111 + Cu^{II} + Cl]⁺ calcd. for C₃₃H₃₁ClCuN₅ 595.15640; found 595.15876.

Me-333-Cu ([Cu(Me-333)](ClO₄)₂)

To a solution of **Me-333** (15.1 mg, 30.3 µmol) in ethanol (0.5 mL) was added Cu(ClO₄)₂·6H₂O (12.0 mg, 32.4 µmol) in ethanol (0.5 mL). After stirring for 5 min, resulting precipitate was collected by filtration and washed with ethanol to afford **Me-333-Cu** as blue powder (17.4 mg, 22.9 µmol, 76%). Single crystals suitable for X-ray crystallography were obtained by recrystallization from acetonitrile.

λ_{max} : 683 nm (CH₃CN), 676 nm (CH₃OH).

Anal Calcd. for C₃₃H₃₆Cl₂CuN₅O_{10.5} (**Me-333-Cu**·2.5H₂O): C, 49.23; H, 4.51; N, 8.70. Found: C, 49.33; H, 4.22; N, 8.80.

Me-XXX-Cu

To a solution of **Me-XXX** (12.2 mg, 24.4 µmol) in ethanol (0.5 mL) was added Cu(ClO₄)₂·6H₂O (9.6 mg, 26 µmol) in ethanol (0.5 mL). After stirring for 5 min, resulting precipitate was collected by filtration and washed with ethanol to afford **Me-XXX** as yellow-green powder (12.3 mg, 61.1 µmol, 66%).

λ_{max} : 641 nm (CH₃CN).

HRMS (ESI) *m/z*: [Me-XXX + Cu^I]⁺ calcd. for C₃₀H₂₈CuN₈ 563.17329; found 563.16825.

Bn-PPP-Cu ([Cu(Bn-PPP)](ClO₄)₂)

To a solution of **Bn-PPP** (12.7 mg, 30.0 µmol) in ethanol (0.5 mL) was added Cu(ClO₄)₂·6H₂O (12.0 mg, 32.4 µmol) in ethanol (0.5 mL). After stirring for 5 min, resulting precipitate was collected by filtration and washed with ethanol to afford **Bn-PPP-Cu** as blue powder (18.6 mg, 27.1 µmol, 90%). Single crystals suitable for X-ray crystallography were obtained by recrystallization from acetonitrile.

λ_{max} : 696 nm (CH₃CN), 690 nm (CH₃OH).

Anal Calcd. for C₂₇H₂₉Cl₂CuN₅O₈ (**Bn-PPP-Cu**): C, 47.27; H, 4.26; N, 10.21. Found: C, 47.14; H, 4.30; N, 10.07.

Bn-QQQ-Cu

To a solution of **Bn-QQQ** (14.6 mg, 25.4 μmol) in ethanol (0.5 mL) was added $\text{Cu}(\text{ClO}_4)_2 \cdot 6\text{H}_2\text{O}$ (9.8 mg, 26 μmol) in ethanol (0.5 mL). After stirring for 5 min, resulting precipitate was collected by filtration and washed with ethanol to afford **Bn-QQQ-Cu** as a green powder (17.2 mg, 20.6 μmol , 82%).

λ_{max} : 661 nm (CH₃CN), 660 nm (CH₃OH).

HRMS (ESI) *m/z*: [Bn-QQQ + Cu^I]⁺ calcd. for C₃₉H₃₅CuN₅ 636.21885; found 636.21728.

Bn-111-Cu ([Cu(Bn-111)](ClO₄)₂)

To a solution of **Bn-111** (17.2 mg, 30.0 μmol) in ethanol (2.5 mL) was added $\text{Cu}(\text{ClO}_4)_2 \cdot 6\text{H}_2\text{O}$ (13.0 mg, 35.0 μmol) in ethanol (2.0 mL). After stirring for 5 min, resulting precipitate was dissolved by addition of DMF. The blue solution was kept at 4 °C to precipitate the complex, which was collected by filtration and washed with ethanol to afford **Bn-111-Cu** as blue crystals suitable for X-ray crystallography (29.2 mg, 35.0 μmol , 43%).

λ_{max} : 703 nm (CH₃CN), 699 nm (CH₃OH).

Anal Calcd. for C₃₉H₃₇Cl₂CuN₅O₉ (**Bn-111-Cu·H₂O**): C, 54.83; H, 4.37; N, 8.20. Found: C, 54.73; H, 4.34; N, 8.29.

Bn-333-Cu ([Cu(Bn-333)](ClO₄)₂)

To a solution of **Bn-333** (15.4 mg, 26.6 μmol) in ethanol (0.5 mL) was added $\text{Cu}(\text{ClO}_4)_2 \cdot 6\text{H}_2\text{O}$ (9.85 mg, 26.8 μmol) in ethanol (1.5 mL). After stirring for 5 min, resulting precipitate was collected by filtration and washed with ethanol to afford **Bn-333-Cu** as blue powder (16.0 mg, 19.1 μmol , 72%). Single crystals suitable for X-ray crystallography were obtained by recrystallization from acetonitrile.

λ_{max} : 694 nm (CH₃CN), 692 nm (CH₃OH).

Anal Calcd. for C₃₉H₃₇Cl₂CuN₅O₉ (**Bn-333-Cu·H₂O**): C, 54.83; H, 4.37; N, 8.20. Found: C, 54.83; H, 4.03; N, 8.25.

Bn-XXX-Cu

To a solution of **Bn-XXX** (14.7 mg, 25.5 μ mol) in ethanol (0.5 mL) was added Cu(ClO₄)₂·6H₂O (9.8 mg, 26 μ mol) in ethanol (0.5 mL). After stirring for 5 min, resulting precipitate was collected by filtration and washed with ethanol to afford **Bn-XXX-Cu** as a yellow-green powder (15.4 mg, 18.4 μ mol, 74%).

λ_{max} : 636 nm (CH₃CN).

HRMS (ESI) *m/z*: [Bn-XXX + Cu^I]⁺ calcd. for C₃₆H₃₂CuN₈ 639.20459; found 639.20499.

Ph-PPP-Cu ([Cu(Ph-PPP)(ClO₄)]ClO₄)

To a solution of **Ph-PPP** (10.2 mg, 25.0 μ mol) in ethanol (0.5 mL) was added Cu(ClO₄)₂·6H₂O (9.5 mg, 26 μ mol) in ethanol (0.5 mL). After stirring for 5 min, resulting precipitate was collected by filtration and washed with ethanol to afford **Ph-PPP-Cu** as a blue powder (13.4 mg, 19.9 μ mol, 80%). Single crystals suitable for X-ray crystallography were obtained from recrystallization from acetonitrile (0.1 mL) in the presence of NaClO₄ (10.8 mg, 76.9 μ mol) under ether diffusion condition.

Anal Calcd. for C₂₆H₂₇Cl₂CuN₅O₈ (**Ph-PPP-Cu**): C, 46.47; H, 4.05; N, 10.42. Found: C, 45.73; H, 3.78; N, 10.28.

On the other hand, recrystallization from acetonitrile (0.2 mL) in the presence of NH₄PF₆ (4.2 mg, 26 μ mol) afforded **Ph-PPP-Cu'** ([Cu(Ph-PPP)(ClO₄)]PF₆) as single crystals suitable for X-ray crystallography.

λ_{max} : 655 nm (CH₃CN), 633 nm (CH₃OH).

Anal Calcd. for C₂₆H₃₀ClCuF₆N₅O_{5.5}P (**Ph-PPP-Cu'**·1.5H₂O): C, 41.94; H, 4.06; N, 9.41. Found: C, 41.66; H, 3.71; N, 9.87.

Ph-QQQ-Cu ([Cu(Ph-QQQ)](ClO₄)₂)

To a solution of **Ph-QQQ** (14.3 mg, 25.5 μ mol) in ethanol (0.5 mL) was added Cu(ClO₄)₂·6H₂O (9.4 mg, 25 μ mol) in ethanol (0.5 mL). After stirring for 5 min, resulting precipitate was collected by filtration and washed with ethanol to afford **Ph-QQQ-Cu** as a green powder (16.3 mg, 19.8 μ mol, 78%). Single crystals suitable for X-

ray crystallography were obtained from recrystallization from acetonitrile (0.1 mL) in the presence of NaClO₄ (3.3 mg, 23 μmol) under ether diffusion condition.

λ_{max} : 643 nm (CH₃CN), 650 nm (CH₃OH).

Anal Calcd. for C₄₀H₃₆Cl₃CuN₆NaO₁₂ (**Ph-QQQ-Cu·NaClO₄·CH₃CN**): C, 48.74; H, 3.68; N, 8.53. Found: C, 48.80; H, 3.70; N, 8.13.

Ph-111-Cu

To a solution of **Ph-111** (14.1 mg, 25.2 μmol) in ethanol (0.5 mL) was added Cu(ClO₄)₂·6H₂O (9.8 mg, 26 μmol) in ethanol (0.5 mL). After stirring for 5 min, resulting precipitate was collected by filtration and washed with ethanol to afford **Ph-111-Cu** as a blue powder (12.0 mg, 14.6 μmol, 58%).

λ_{max} : 674 nm (CH₃CN), 641 nm (CH₃OH).

HRMS (ESI) *m/z*: [Ph-111 + Cu^{II} + ClO₄]⁺ calcd. for C₃₈H₃₃ClCuN₅O₄ 721.15171; found 721.14981.

Ph-333-Cu

To a solution of **Ph-333** (13.6 mg, 24.3 μmol) in ethanol (0.5 mL) was added Cu(ClO₄)₂·6H₂O (9.9 mg, 27 μmol) in ethanol (0.5 mL). After stirring for 5 min, resulting precipitate was collected by filtration and washed with ethanol to afford **Ph-333-Cu** as a blue powder (17.4 mg, 21.2 μmol, 88%).

λ_{max} : 650 nm (CH₃CN), 641 nm (CH₃OH).

HRMS (ESI) *m/z*: [Ph-333 + Cu^{II} + ClO₄]⁺ calcd. for C₃₈H₃₃ClCuN₅O₄ 721.15171; found 721.14920.

Ph-XXX-Cu

To a solution of **Ph-XXX** (14.0 mg, 24.9 μmol) in ethanol (0.5 mL) was added Cu(ClO₄)₂·6H₂O (9.8 mg, 26 μmol) in ethanol (0.5 mL). After stirring for 5 min, resulting precipitate was collected by filtration and washed with ethanol to afford **Ph-XXX-Cu** as a yellow green powder (12.2 mg, 14.8 μmol, 60%).

HRMS (ESI) *m/z*: [Ph-XXX + Cu^I]⁺ calcd. for C₃₅H₃₀CuN₈ 625.18894; found 625.19341.

Ph-PPQ-Cu

To a solution of **Ph-PPQ** (22.5 mg, 49.0 μmol) in ethanol (0.5 mL) was added Cu(ClO₄)₂·6H₂O (20.4 mg, 55.1 μmol) in ethanol (0.5 mL). After stirring for 5 min, resulting precipitate was collected by filtration and washed with ethanol to afford **Ph-PPQ-Cu** as a green powder (23.0 mg, 31.8 μmol, 64%). Single crystals suitable for X-ray crystallography were obtained by recrystallization from methanol.

λ_{max}: 714 nm (CH₃CN), 645 nm (CH₃OH).

HRMS (ESI) *m/z*: [Ph-PPQ + Cu^I]⁺ calcd. for C₃₀H₂₉CuN₅ 522.17190; found 522.16860.

Ph-PQP-Cu

To a solution of **Ph-PQP** (22.7 mg, 49.4 μmol) in ethanol (0.5 mL) was added Cu(ClO₄)₂·6H₂O (20.4 mg, 55.1 μmol) in ethanol (0.5 mL). After stirring for 5 min, resulting precipitate was collected by filtration and washed with ethanol to afford **Ph-PQP-Cu** as a green powder (23.0 mg, 31.8 μmol, 64%).

λ_{max}: 638 nm (CH₃CN), 645 nm (CH₃OH).

HRMS (ESI) *m/z*: [Ph-PQP + Cu^I]⁺ calcd. for C₃₀H₂₉CuN₅ 522.17190; found 522.16937.

Ph-PQQ-Cu ([Cu(Ph-PQQ)](ClO₄)₂)

To a solution of **Ph-PQQ** (25.5 mg, 50.0 μmol) in ethanol (0.5 mL) was added Cu(ClO₄)₂·6H₂O (20.4 mg, 55.1 μmol) in ethanol (0.5 mL). After stirring for 5 min, resulting precipitate was collected by filtration and washed with ethanol to afford **Ph-PQQ-Cu** as green powder (20.1 mg, 26.0 μmol, 52%). Single crystals suitable for X-ray crystallography were obtained by recrystallization from acetonitrile.

λ_{max}: 742 nm (CH₃CN), 738 nm (CH₃OH).

Anal Calcd. for C₃₄H₃₁Cl₂CuN₅O₈ (**Ph-PQQ-Cu**): C, 52.89; H, 4.05; N, 9.07. Found: C, 52.56; H, 4.06; N, 9.67.

Ph-QQP-Cu ([Cu(Ph-QQP)](ClO₄)₂)

To a solution of **Ph-QQP** (12.7 mg, 25.0 μmol) in methanol (0.5 mL) was added Cu(ClO₄)₂·6H₂O (10.9 mg, 29 μmol) in methanol (0.5 mL). The green solution was kept at 4 °C to precipitate the complex, which was collected by filtration. The green powder was recrystallized from acetonitrile (0.6 mL) at 4 °C under ether diffusion conditions to afford **Ph-QQP-Cu** as green crystals suitable for X-ray crystallography (17.7 mg, 22.9 μmol, 92%).

λ_{max}: 636 nm (CH₃CN), 637 nm (CH₃OH).

Anal Calcd. for C₃₄H₃₁Cl₂CuN₅O₈ (**Ph-QQP-Cu**): C, 52.89; H, 4.05; N, 9.07. Found: C, 53.04; H, 4.10; N, 9.48.

X-ray crystallography**Table S1.** Crystallographic data for [Cu(Me-PPP)](ClO₄)₂·CH₃CN (**Me-PPP-Cu**·CH₃CN) and [Cu(Me-QQQ)](ClO₄)₂·1.75CH₃CN (**Me-QQQ-Cu**·1.75CH₃CN)

	Me-PPP-Cu ·CH ₃ CN	Me-QQQ-Cu ·1.75CH ₃ CN
Formula	C ₂₃ H ₂₈ Cl ₂ CuN ₆ O ₈	C _{36.5} H _{36.25} Cl ₂ CuN _{6.75} O ₈
FW	650.96	831.91
Crystal system	triclinic	orthorhombic
Space group	P-1	P2 ₁ 2 ₁ 2
<i>a</i> , Å	8.300(4)	19.7113(5)
<i>b</i> , Å	11.361(5)	45.9648(14)
<i>c</i> , Å	15.321(6)	8.4267(2)
α , deg	93.883(6)	90
β , deg	96.666(5)	90
γ , deg	105.289(5)	90
<i>V</i> , Å ³	1376.8(10)	7634.8(4)
<i>Z</i>	2	8
<i>D</i> _{calc} , g cm ⁻³	1.570	1.447
μ , mm ⁻¹	1.0449	0.772
2θ _{max} , deg	55	50.7
temp, K	153	150
no. reflns collected	10754	28038
no. reflns used	6013	13467
no. of params	390	1160
<i>R</i> _{int}	0.0219	0.0354
Final <i>R</i> 1 (<i>I</i> > 2σ(<i>I</i>)) ^a	0.0476	0.0484
<i>wR</i> 2 (all data) ^b	0.1366	0.1260
GOF	1.043	1.037

^a*R*1 = Σ ||*F*_o|| - ||*F*_c|| / Σ ||*F*_o||. ^b*wR*2 = [Σ*w*[(*F*_o² - *F*_c²)²] / Σ [*w*(*F*_o²)²]]^{1/2}.

Table S2. Crystallographic data for [Cu(Me-333)](ClO₄)₂·CH₃OH·0.5CH₃CN·0.5CHCl₃ (**Me-333-Cu**·CH₃OH·0.5CH₃CN·0.5CHCl₃) and [Cu(Bn-PPP)](ClO₄)₂ (**Bn-PPP-Cu**)

	Me-333-Cu ·CH ₃ OH ·0.5CH ₃ CN·0.5CHCl ₃	Bn-PPP-Cu
Formula	C _{35.5} H ₃₇ Cl _{3.5} CuN _{5.5} O ₉	C ₂₇ H ₂₉ Cl ₂ CuN ₅ O ₈
FW	872.32	686.01
Crystal system	monoclinic	orthorhombic
Space group	P2 ₁ /c	Pbca
a, Å	18.6631(5)	14.5386(19)
b, Å	15.1459(3)	18.525(3)
c, Å	28.2417(9)	21.715(3)
β, deg	105.021(3)	90
V, Å ³	7710.3(4)	5848.4(15)
Z	8	8
D _{calc} , g cm ⁻³	1.503	1.558
μ, mm ⁻¹	0.870	0.9877
2θ _{max} , deg	60.3	55
temp, K	150	153
no. reflns collected	55167	45067
no. reflns used	18533	6526
no. of params	1028	388
R _{int}	0.0450	0.0481
Final R1 (I > 2σ(I)) ^a	0.0706	0.0435
wR2 (all data) ^b	0.2224	0.1122
GOF	1.042	1.052

^aR1 = Σ ||F_o| - |F_c| | / Σ |F_o|. ^bwR2 = [Σw[(F_o² - F_c²)²] / Σ[w(F_o²)²]]^{1/2}.

Table S3. Crystallographic data for $[\text{Cu}(\text{Bn-111})](\text{ClO}_4)_2 \cdot \text{DMF}$ (**Bn-111-Cu·DMF**) and $[\text{Cu}(\text{Bn-333})](\text{ClO}_4)_2 \cdot 1.25\text{CH}_3\text{CN}$ (**Bn-333-Cu·1.25CH₃CN**)

	Bn-111-Cu·DMF	Bn-333-Cu·1.25CH₃CN
Formula	$\text{C}_{42}\text{H}_{42}\text{Cl}_2\text{CuN}_6\text{O}_9$	$\text{C}_{41.5}\text{H}_{38.75}\text{Cl}_2\text{CuN}_{6.25}\text{O}_8$
FW	909.28	887.48
Crystal system	triclinic	triclinic
Space group	<i>P</i> -1	<i>P</i> -1
<i>a</i> , Å	11.805(3)	13.425(6)
<i>b</i> , Å	13.196(4)	15.738(7)
<i>c</i> , Å	13.294(4)	19.413(8)
α , deg	86.264(7)	76.205(10)
β , deg	75.769(6)	86.332(9)
γ , deg	88.616(6)	87.694(8)
<i>V</i> , Å ³	2003.0(10)	3974(3)
<i>Z</i>	2	4
<i>D</i> _{calc} , g cm ⁻³	1.507	1.483
μ , mm ⁻¹	0.7442	0.747
2 <i>θ</i> _{max} , deg	61.5	55
temp, K	153	153
no. reflns collected	24105	40334
no. reflns used	11187	17833
no. of params	389	1187
<i>R</i> _{int}	0.0242	0.0474
Final <i>R</i> 1 (<i>I</i> > 2σ(<i>I</i>)) ^a	0.0443	0.0635
<i>wR</i> 2 (all data) ^b	0.1267	0.2045
GOF	1.072	1.073

^a*R*1 = $\sum ||F_o| - |F_c|| / \sum |F_o|$. ^b*wR*2 = $[\sum w[(F_o^2 - F_c^2)^2] / \sum [w(F_o^2)^2]]^{1/2}$.

Table S4. Crystallographic data for $[\text{Cu}(\text{Ph-PPP})(\text{ClO}_4)]\text{ClO}_4$ (**Ph-PPP-Cu**) and $[\text{Cu}(\text{Ph-PPP})(\text{ClO}_4)]\text{PF}_6$ (**Ph-PPP-Cu'**)

	Ph-PPP-Cu	Ph-PPP-Cu'
Formula	$\text{C}_{26}\text{H}_{27}\text{Cl}_2\text{CuN}_5\text{O}_8$	$\text{C}_{26}\text{H}_{27}\text{ClCuF}_6\text{N}_5\text{O}_4\text{P}$
FW	671.98	717.49
Crystal system	monoclinic	monoclinic
Space group	$P2_1/c$	$P2_1/c$
a , Å	20.820(4)	21.039(10)
b , Å	7.9052(15)	7.934(4)
c , Å	18.113(4)	18.056(9)
β , deg	110.212(3)	110.078(7)
V , Å ³	2797.6(10)	2831(2)
Z	4	4
D_{calc} , g cm ⁻³	1.595	1.683
μ , mm ⁻¹	1.0306	1.0060
$2\theta_{\text{max}}$, deg	55	55
temp, K	153	153
no. reflns collected	20997	18245
no. reflns used	6338	6360
no. of params	403	399
R_{int}	0.0288	0.0365
Final $R1$ ($I > 2\sigma(I)$) ^a	0.0791	0.0561
$wR2$ (all data) ^b	0.2397	0.1684
GOF	1.116	1.036

^a $R1 = \sum ||F_o| - |F_c|| / \sum |F_o|$. ^b $wR2 = [\sum w[(F_o^2 - F_c^2)^2] / \sum [w(F_o^2)^2]]^{1/2}$.

Table S5. Crystallographic data for $[\text{Cu}(\text{Ph}-\text{QQQ})](\text{ClO}_4)_2 \cdot \text{NaClO}_4 \cdot \text{CH}_3\text{CN}$ (**Ph-QQQ-Cu**) and $[\text{Cu}(\text{Ph}-\text{PQQ})](\text{ClO}_4)_2 \cdot \text{CH}_3\text{CN}$ (**Ph-PQQ-Cu**·0.5CH₃CN)

	Ph-QQQ-Cu·NaClO₄·CH₃CN	Ph-PQQ-Cu·0.5CH₃CN
Formula	C ₄₀ H ₃₈ Cl ₃ CuN ₆ NaO ₁₃	C ₃₅ H _{32.5} Cl ₂ CuN _{5.5} O ₈
FW	1003.67	792.60
Crystal system	triclinic	monoclinic
Space group	<i>P</i> -1	<i>I</i> 2/ <i>a</i>
<i>a</i> , Å	10.7240(19)	9.9174(2)
<i>b</i> , Å	13.815(3)	18.90674)
<i>c</i> , Å	15.435(3)	37.0398(7)
α, deg	84.3269(10)	90
β, deg	74.387(8)	91.504(2)
γ, deg	71.884(6)	90
<i>V</i> , Å ³	2092.9(7)	6942.8(2)
<i>Z</i>	2	8
<i>D</i> _{calc} , g cm ⁻³	1.593	1.517
μ, mm ⁻¹	0.7979	0.844
2θ _{max} , deg	55	59
temp, K	153	150
no. reflns collected	17126	26753
no. reflns used	9180	8373
no. of params	578	497
<i>R</i> _{int}	0.0260	0.0240
Final <i>R</i> 1 (<i>I</i> > 2σ(<i>I</i>)) ^a	0.0546	0.0472
<i>wR</i> 2 (all data) ^b	0.1631	0.1402
GOF	1.042	1.066

^a*R*1 = Σ ||*F*_o|| - ||*F*_c|| / Σ ||*F*_o||. ^b*wR*2 = [Σ*w*[(*F*_o² - *F*_c²)²] / Σ [*w*(*F*_o²)²]]^{1/2}.

Table S6. Crystallographic data for $[\text{Cu}(\text{Ph-QQP})](\text{ClO}_4)_2$ (**Ph-QQP-Cu**) and $[\text{Cu}(\text{Ph-PPQ})](\text{ClO}_4)_2 \cdot 0.75\text{CH}_3\text{OH} \cdot 0.125\text{H}_2\text{O}$ (**Ph-PPQ-Cu·0.75CH₃OH·0.125H₂O**)

	Ph-QQP-Cu	Ph-PPQ-Cu·0.75CH₃OH·0.125H₂O
Formula	$\text{C}_{34}\text{H}_{31}\text{Cl}_2\text{CuN}_5\text{O}_8$	$\text{C}_{30.75}\text{H}_{32.25}\text{Cl}_2\text{CuN}_5\text{O}_{8.875}$
FW	772.10	748.30
Crystal system	orthorhombic	monoclinic
Space group	$Pna2_1$	$P2_1/c$
a , Å	14.734(2)	8.1238(2)
b , Å	21.124(3)	37.8829(8)
c , Å	10.5506(16)	41.6362(12)
β , deg	90	92.788(2)
V , Å ³	3283.8(8)	12798.5(6)
Z	4	16
D_{calc} , g cm ⁻³	1.562	1.553
μ , mm ⁻¹	0.8895	0.912
2 θ_{max} , deg	55	50.7
temp, K	153	150
no. reflns collected	26183	23294
no. reflns used	6043	13744
no. of params	451	1879
R_{int}	0.0391	0.0635
Final $R1$ ($I > 2\sigma(I)$) ^a	0.0413	0.0572
$wR2$ (all data) ^b	0.1118	0.1549
GOF	1.042	1.081

^a $R1 = \sum ||F_o| - |F_c|| / \sum |F_o|$. ^b $wR2 = [\sum w[(F_o^2 - F_c^2)^2] / \sum [w(F_o^2)^2]]^{1/2}$.

Table S7. Selected Bond Angles ($^{\circ}$) for **Me-PPP-Cu**, **Me-QQQ-Cu**, **Me-333-Cu**, **Bn-PPP-Cu**, **Bn-111-Cu** and **Bn-333-Cu**

	Me-PPP -Cu	Me-QQQ -Cu^a	Me-333 -Cu^a	Bn-PPP -Cu	Bn-111 -Cu	Bn-333 -Cu^a
N1-Cu-N2	87.5	85.3	85.9	87.1	87.2	86.2
N1-Cu-N3	82.6	80.6	82.4	83.5	83.3	82.9
N1-Cu-N4	82.3	81.9	82.5	82.8	83.1	83.1
N1-Cu-N5	168.1	163.3	166.6	167.9	167.1	168.1
N2-Cu-N3	107.2	161.9	104.1	106.7	132.7	103.3
N2-Cu-N4	138.8	98.9	139.7	138.3	107.3	143.4
N2-Cu-N5	82.0	79.1	82.5	82.3	81.2	82.8
N3-Cu-N4	110.8	90.4	112.3	112.2	117.2	109.8
N3-Cu-N5	106.0	113.5	107.2	105.2	100.5	103.3
N4-Cu-N5	101.8	106.1	105.9	101.3	105.7	103.8

^a Average values for two crystallographically independent complexes.

Table S8. Selected Bond Angles ($^{\circ}$) for **Ph-PPP-Cu**, **Ph-PPP-Cu'**, **Ph-QQQ-Cu**, **Ph-PQQ-Cu** and **Ph-QQP-Cu**

	Ph-PPP -Cu	Ph-PPP -Cu'	Ph-QQQ -Cu	Ph-PQQ -Cu	Ph-QQP -Cu
N1-Cu-N2	84.7	84.8	85.7	86.5	85.3
N1-Cu-N3	82.6	82.4	81.0	131.5	80.7
N1-Cu-N4	83.4	83.6	81.7	82.6	82.7
N1-Cu-N5	161.0	161.2	163.2	161.0	116.5
N2-Cu-N3	91.0	90.0	161.3	131.5	164.2
N2-Cu-N4	100.4	100.0	98.9	100.5	93.6
N2-Cu-N5	76.8	76.9	79.3	80.9	83.8
N3-Cu-N4	161.0	161.3	92.0	124.4	91.8
N3-Cu-N5	101.8	101.8	111.7	95.0	96.1
N4-Cu-N5	95.7	95.4	107.9	113.6	160.2
O1-Cu-N1	111.1	110.3	—	—	—
O1-Cu-N2	161.7	161.7	—	—	—
O1-Cu-N3	82.3	81.5	—	—	—
O1-Cu-N4	90.9	91.8	—	—	—
O1-Cu-N5	87.9	88.4	—	—	—

Table S9. Selected Bond Angles ($^{\circ}$) for Ph-PPQ-Cu

	Ph-PPQ- Cu-1	Ph-PPQ- Cu-2	Ph-PPQ- Cu-3	Ph-PPQ- Cu-4
N1-Cu-N2	85.0	85.9	85.9	86.6
N1-Cu-N3	84.7	84.2	84.4	83.0
N1-Cu-N4	83.8	84.1	83.5	83.8
N1-Cu-N5	164.3	164.8	163.9	166.9
N2-Cu-N3	102.6	104.2	106.3	98.8
N2-Cu-N4	94.1	64.6	93.0	131.7
N2-Cu-N5	79.8	79.9	78.9	81.8
N3-Cu-N4	158.8	157.0	156.4	126.6
N3-Cu-N5	94.9	94.2	94.7	104.7
N4-Cu-N5	101.0	102.2	102.4	99.4

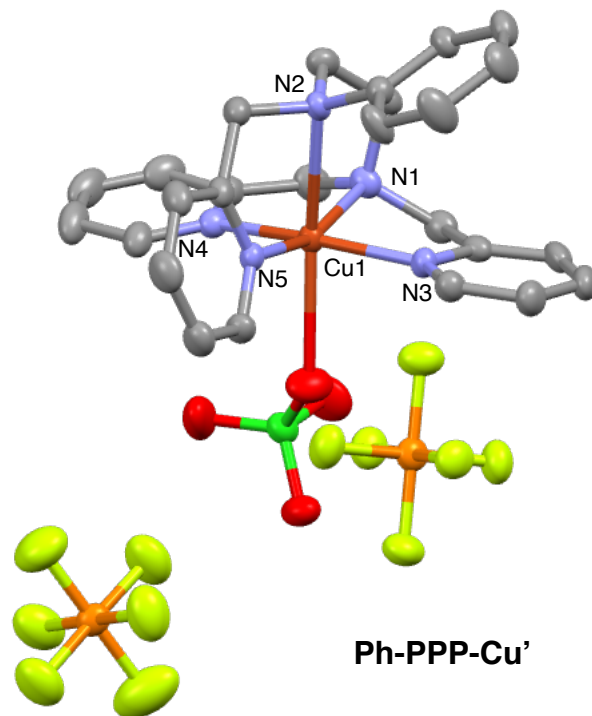


Fig. S1. Perspective view for **Ph-PPP-Cu'** complex ($[\text{Cu}(\text{Ph-PPP})(\text{ClO}_4)]\text{PF}_6$) in 50% probability, where the occupancy of both PF_6^- anion is 0.5. Hydrogen atoms are omitted for clarity.

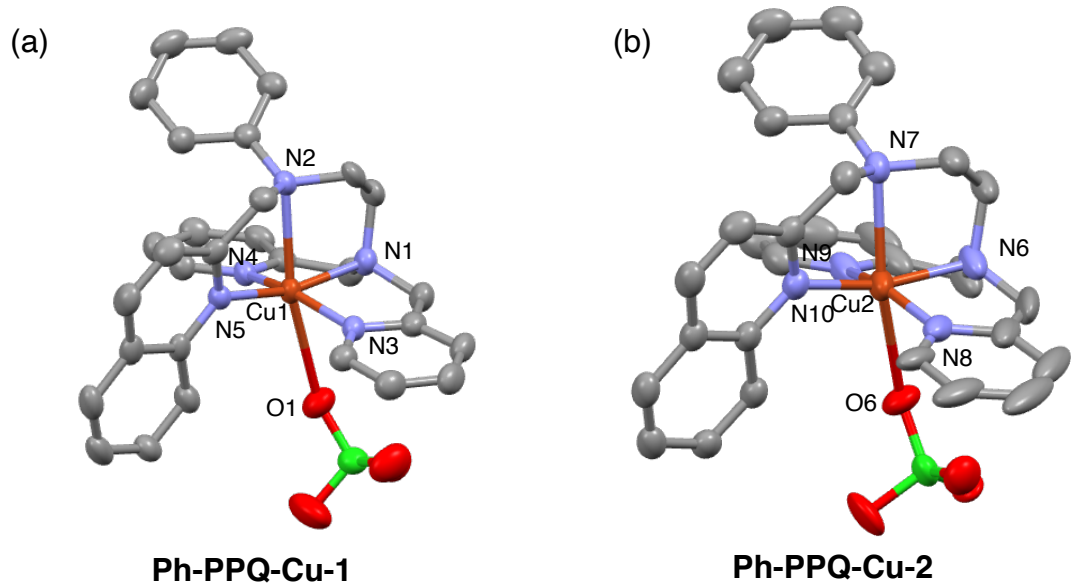
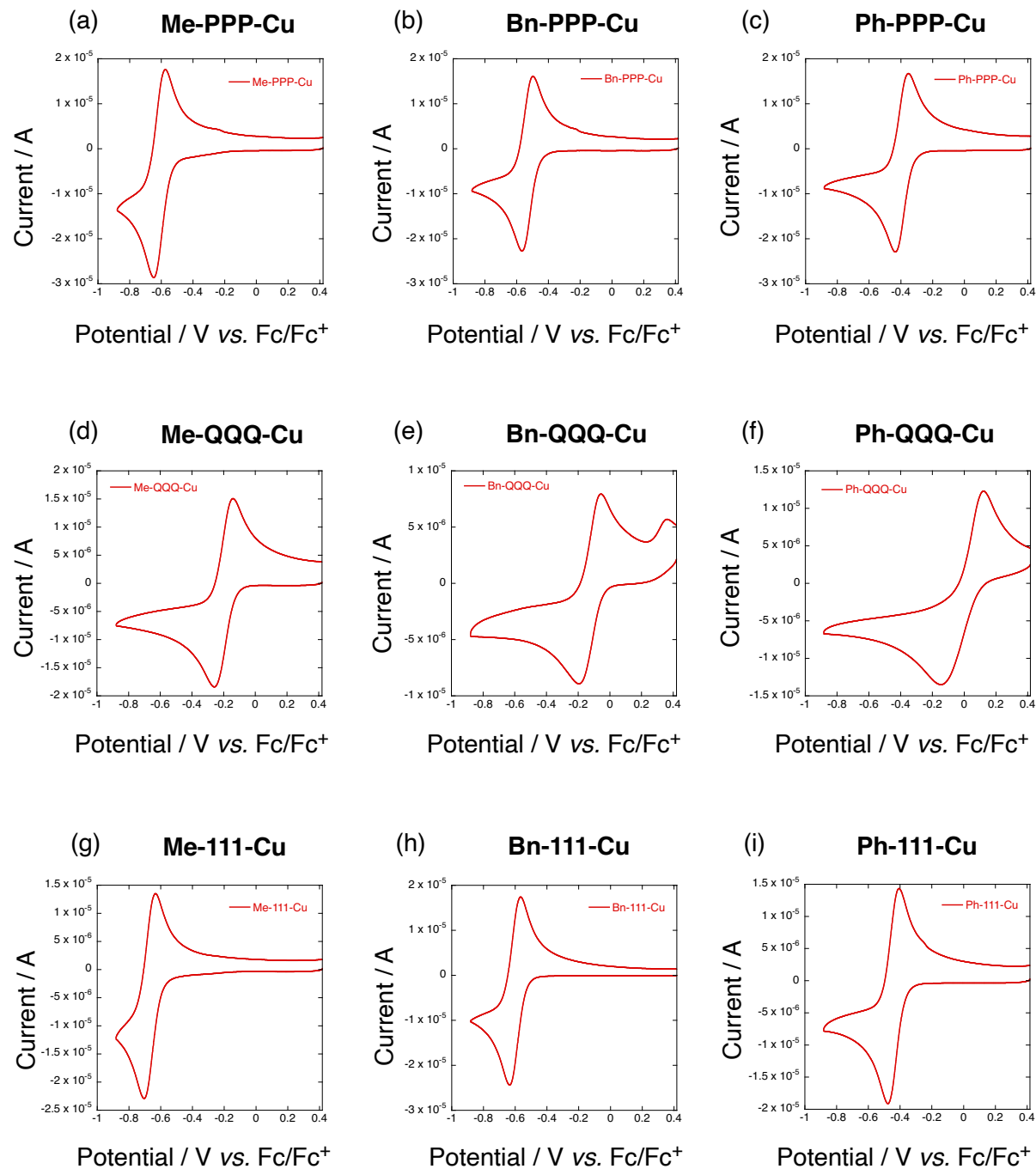


Fig. S2. Perspective view for **Ph-PPQ-Cu** complex in 50% probability. Non-coordinating counter anions, solvents and hydrogen atoms are omitted for clarity.

Cyclic voltammetry

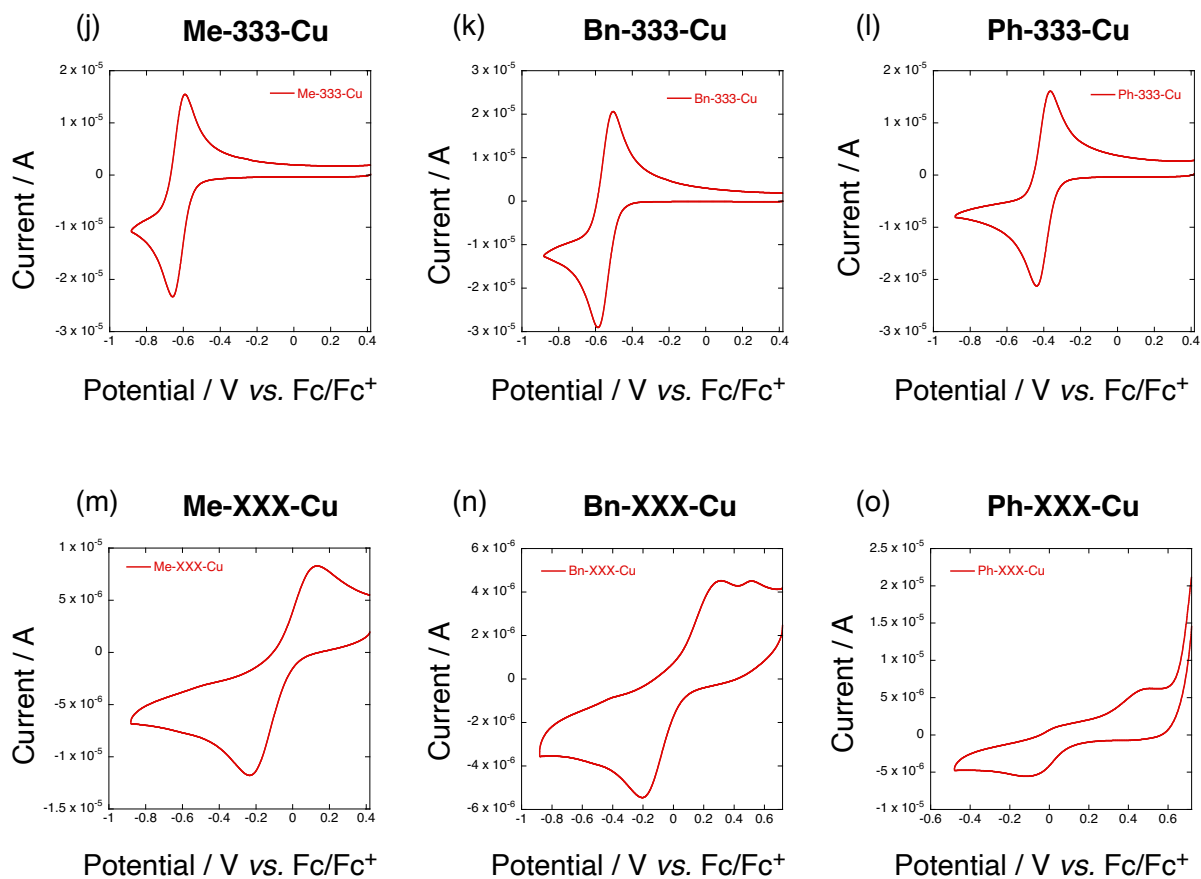


Fig. S3. Cyclic voltammogram of copper(II) complexes in acetonitrile (1 mM, scan rate 100 mV/s). (a) Me-PPP-Cu, (b) Bn-PPP-Cu, (c) Ph-PPP-Cu, (d) Me-QQQ-Cu, (e) Bn-QQQ-Cu, (f) Ph-QQQ-Cu, (g) Me-111-Cu, (h) Bn-111-Cu, (i) Ph-111-Cu, (j) Me-333-Cu, (k) Bn-333-Cu, (l) Ph-333-Cu, (m) Me-XXX-Cu, (n) Bn-XXX-Cu and (o) Ph-XXX-Cu.

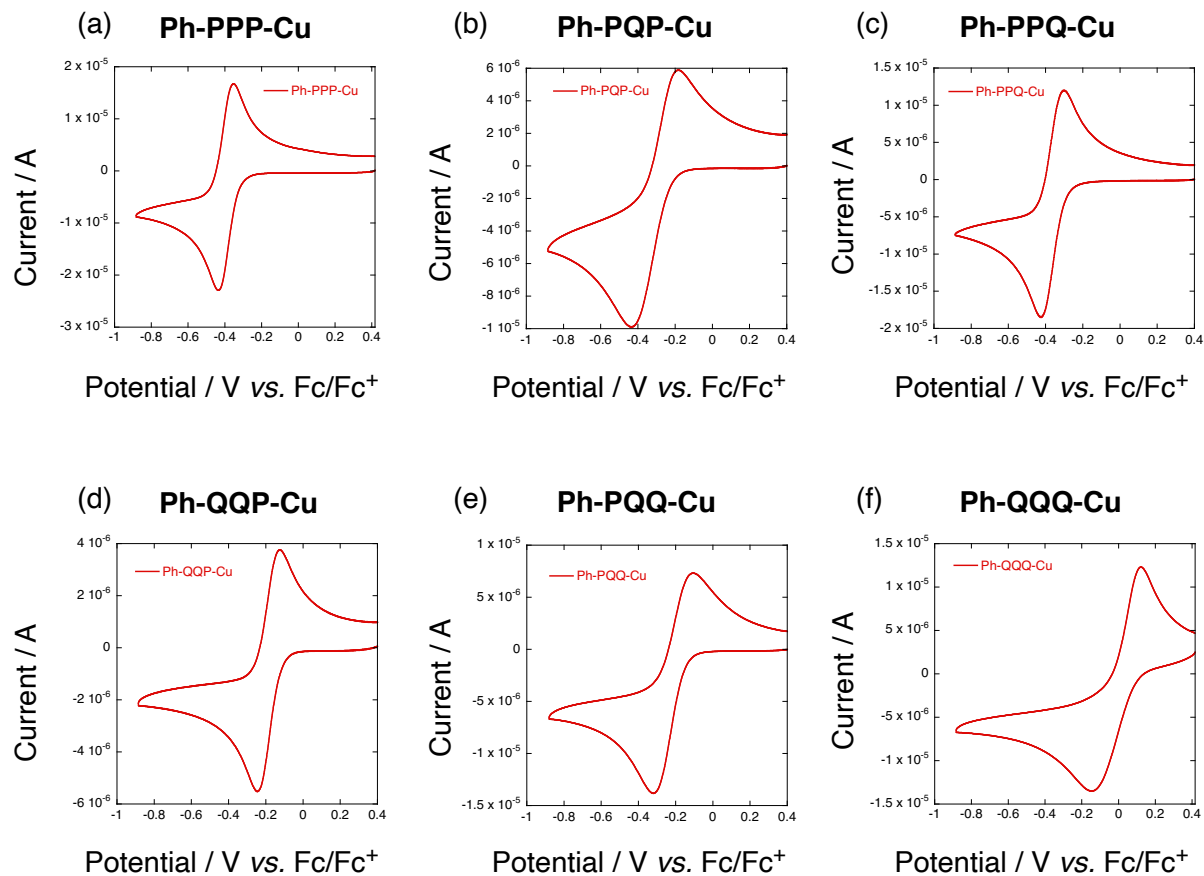


Fig. S4. Cyclic voltammogram of copper(II) complexes in acetonitrile (1 mM, scan rate 100 mV/s). (a) Ph-PPP-Cu, (b) Ph-PQP-Cu, (c) Ph-PPQ-Cu, (d) Ph-QQP-Cu, (e) Ph-PQQ-Cu and (f) Ph-QQQ-Cu.

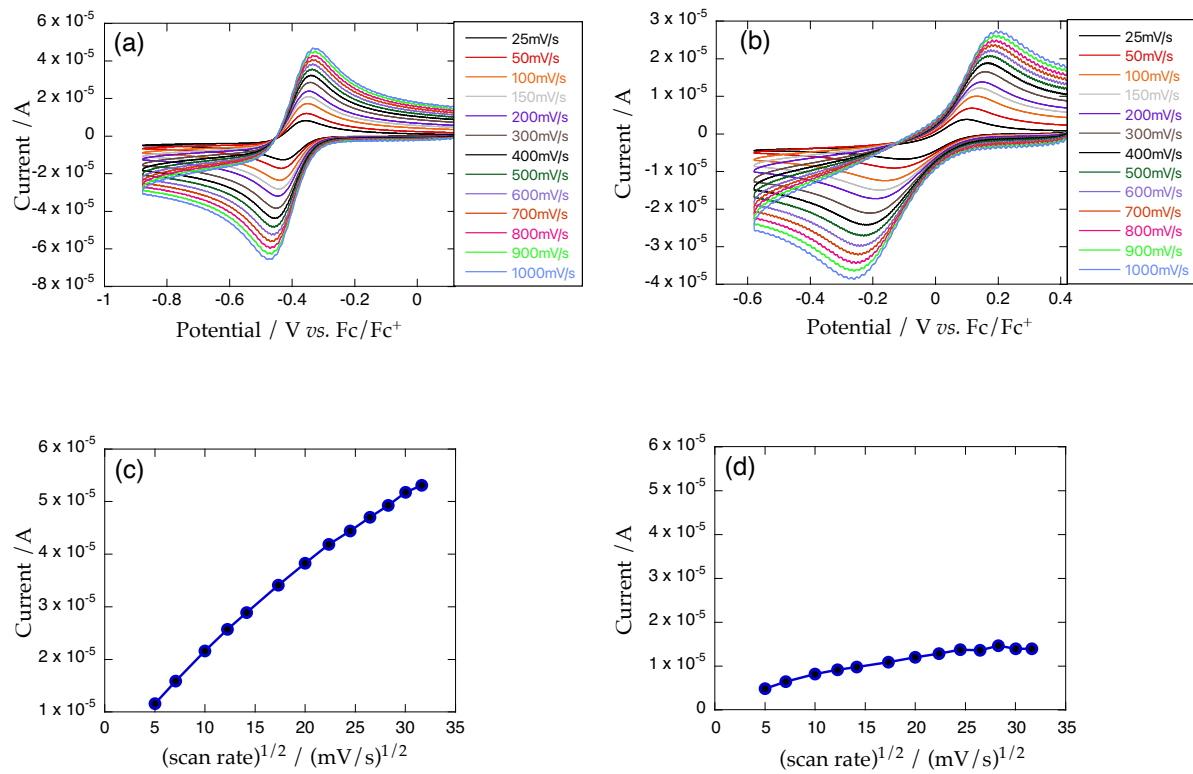
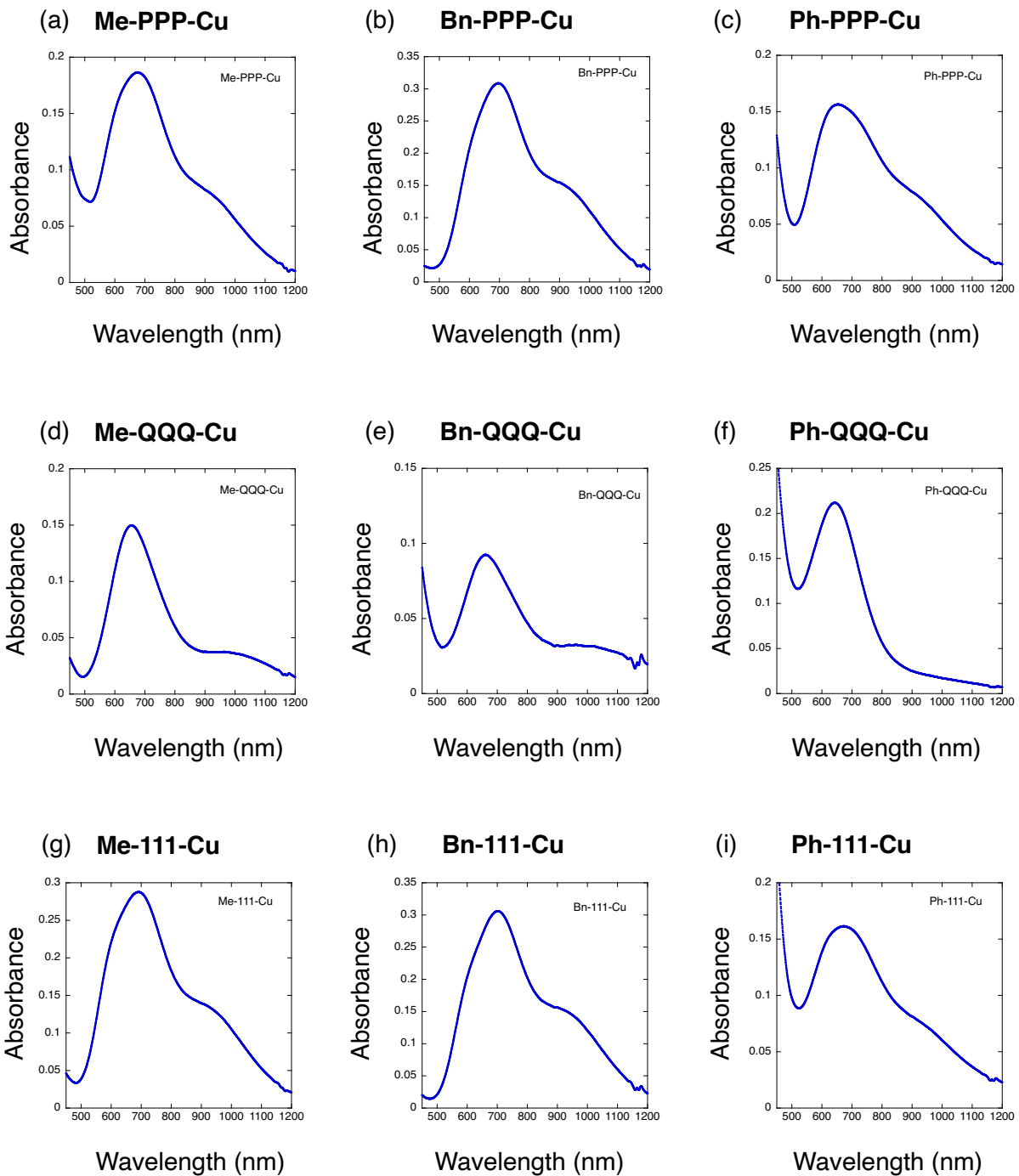


Fig. S5. Cyclic voltammogram of (a) Ph-PPP-Cu and (b) Ph-QQQ-Cu in acetonitrile at various scan rates (1 mM, scan rate 25–1000 mV/s) and plot for current *vs.* (scan rate)^{1/2} for (c) Ph-PPP-Cu and (d) Ph-QQQ-Cu.

Absorption spectrum



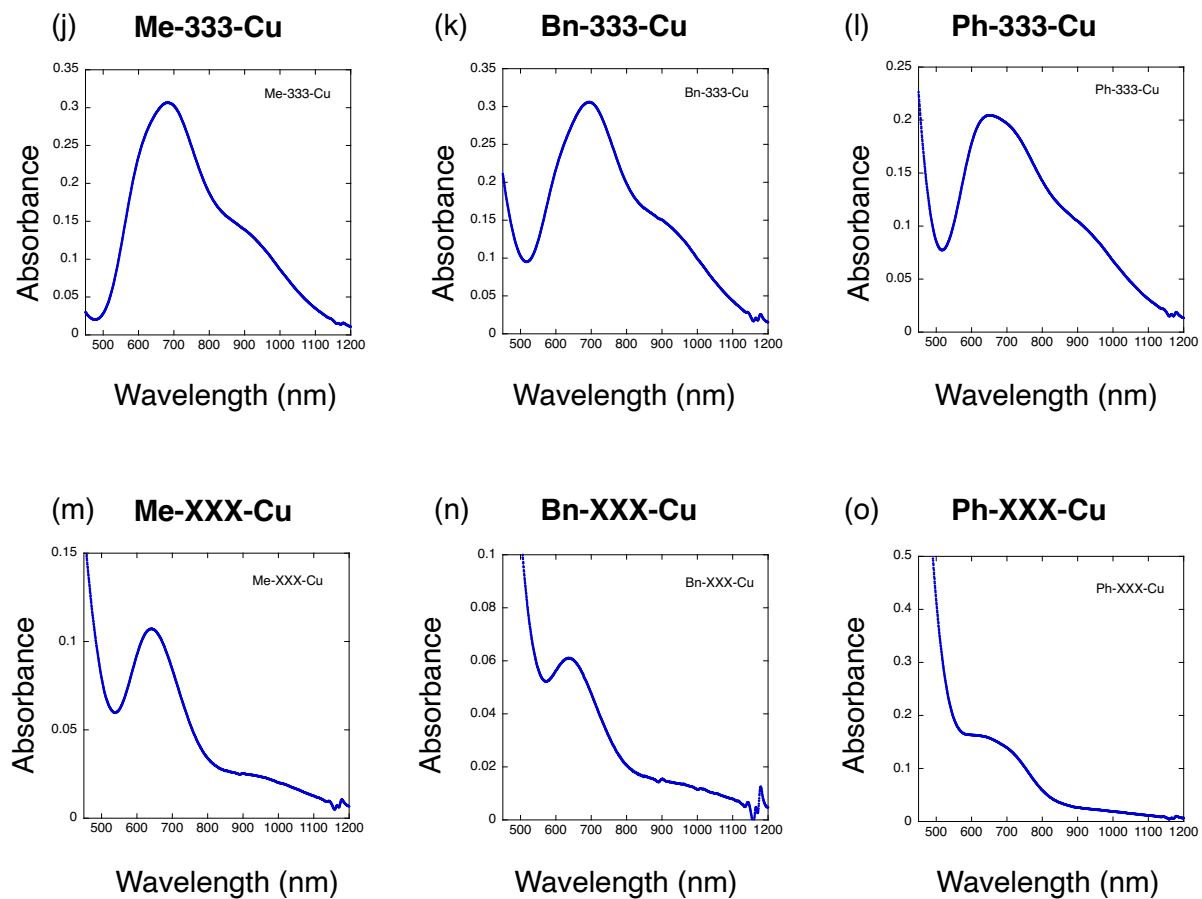


Fig. S6. Absorption spectrum of **R-ArArAr-Cu** in acetonitrile (1 mM). (a) **Me-PPP-Cu**, (b) **Bn-PPP-Cu**, (c) **Ph-PPP-Cu**, (d) **Me-QQQ-Cu**, (e) **Bn-QQQ-Cu**, (f) **Ph-QQQ-Cu**, (g) **Me-111-Cu**, (h) **Bn-111-Cu**, (i) **Ph-111-Cu**, (j) **Me-333-Cu**, (k) **Bn-333-Cu**, (l) **Ph-333-Cu**, (m) **Me-XXX-Cu**, (n) **Bn-XXX-Cu** and (o) **Ph-XXX-Cu**.

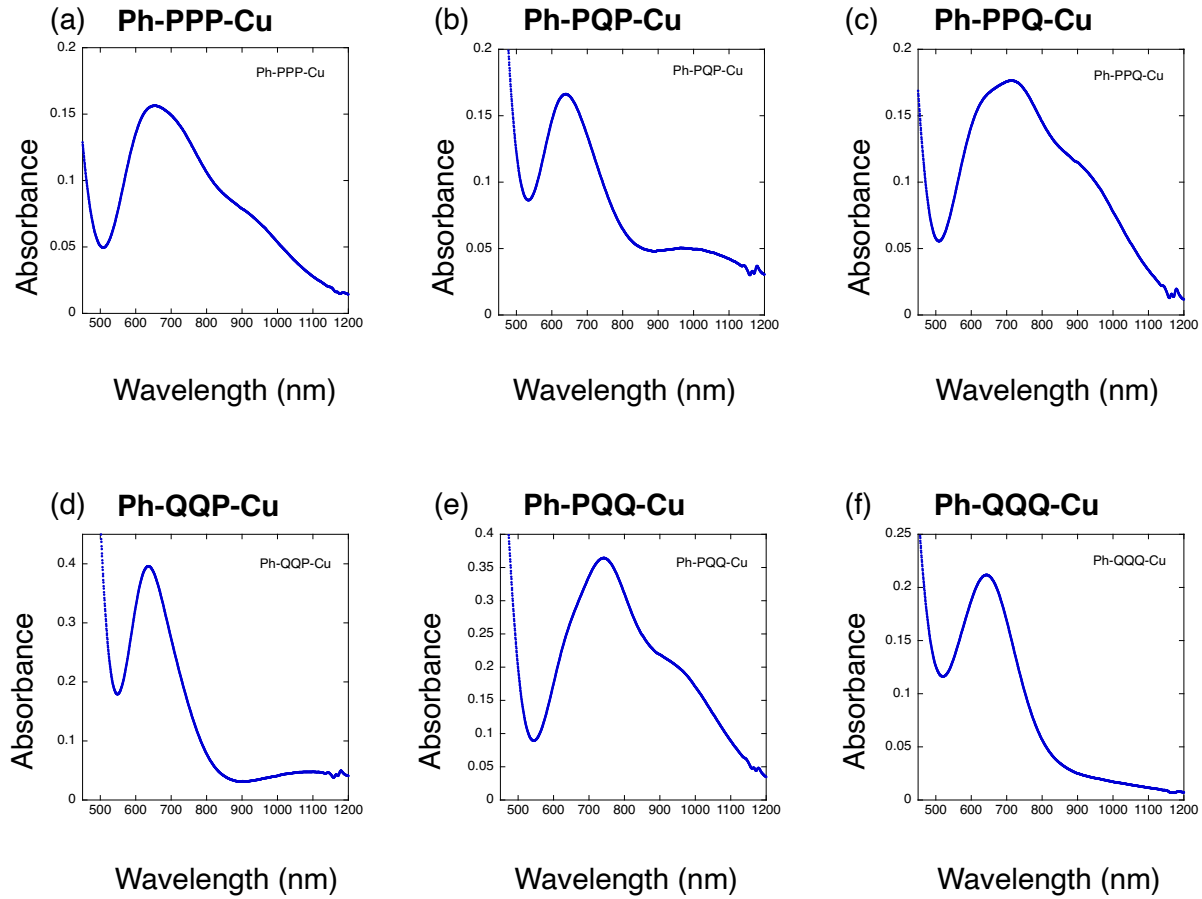
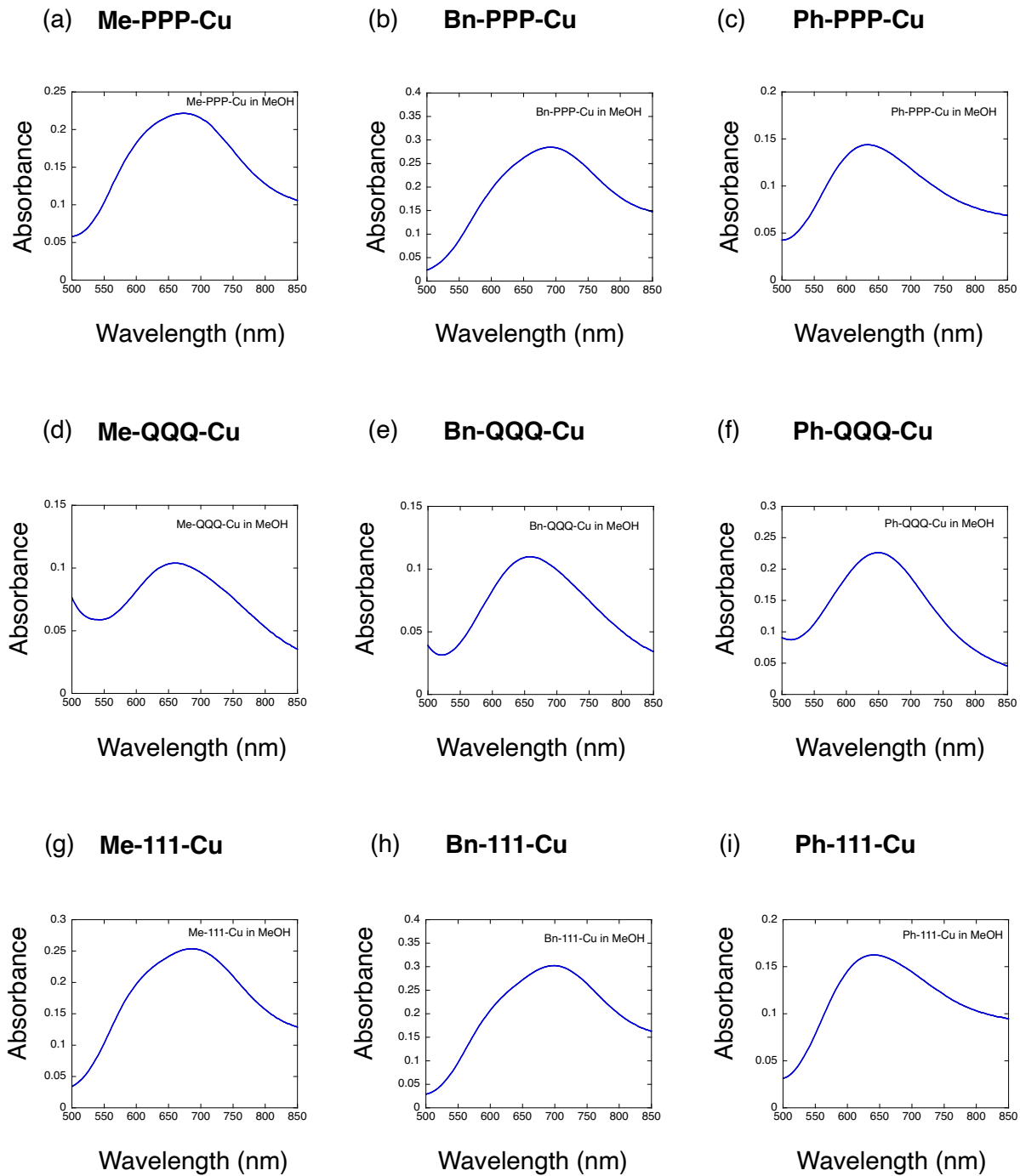


Fig. S7. Absorption spectrum of **Ph-Ar¹Ar²Ar³-Cu** in acetonitrile (1 mM). (a) **Ph-PPP-Cu**, (b) **Ph-PQP-Cu**, (c) **Ph-PPQ-Cu**, (d) **Ph-QQP-Cu**, (e) **Ph-PQQ-Cu** and (f) **Ph-QQQ-Cu**.



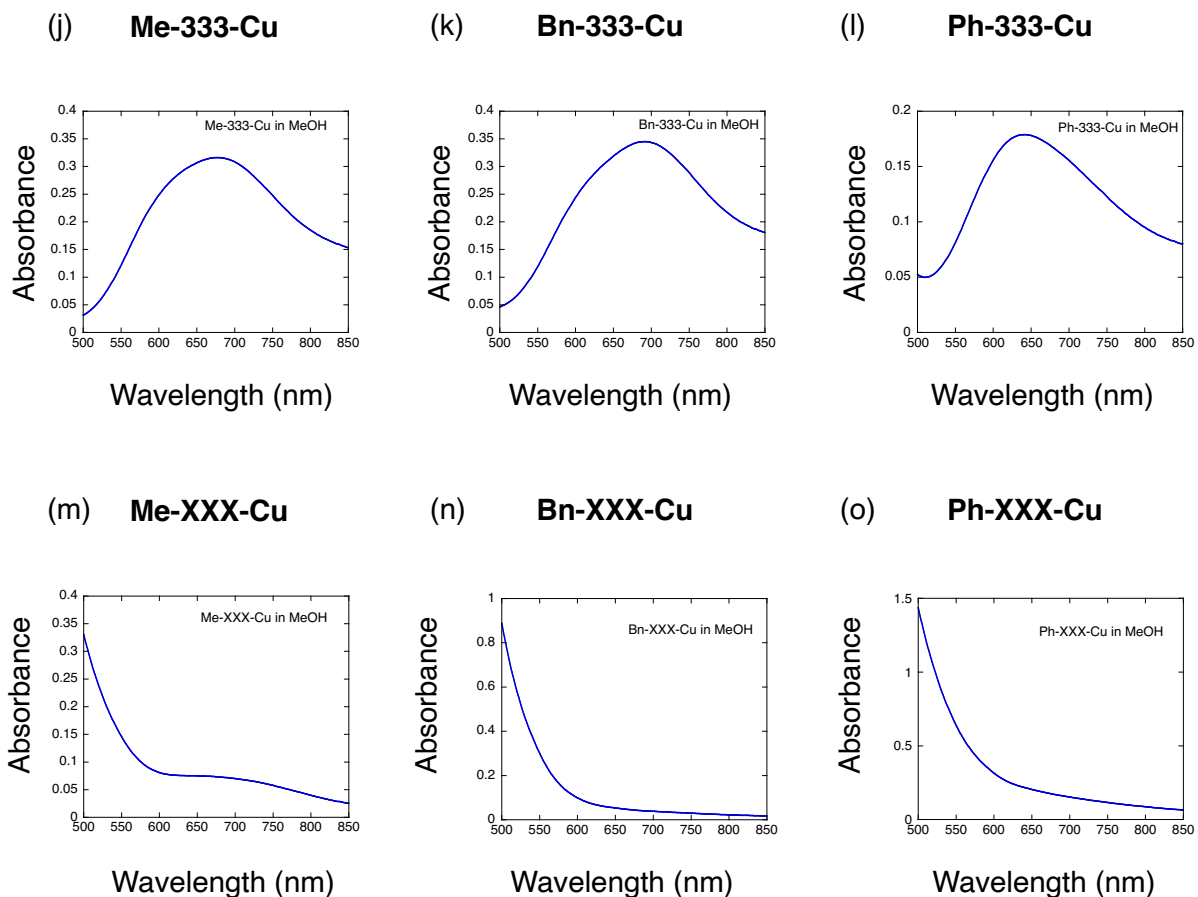


Fig. S8. Absorption spectrum of **R-ArArAr-Cu** in methanol (1 mM). (a) **Me-PPP-Cu**, (b) **Bn-PPP-Cu**, (c) **Ph-PPP-Cu**, (d) **Me-QQQ-Cu**, (e) **Bn-QQQ-Cu**, (f) **Ph-QQQ-Cu**, (g) **Me-111-Cu**, (h) **Bn-111-Cu**, (i) **Ph-111-Cu**, (j) **Me-333-Cu**, (k) **Bn-333-Cu**, (l) **Ph-333-Cu**, (m) **Me-XXX-Cu**, (n) **Bn-XXX-Cu** and (o) **Ph-XXX-Cu**.

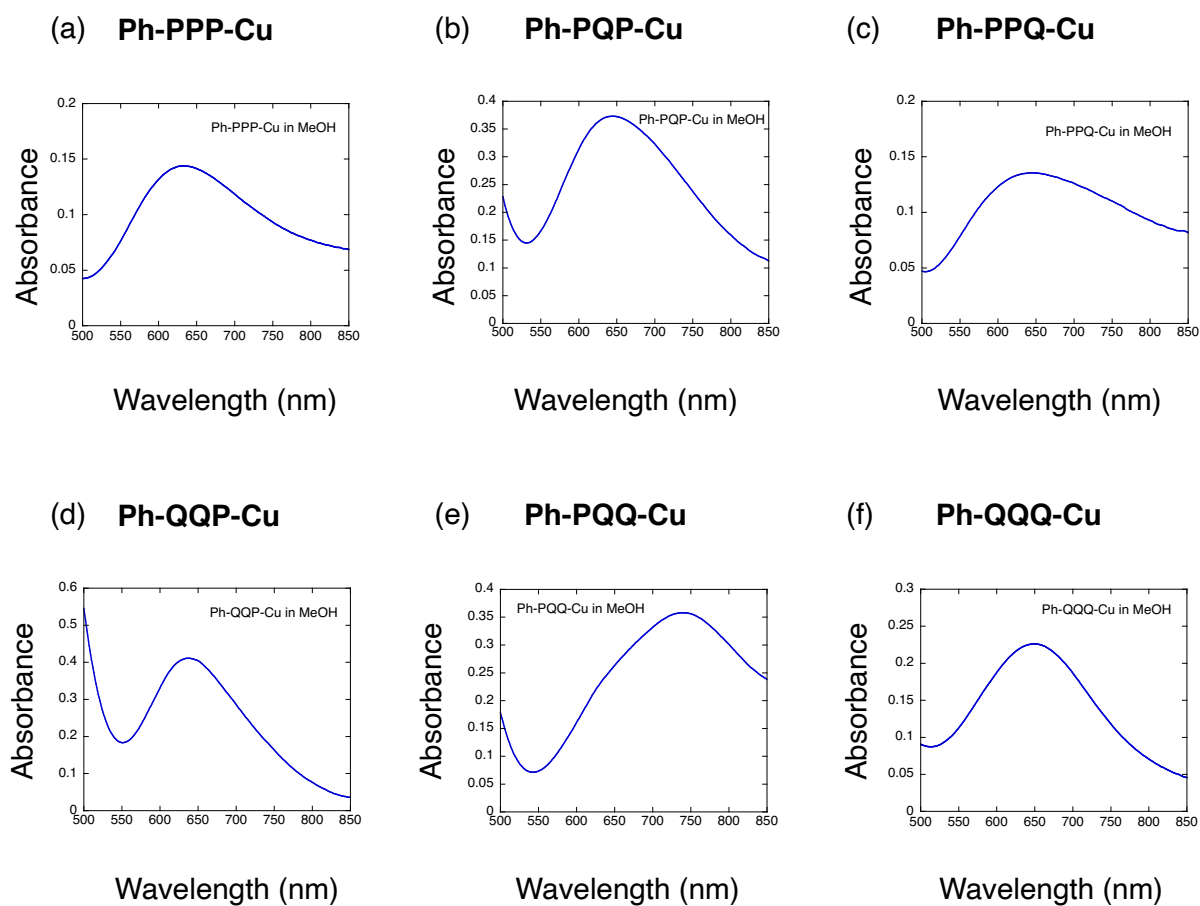


Fig. S9. Absorption spectrum of **Ph-Ar¹Ar²Ar³-Cu** in methanol (1 mM). (a) **Ph-PPP-Cu**, (b) **Ph-PQP-Cu**, (c) **Ph-PPQ-Cu**, (d) **Ph-QQP-Cu**, (e) **Ph-PQQ-Cu** and (f) **Ph-QQQ-Cu**.

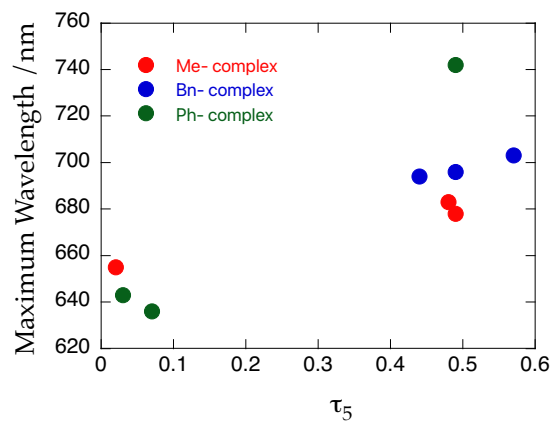
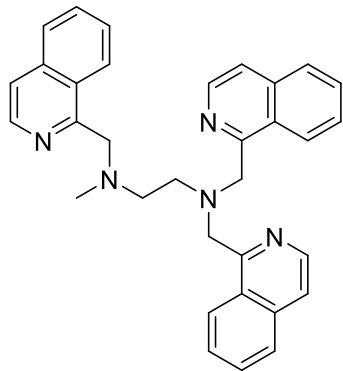
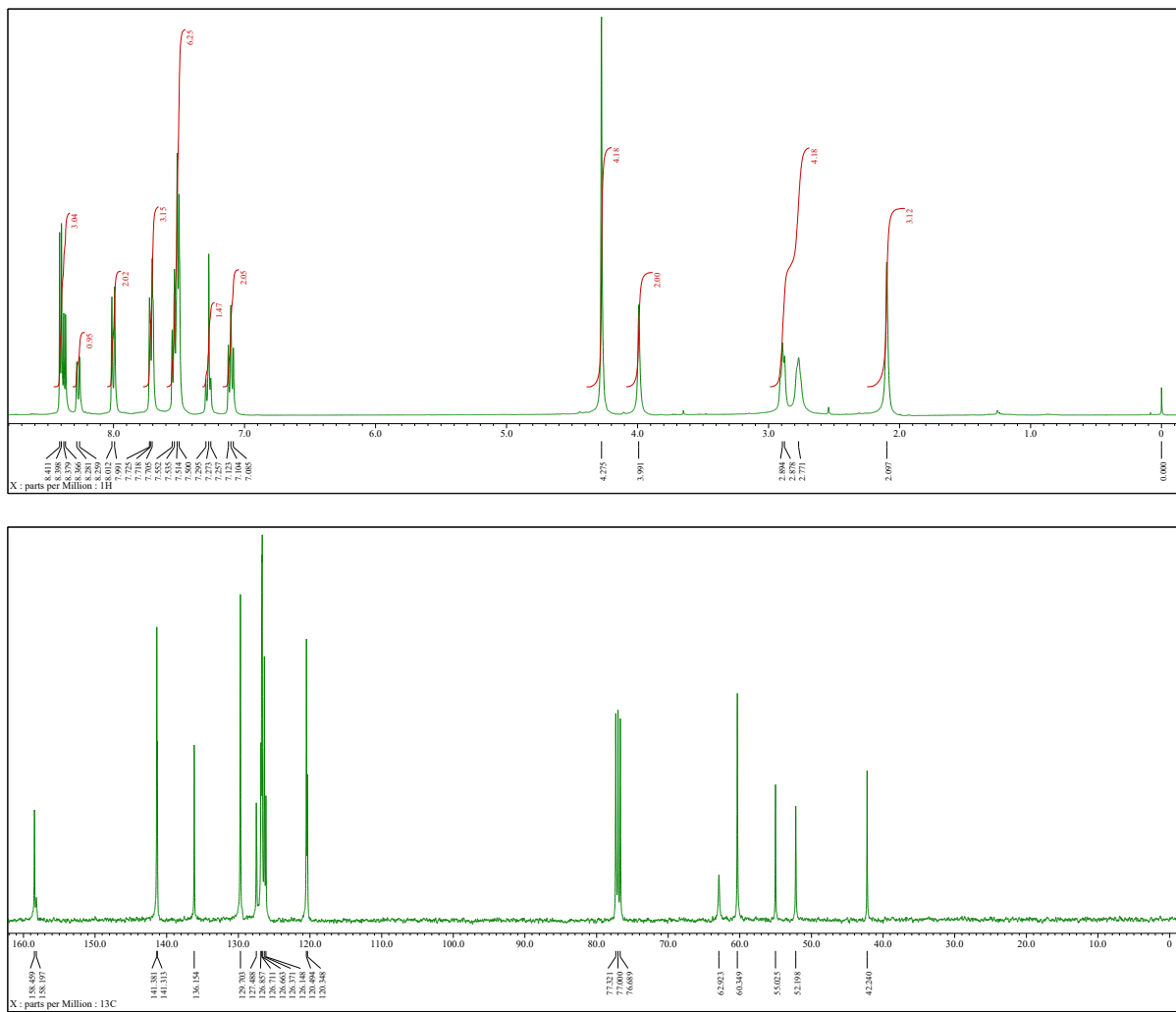
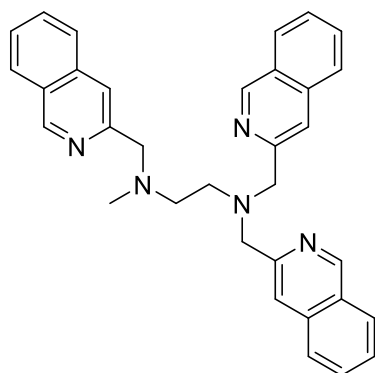


Fig. S10. Plot for absorption maxima of copper complexes measured in acetonitrile against the τ_5 values derived from X-ray crystallography shown in Fig. 2 and 3. The data for **Ph-PPP-Cu** (octahedral geometry) and **Ph-PPQ-Cu** (two geometries with largely different τ_5 values) were not included.

¹H/¹³C NMR spectrum

Me-111





Me-333

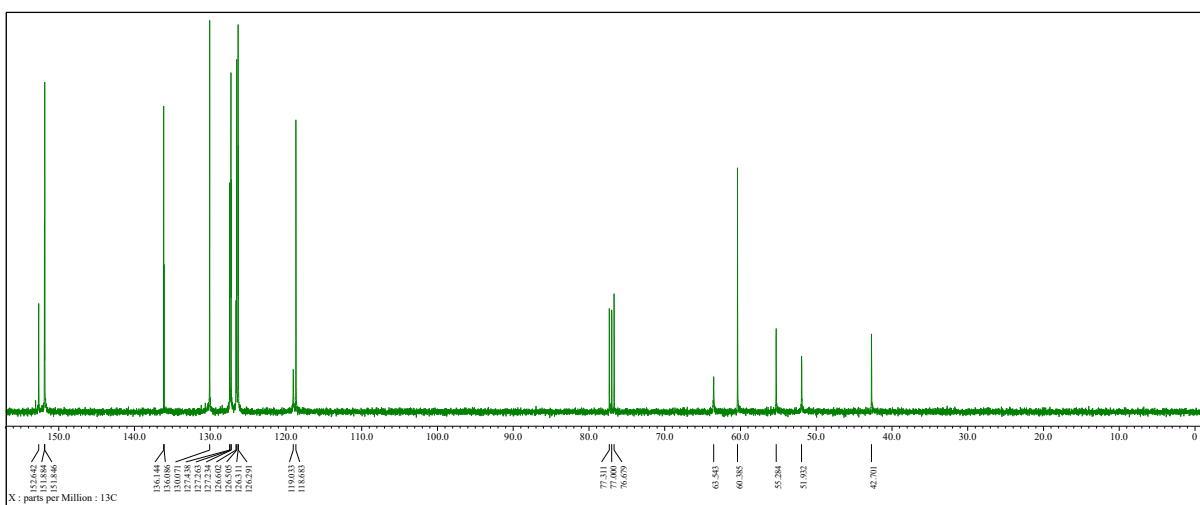
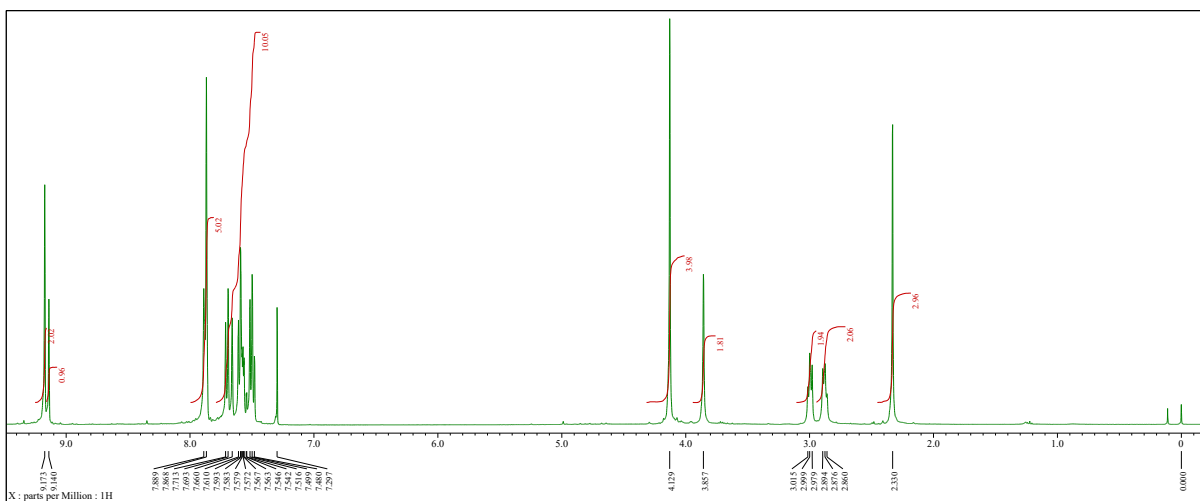
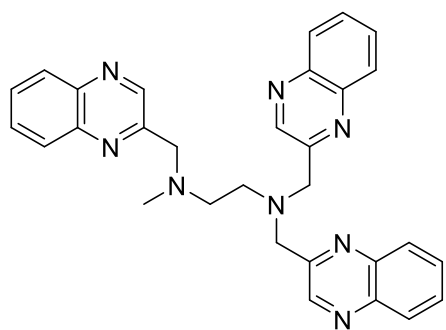


Fig. S12. $^1\text{H}/^{13}\text{C}$ NMR spectrum of Me-333 in CDCl_3 .



Me-XXX

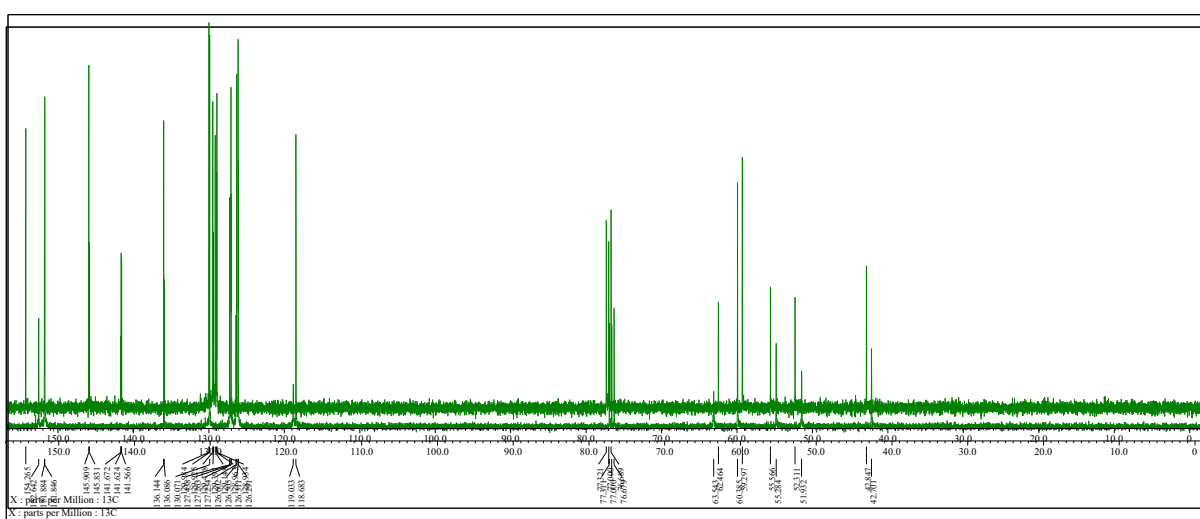
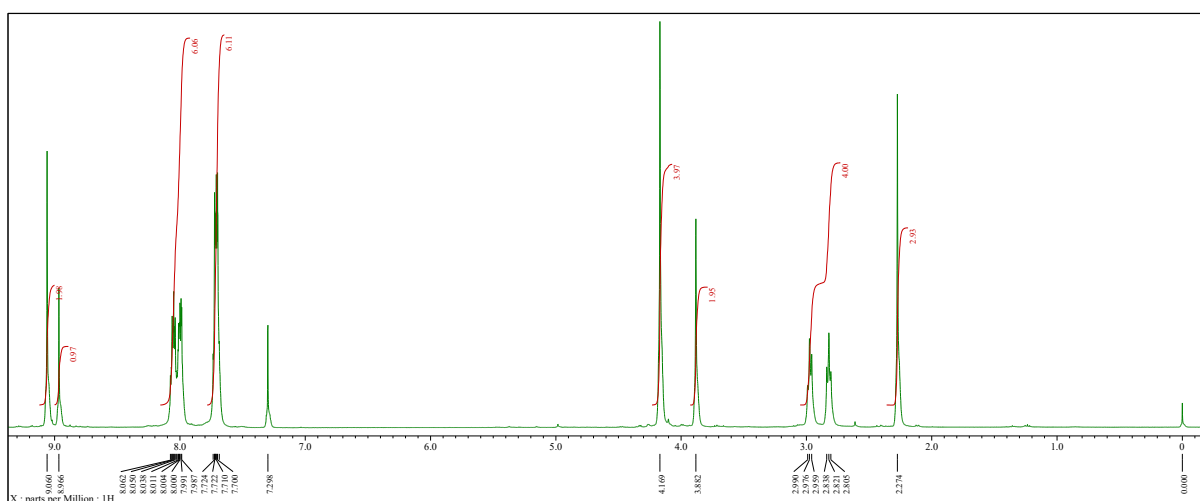
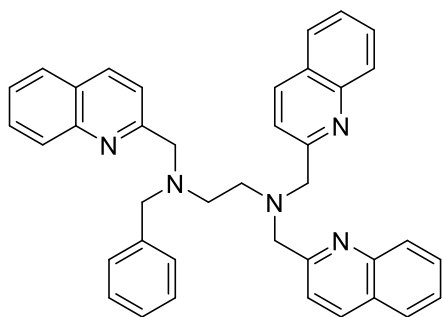


Fig. S13. $^1\text{H}/^{13}\text{C}$ NMR spectrum of Me-XXX in CDCl_3 .



Bn-QQQ

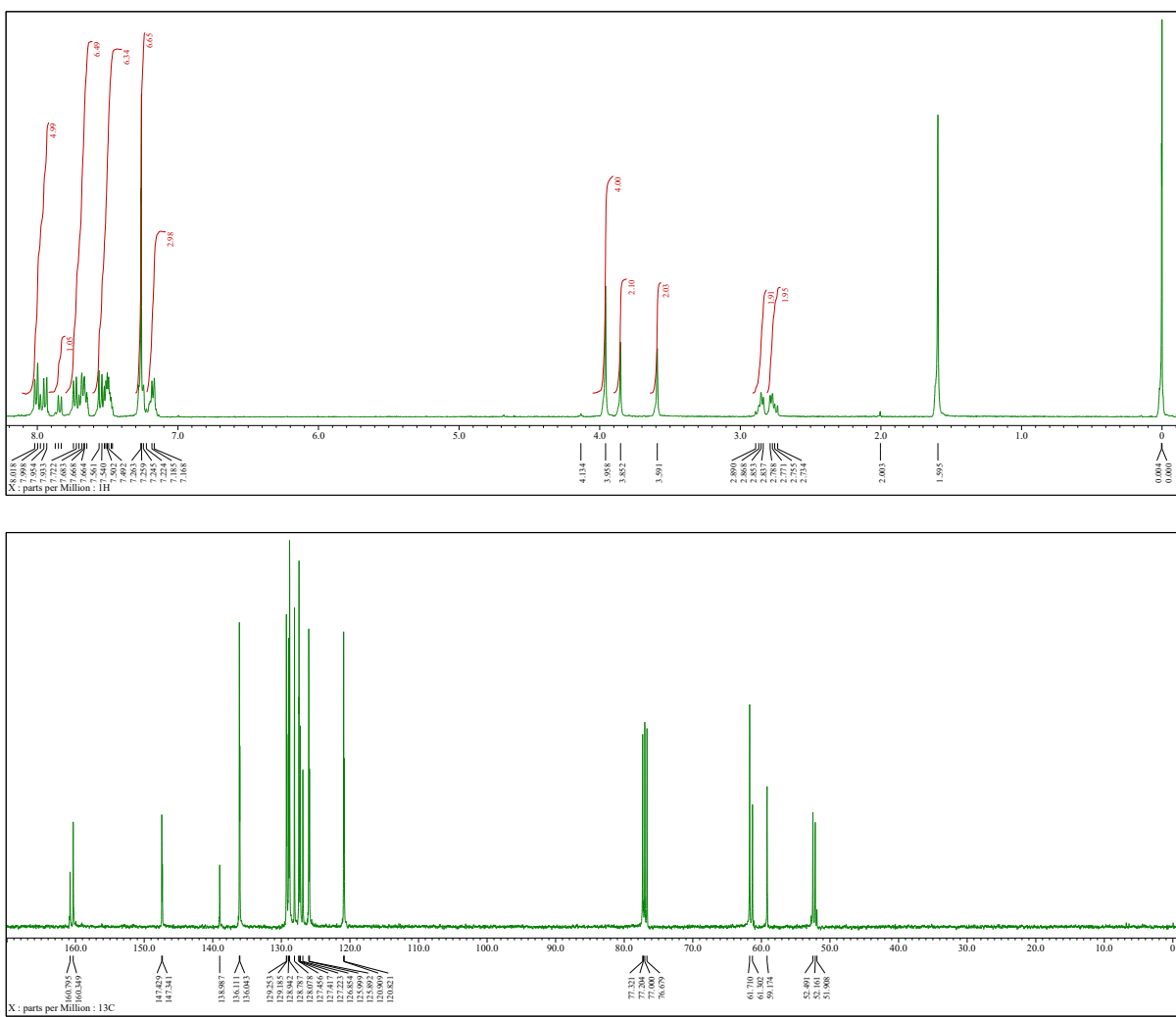
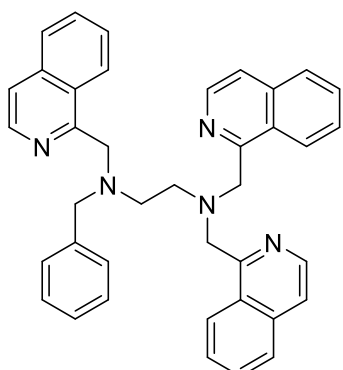


Fig. S14. $^1\text{H}/^{13}\text{C}$ NMR spectrum of Bn-**QQQ** in CDCl_3 .



Bn-111

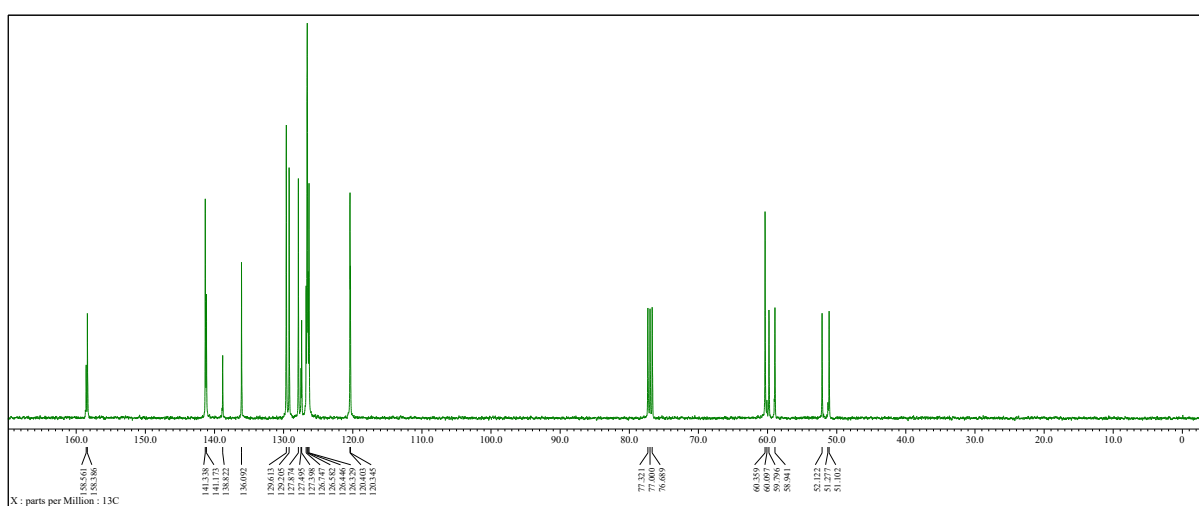
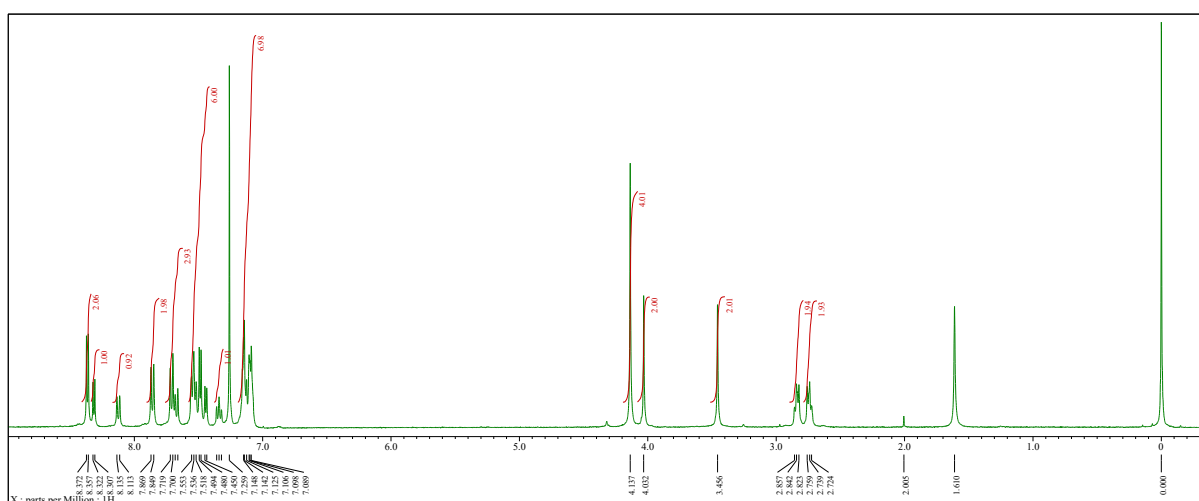
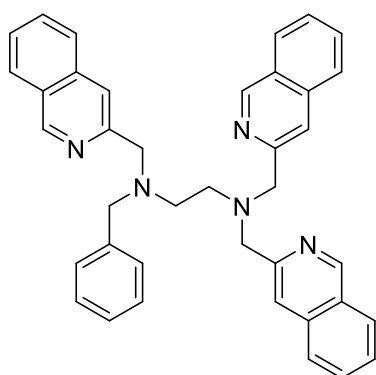


Fig. S15. $^1\text{H}/^{13}\text{C}$ NMR spectrum of **Bn-111** in CDCl_3 .



Bn-333

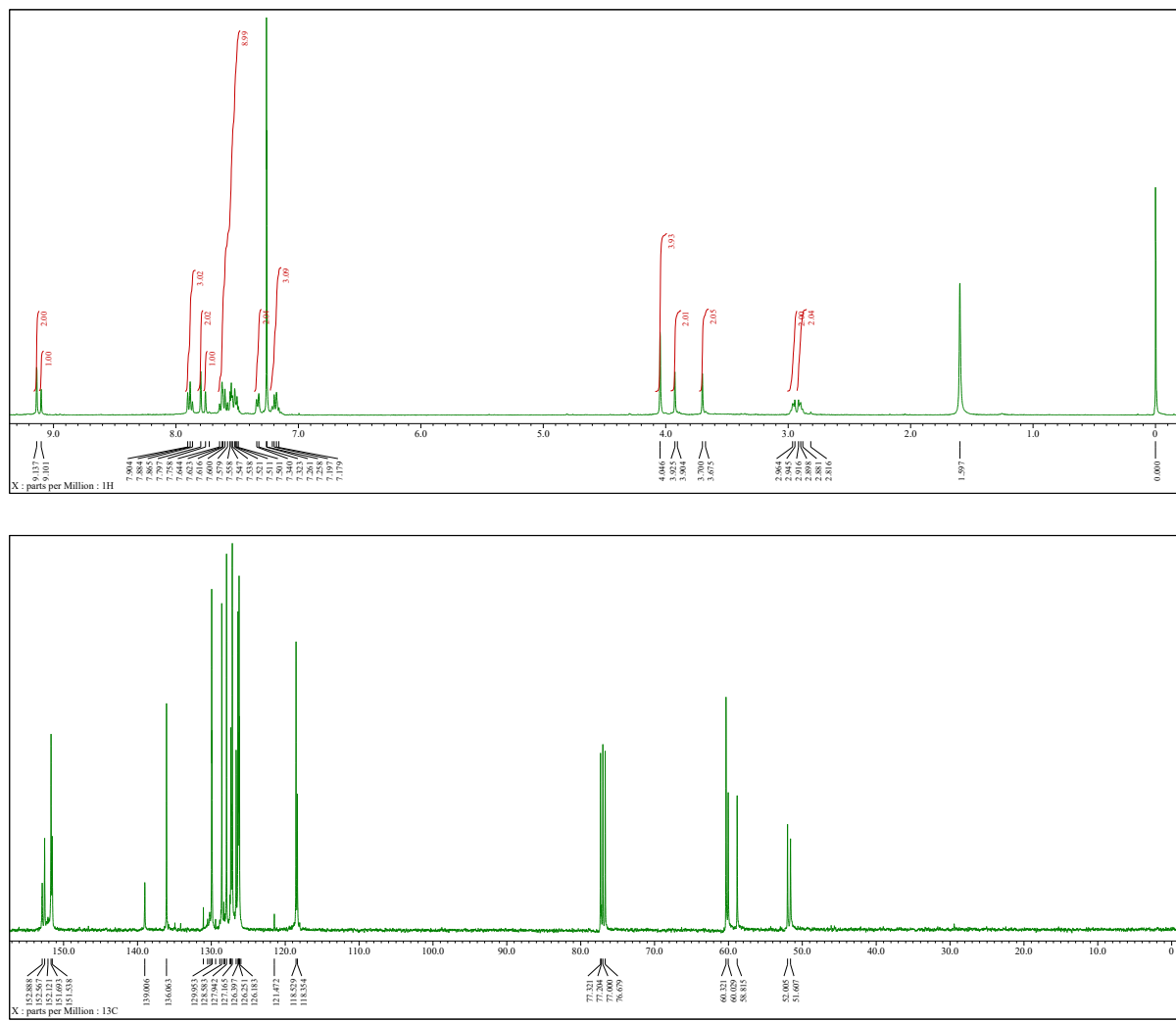


Fig. S16. $^1\text{H}/^{13}\text{C}$ NMR spectrum of Bn-333 in CDCl_3 .

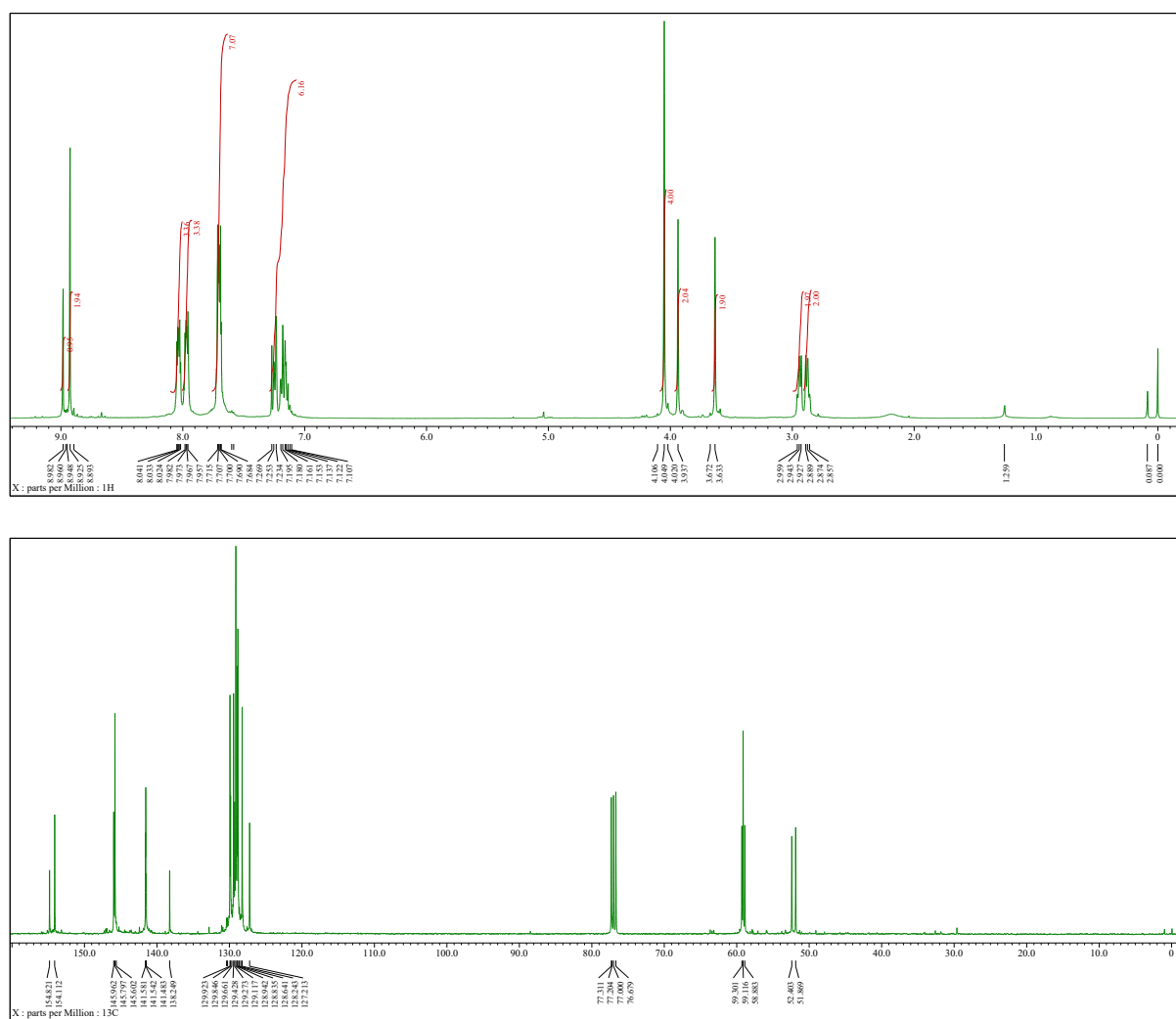
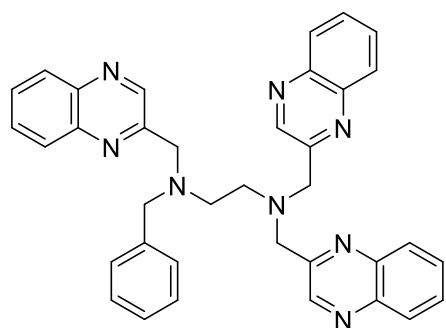
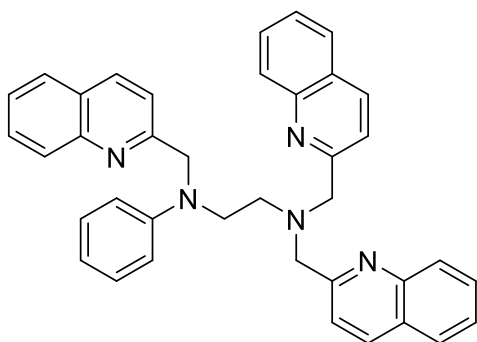
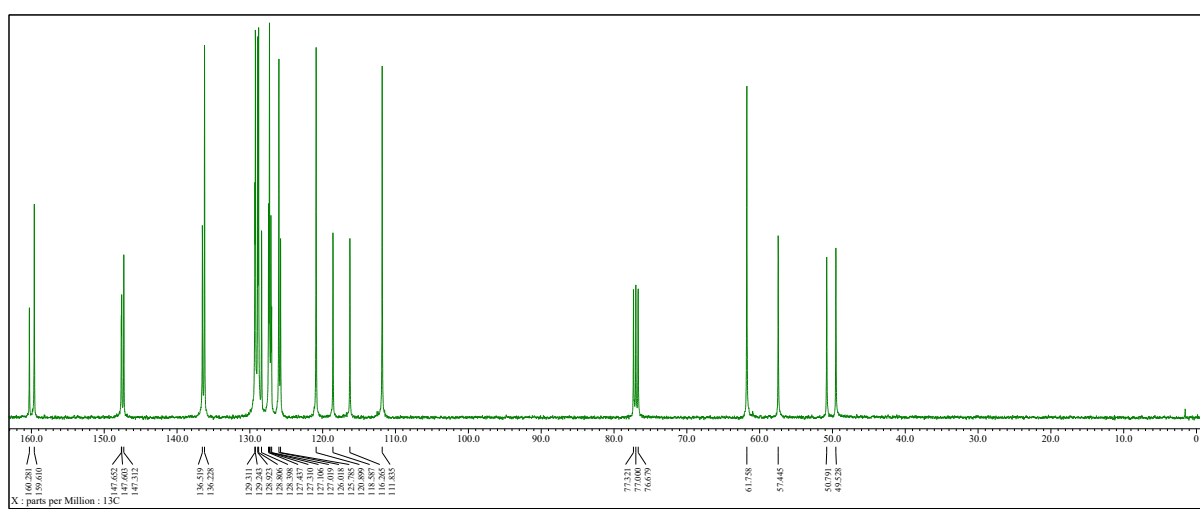
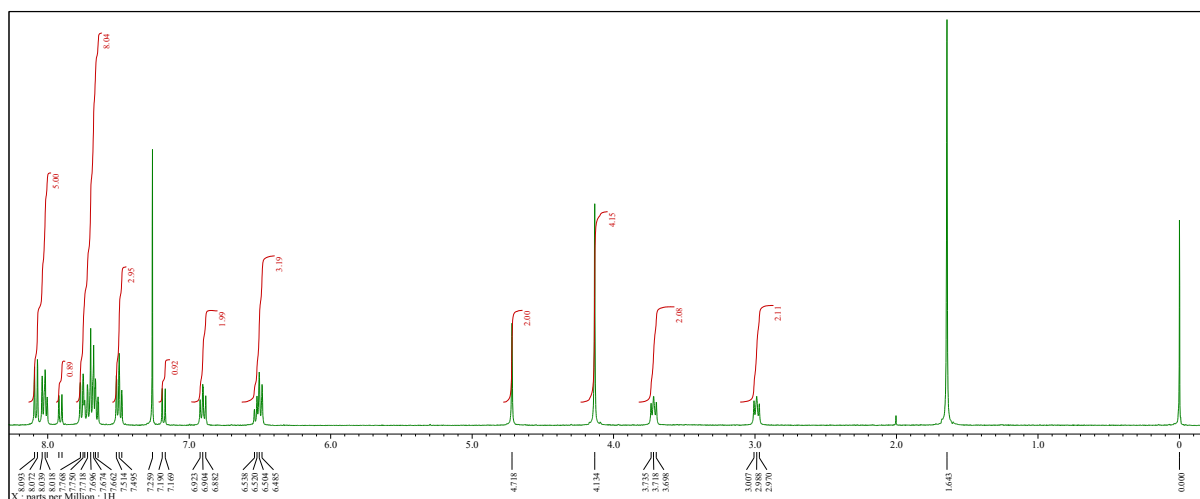
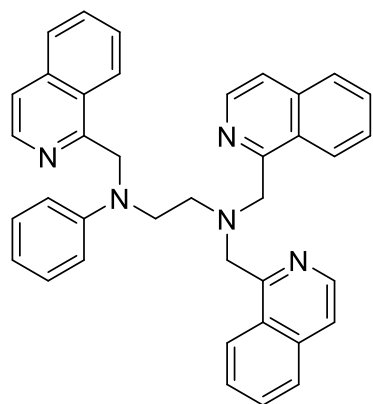
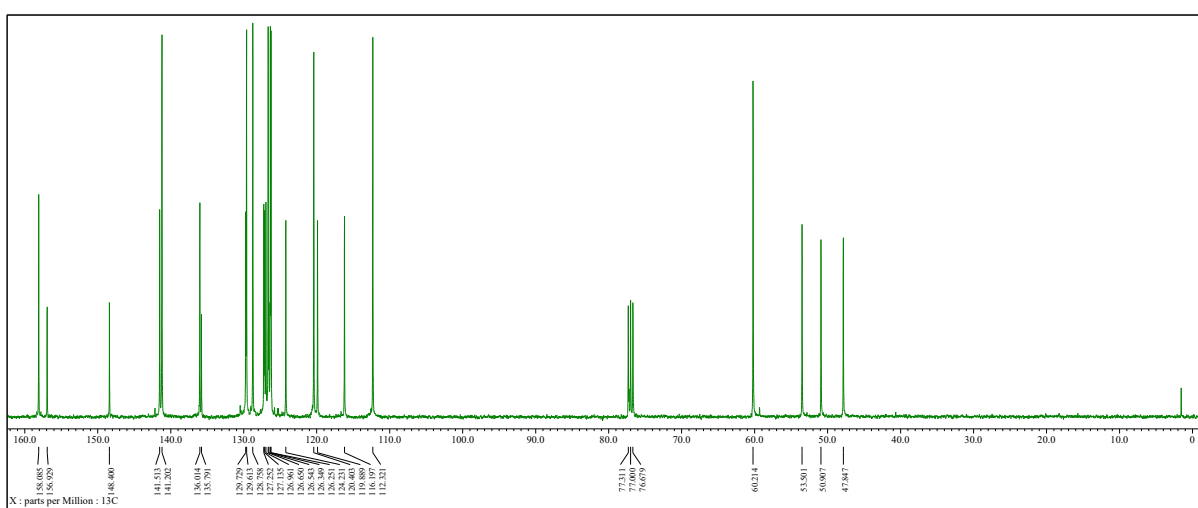
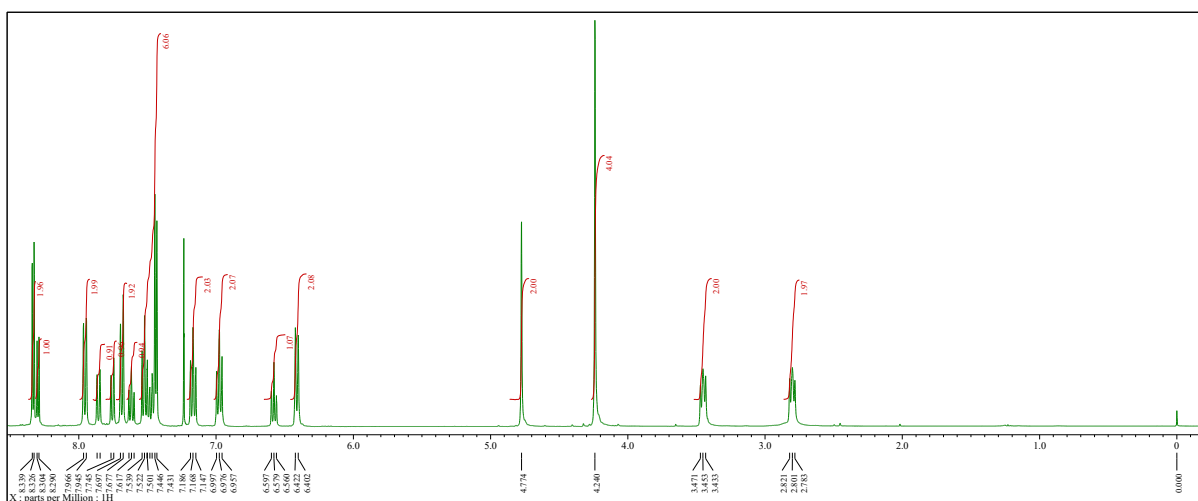


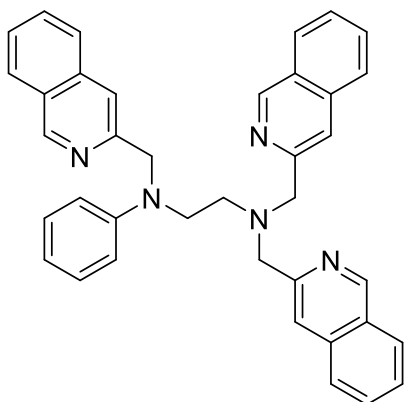
Fig. S17. $^1\text{H}/^{13}\text{C}$ NMR spectrum of **Bn-XXX** in CDCl_3 .



Ph-QQQ



**Ph-111****Fig. S19.** $^1\text{H}/^{13}\text{C}$ NMR spectrum of Ph-111 in CDCl_3 .



Ph-333

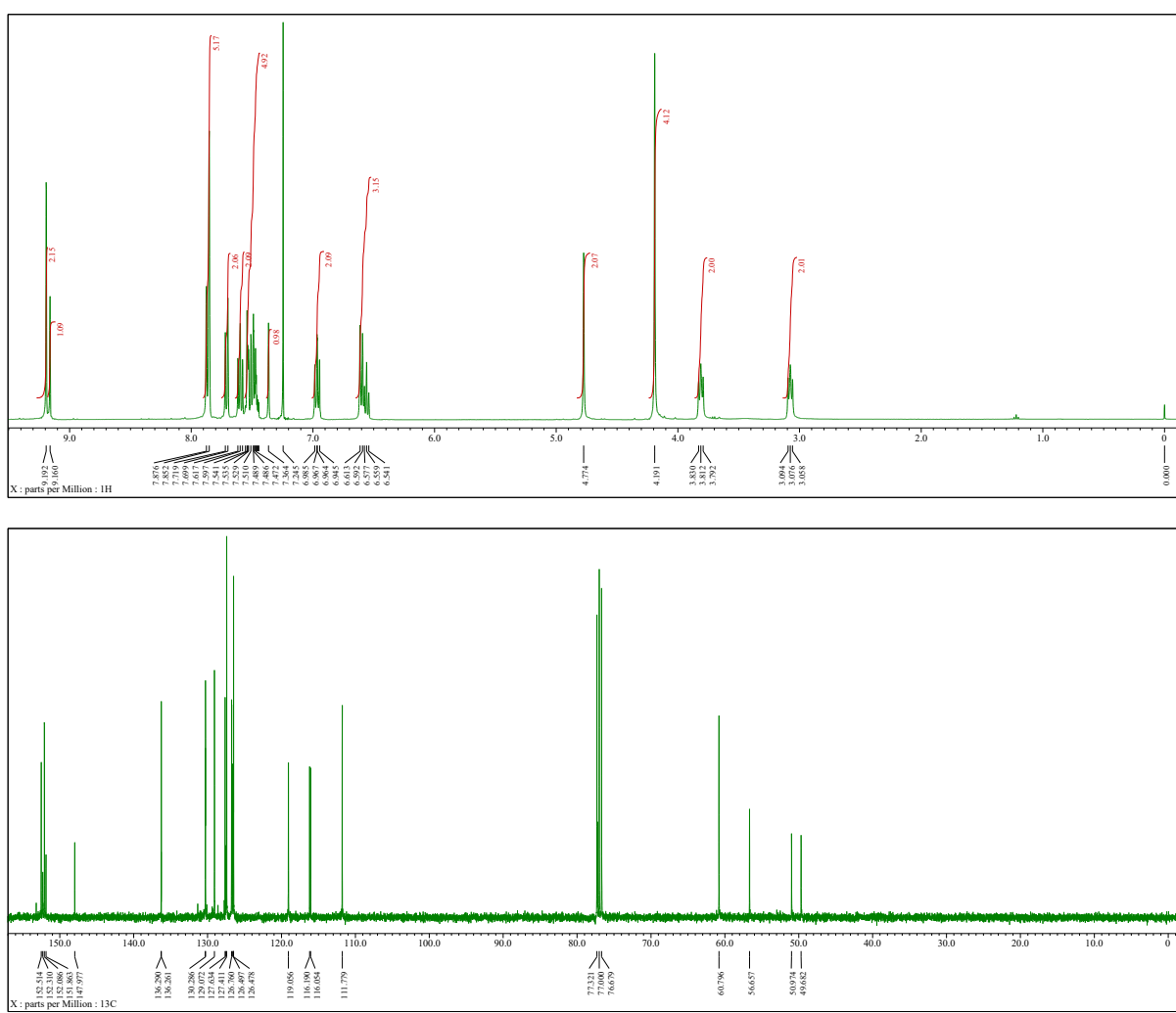
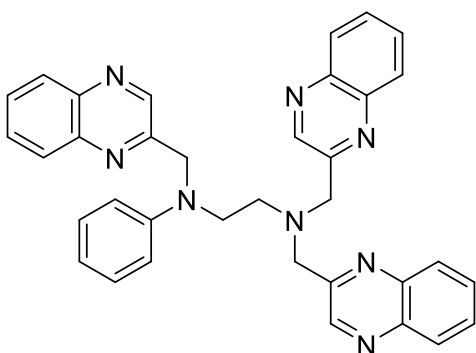
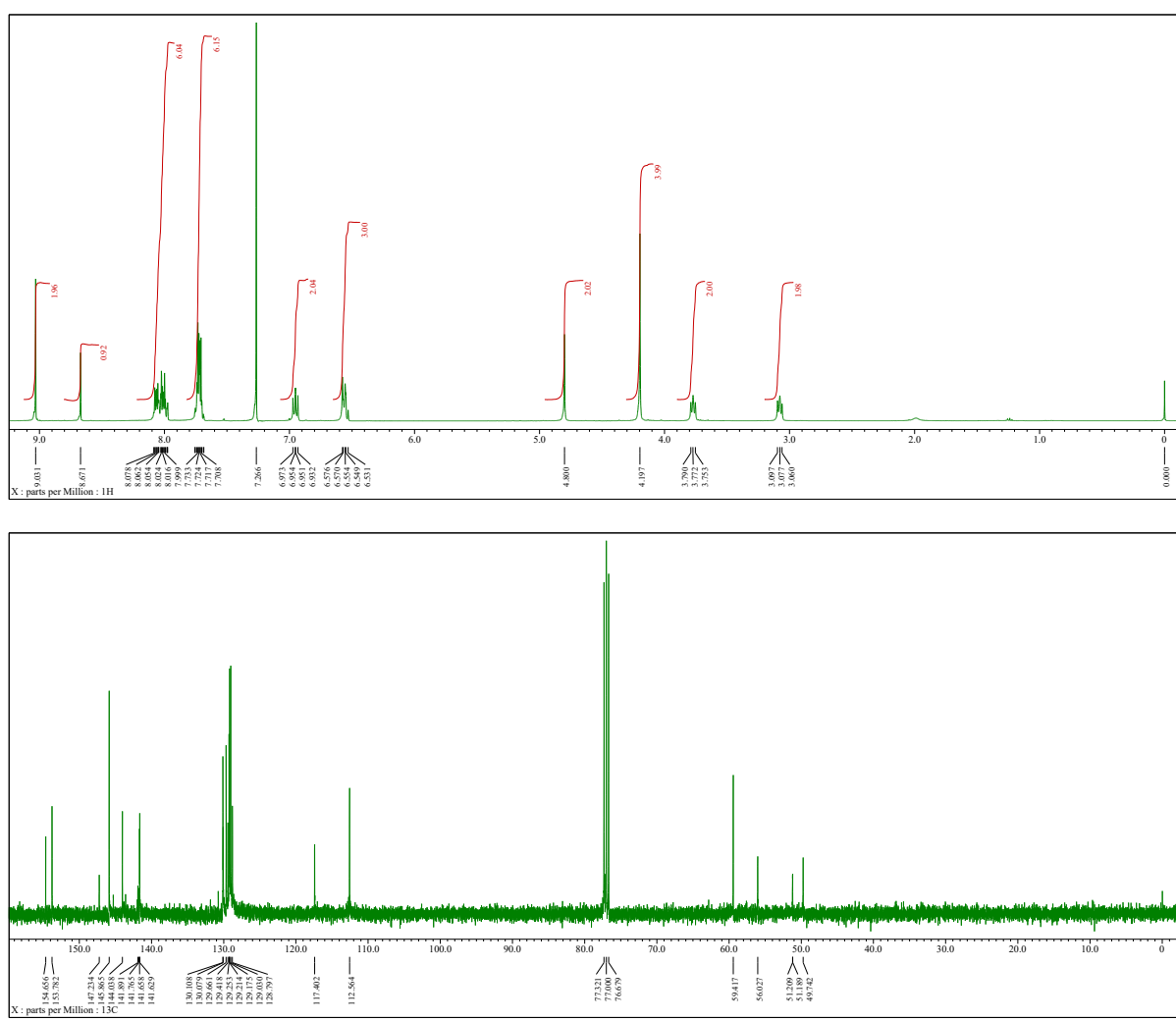
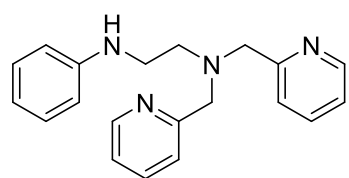


Fig. S20. $^1\text{H}/^{13}\text{C}$ NMR spectrum of Ph-333 in CDCl_3 .



Ph-XXX





N,N-Bis(2-pyridylmethyl)-*N'*-phenylethylenediamine

Ph-PPH

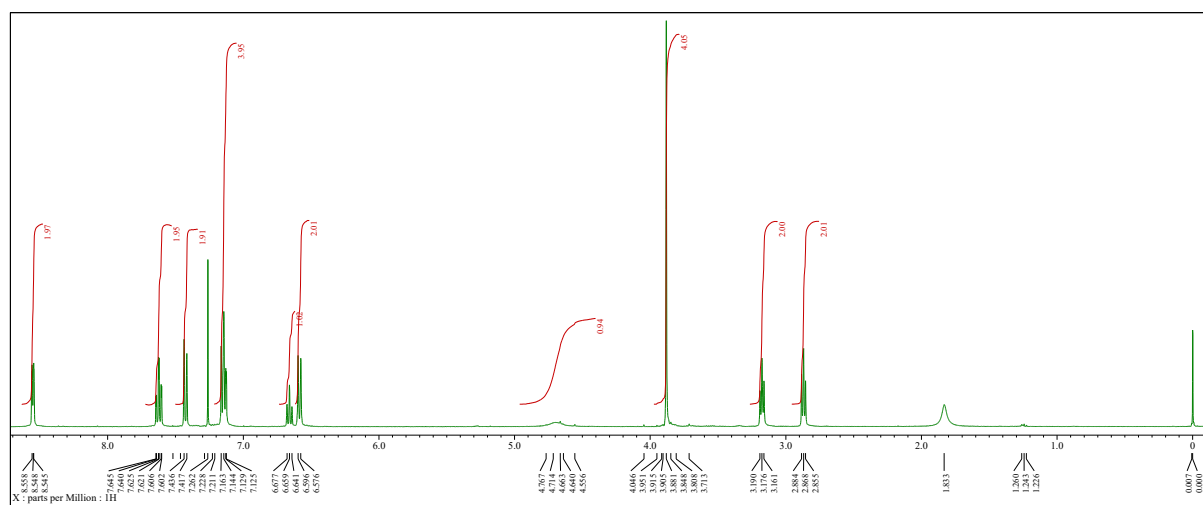
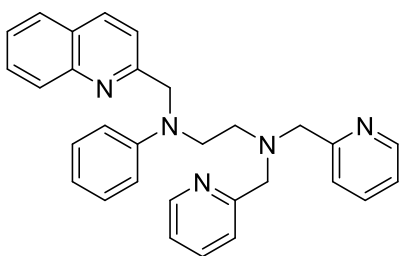
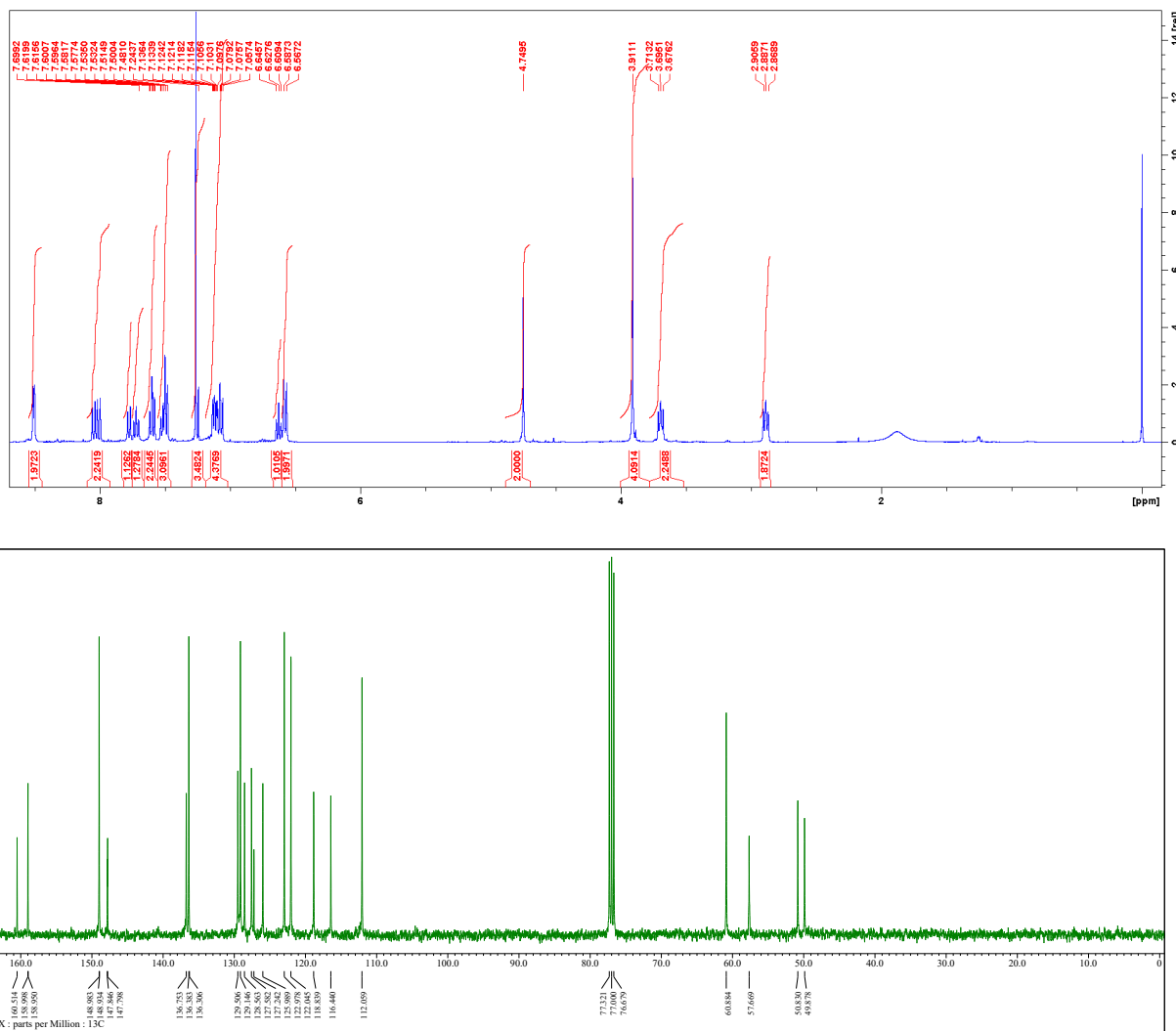
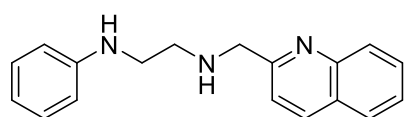


Fig. S22. ^1H NMR spectrum of **Ph-PPH** in CDCl_3 .

**Ph-PPQ****Fig. S23.** ¹H/¹³C NMR spectrum of Ph-PPQ in CDCl₃.



N-(2-quinolylmethyl)-N'-phenylethylenediamine Ph-QHH

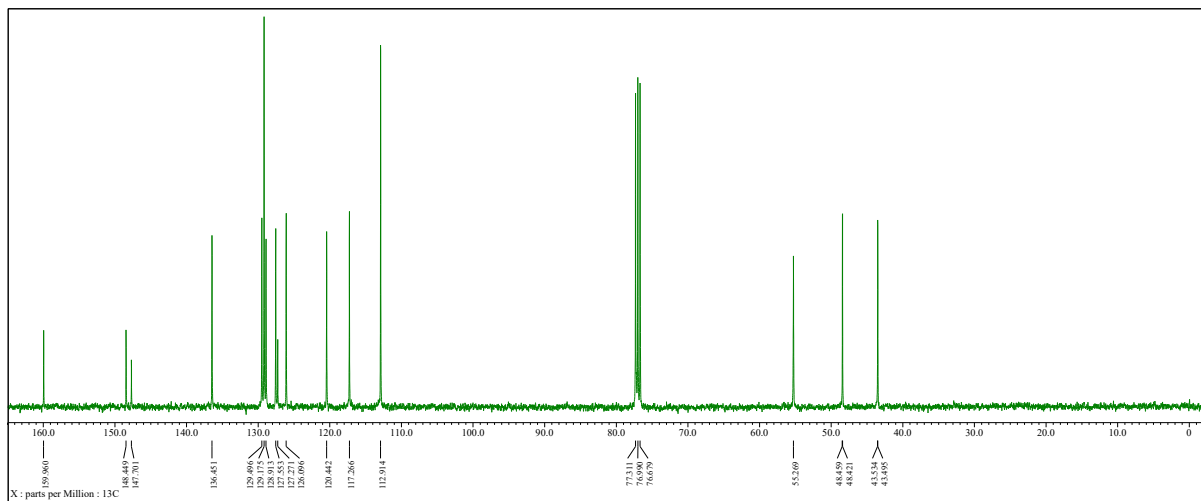
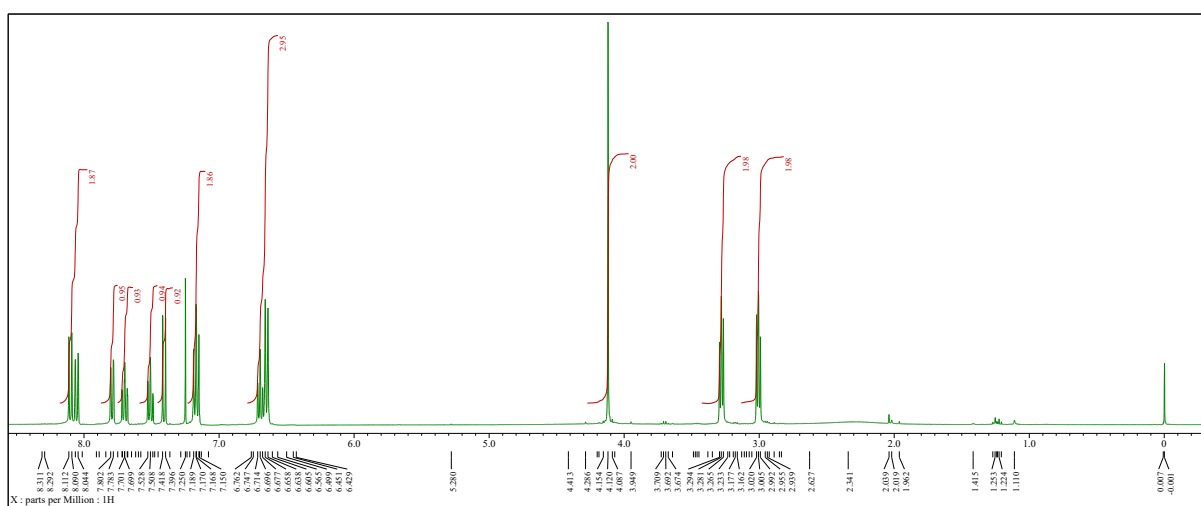
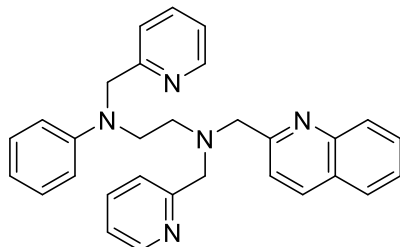
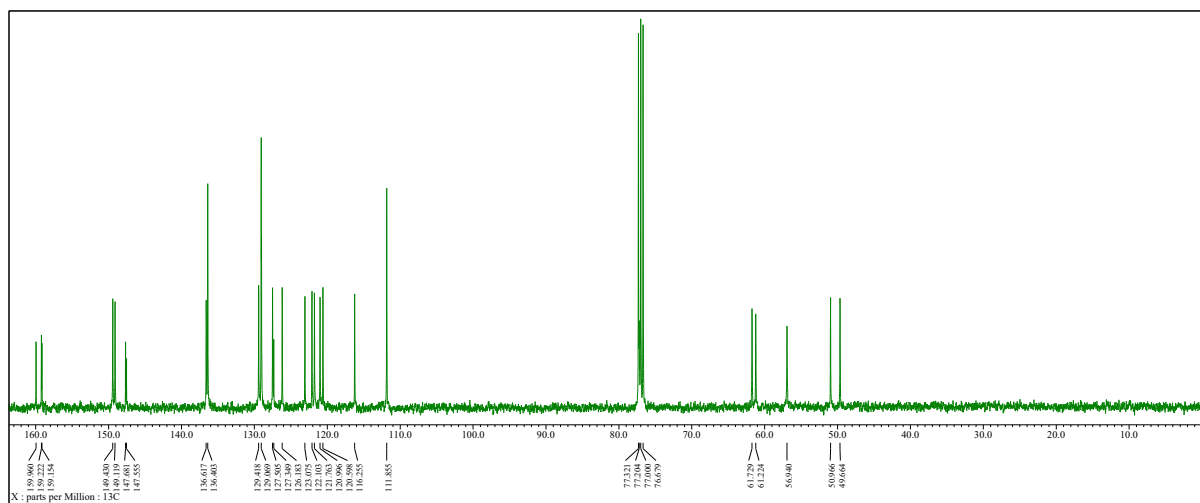
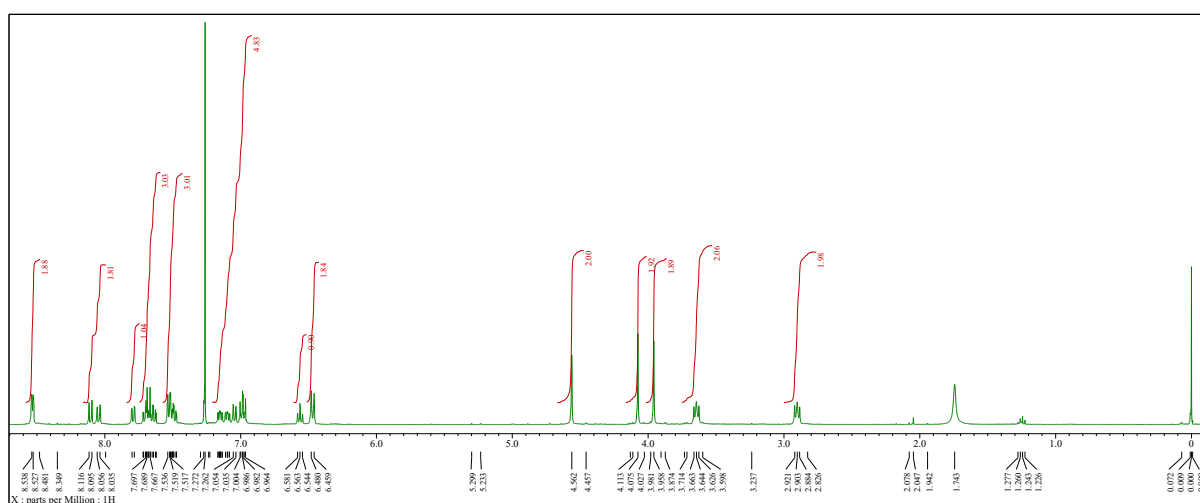
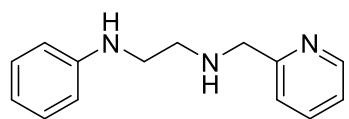


Fig. S24. $^1\text{H}/^{13}\text{C}$ NMR spectrum of Ph-QHH in CDCl_3 .

**Ph-PQP****Fig. S25.** ¹H/¹³C NMR spectrum of Ph-PQP in CDCl₃.



N-(2-pyridylmethyl)-*N'*-phenylethylenediamine

Ph-PHH

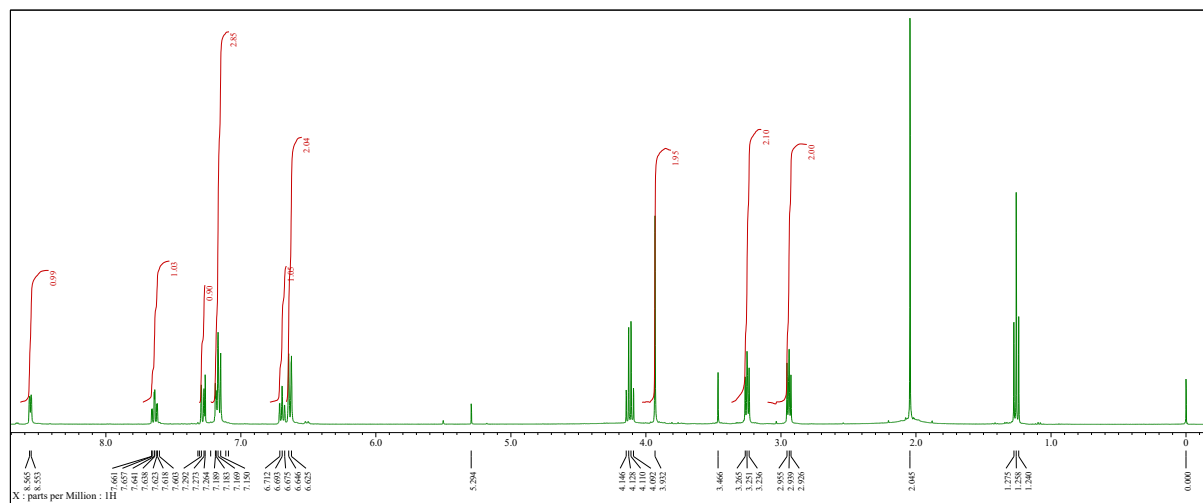
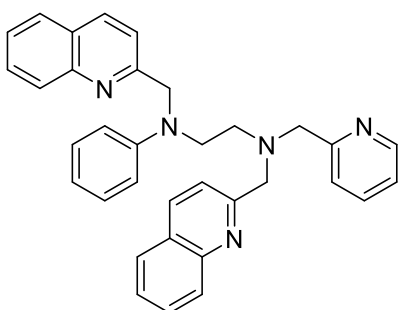


Fig. S26. ^1H NMR spectrum of Ph-PHH in CDCl_3 .



Ph-PQQ

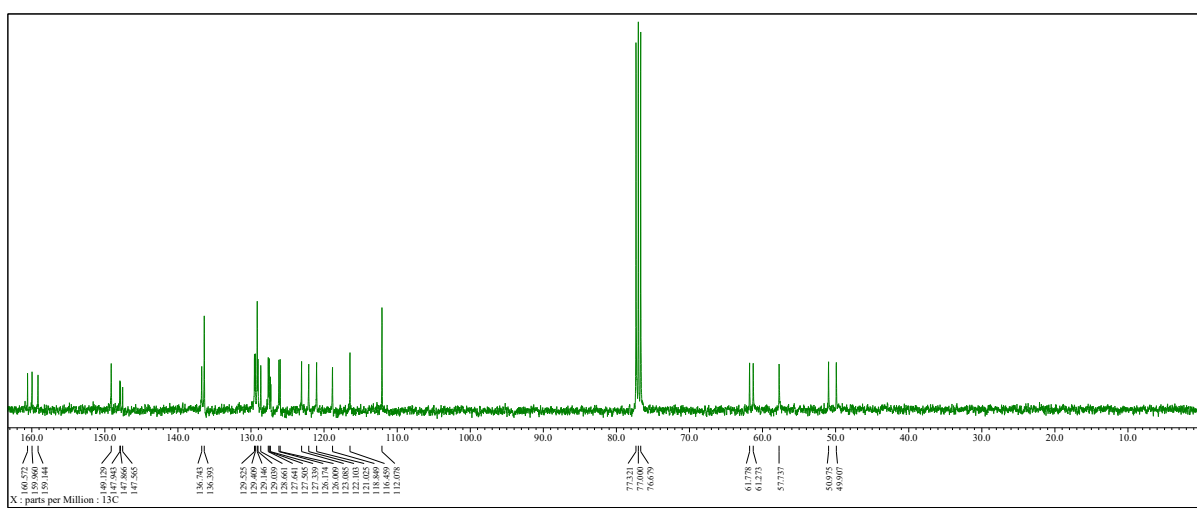
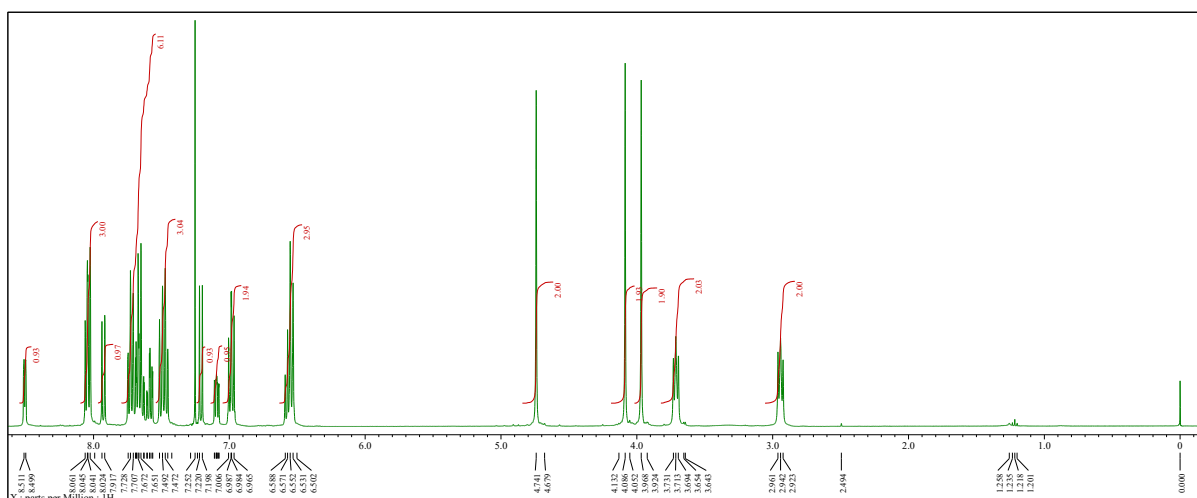
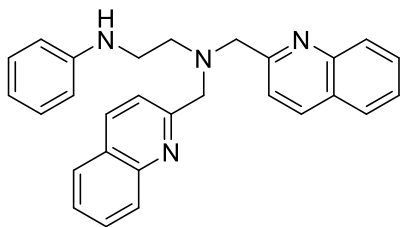


Fig. S27. $^1\text{H}/^{13}\text{C}$ NMR spectrum of Ph-PQQ in CDCl_3 .



N,N-Bis(2-quinolylmethyl)-*N'*-phenylethylenediamine

Ph-QQH

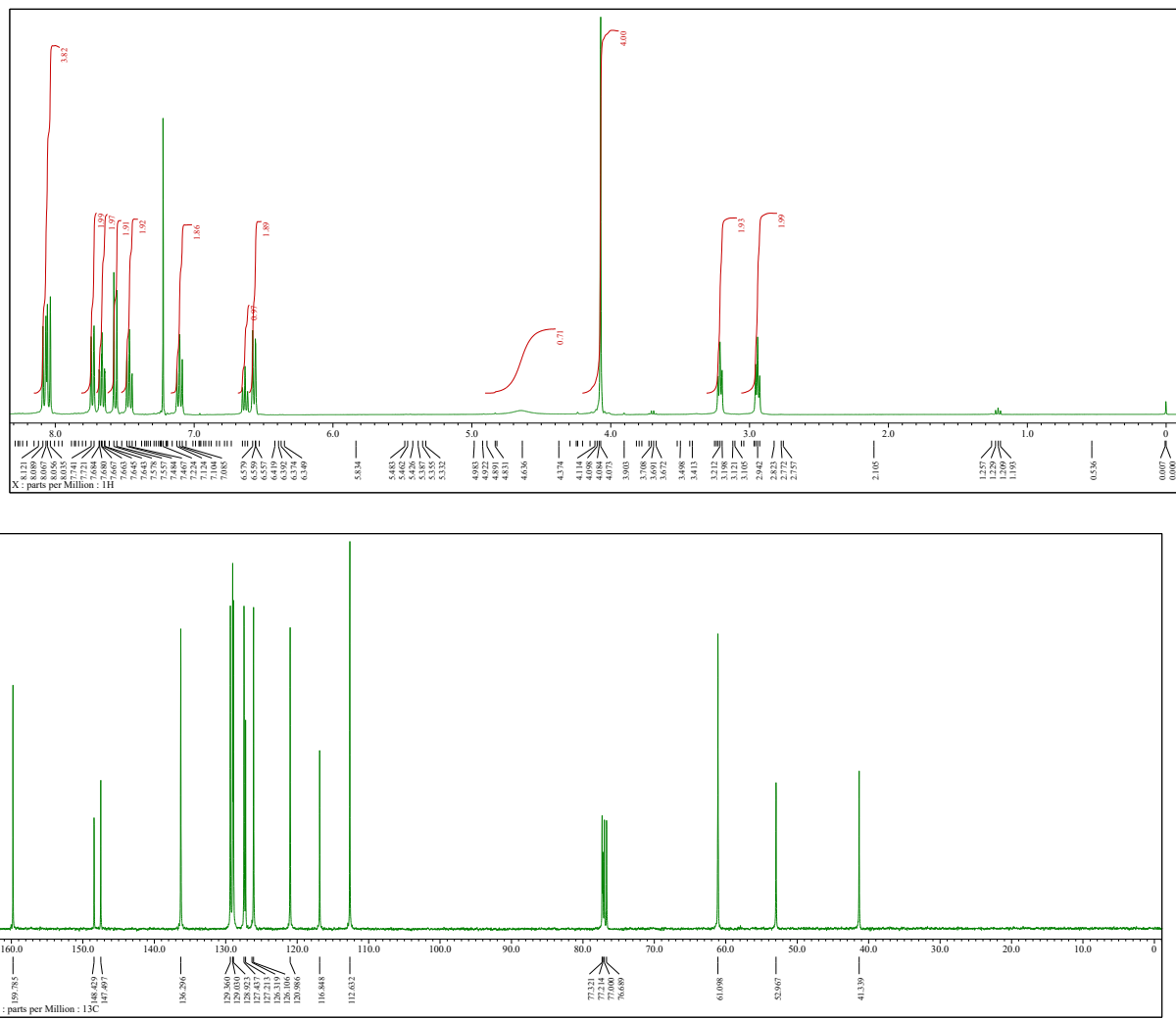
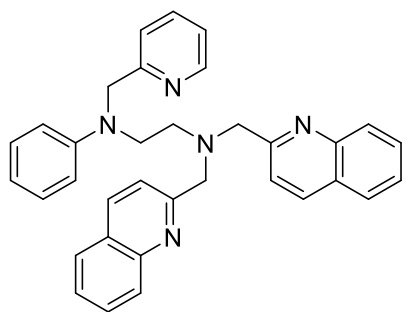
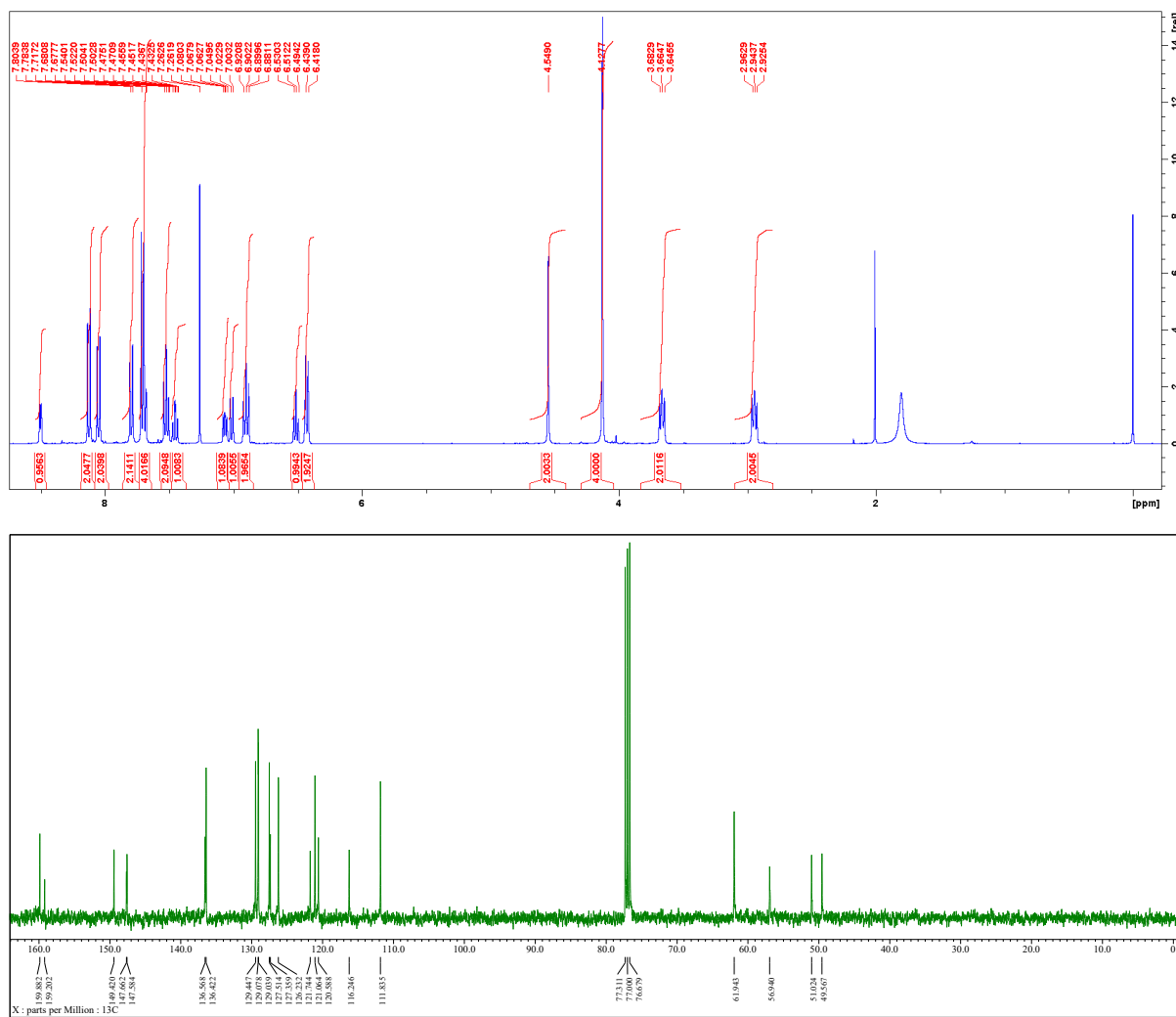
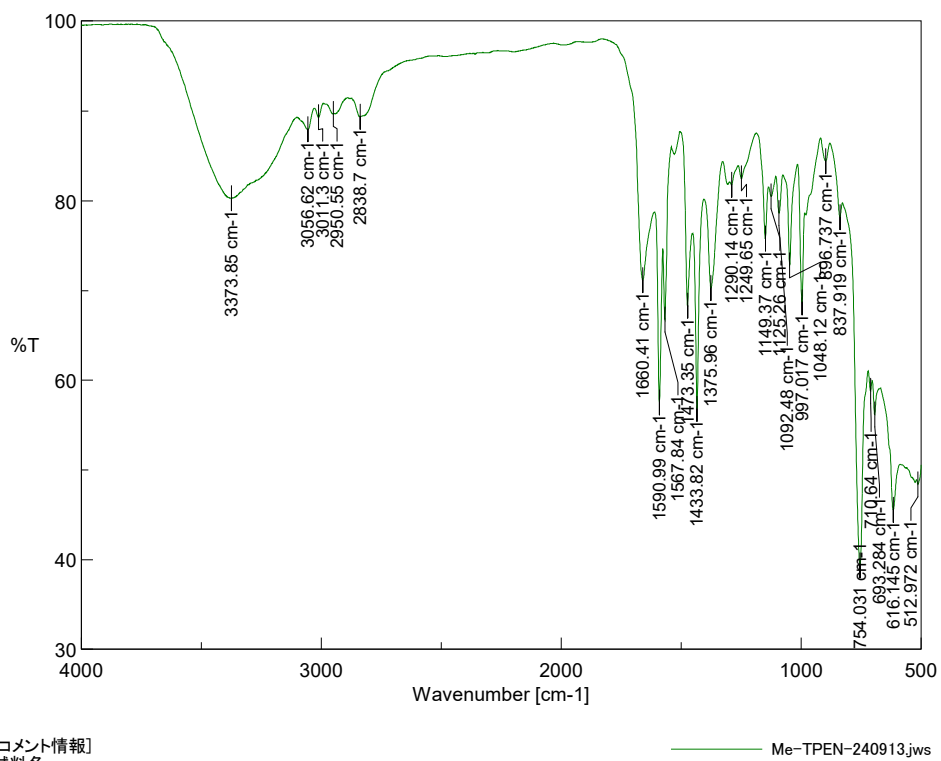
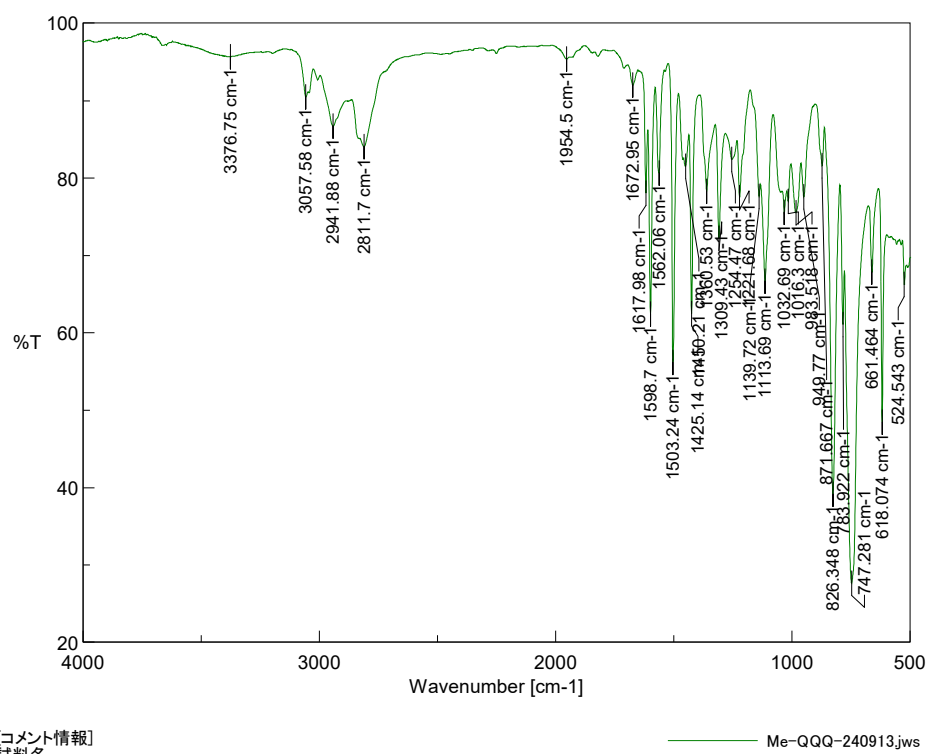


Fig. S28. $^1\text{H}/^{13}\text{C}$ NMR spectrum of Ph-QQH in CDCl_3 .

**Ph-QQP****Fig. S29.** IR spectrum of Ph-QQP in CDCl_3 .

IR spectrum**Fig. S30.** IR spectrum of Me-PPP.**Fig. S31.** IR spectrum of Me-QQQ.

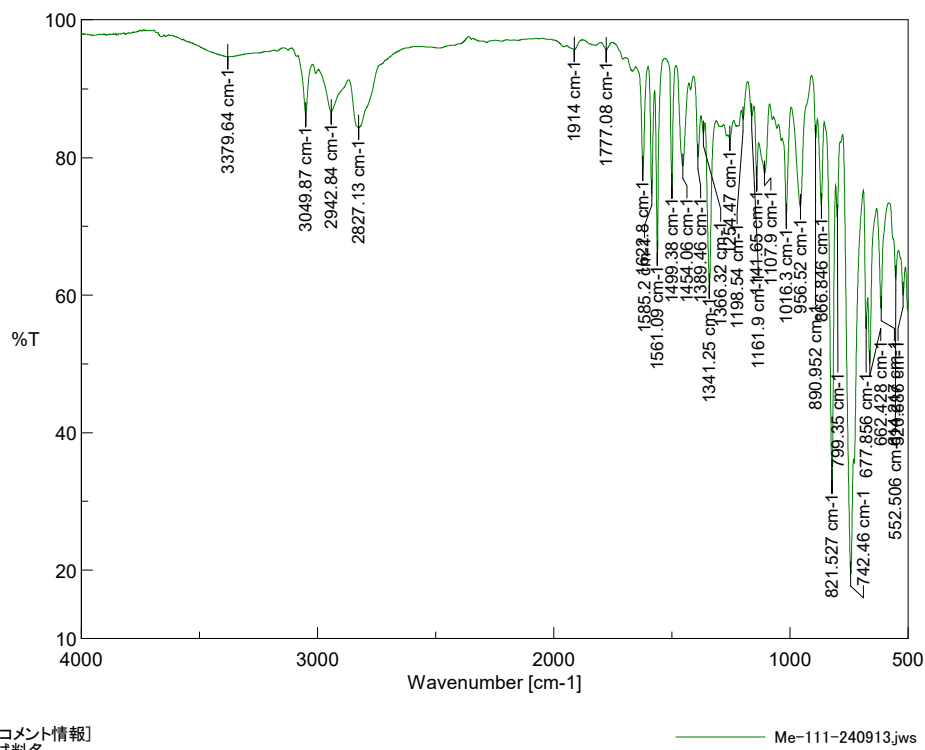


Fig. S32. IR spectrum of Me-111.

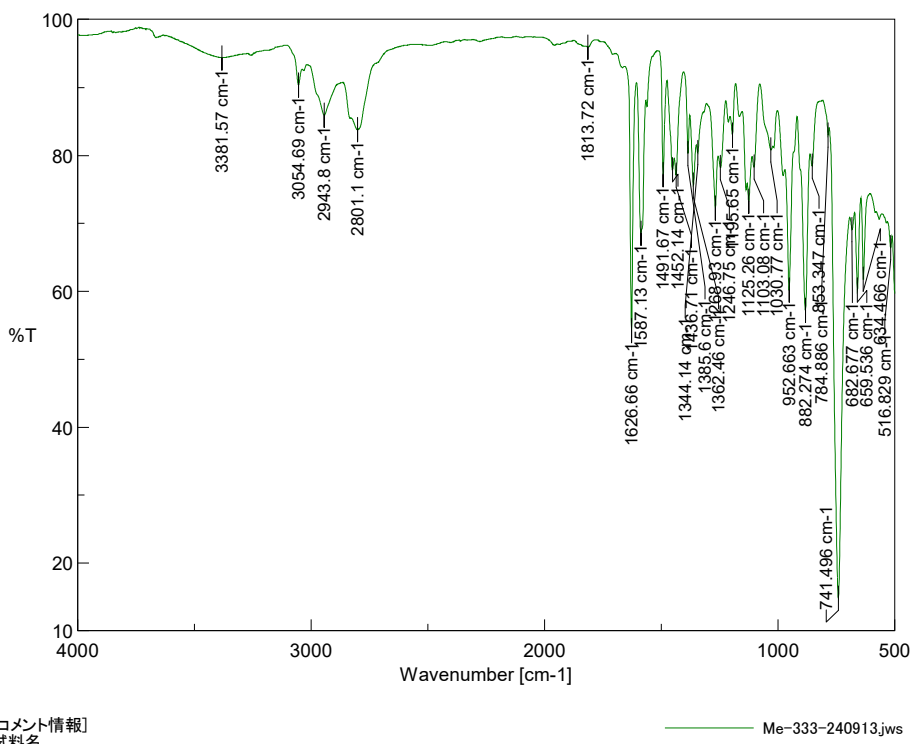


Fig. S33. IR spectrum of Me-333.

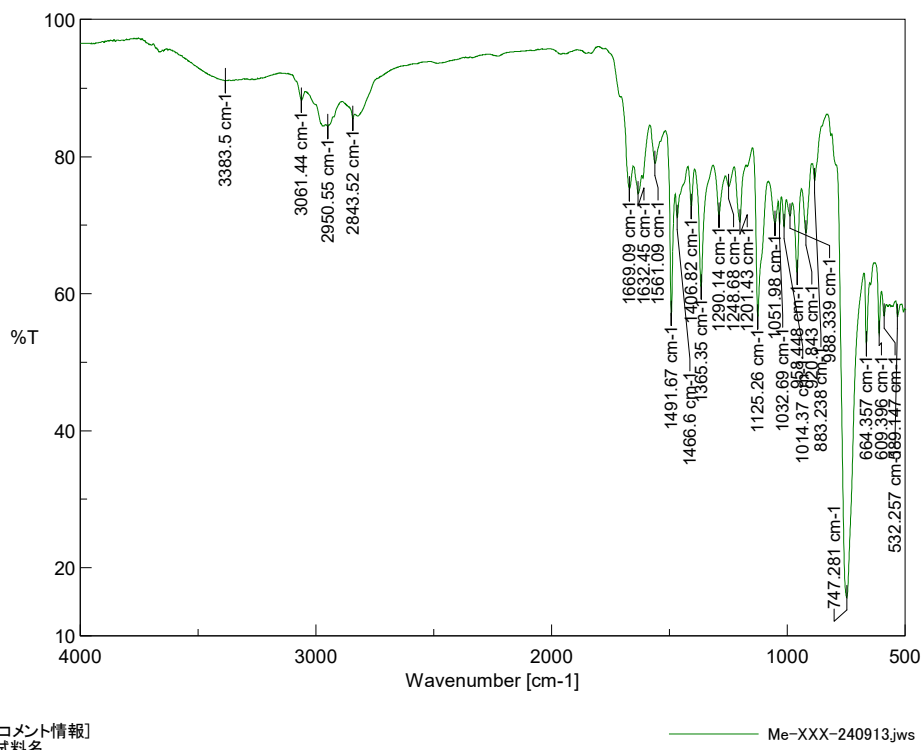


Fig. S34. IR spectrum of Me-XXX.

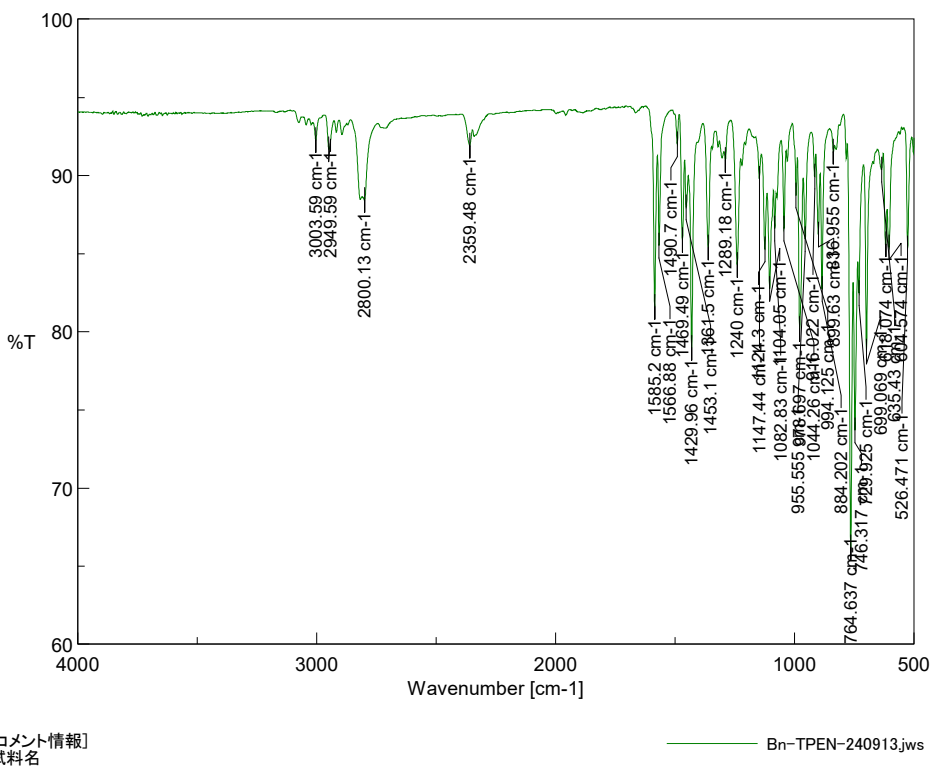


Fig. S35. IR spectrum of Bn-PPP.

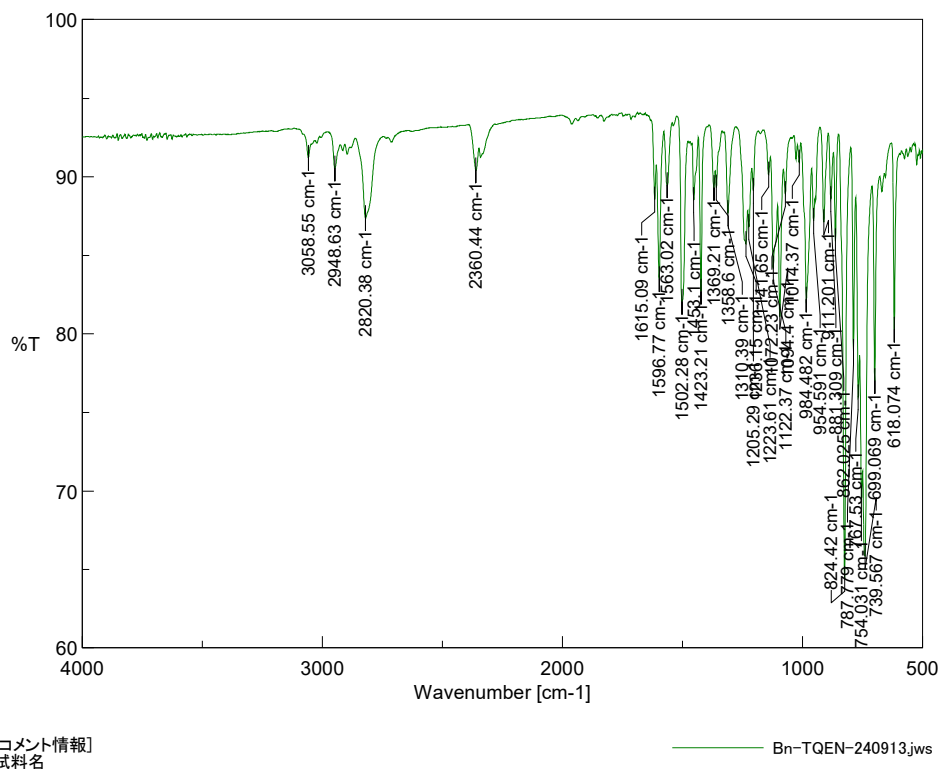


Fig. S36. IR spectrum of Bn-QQQ.

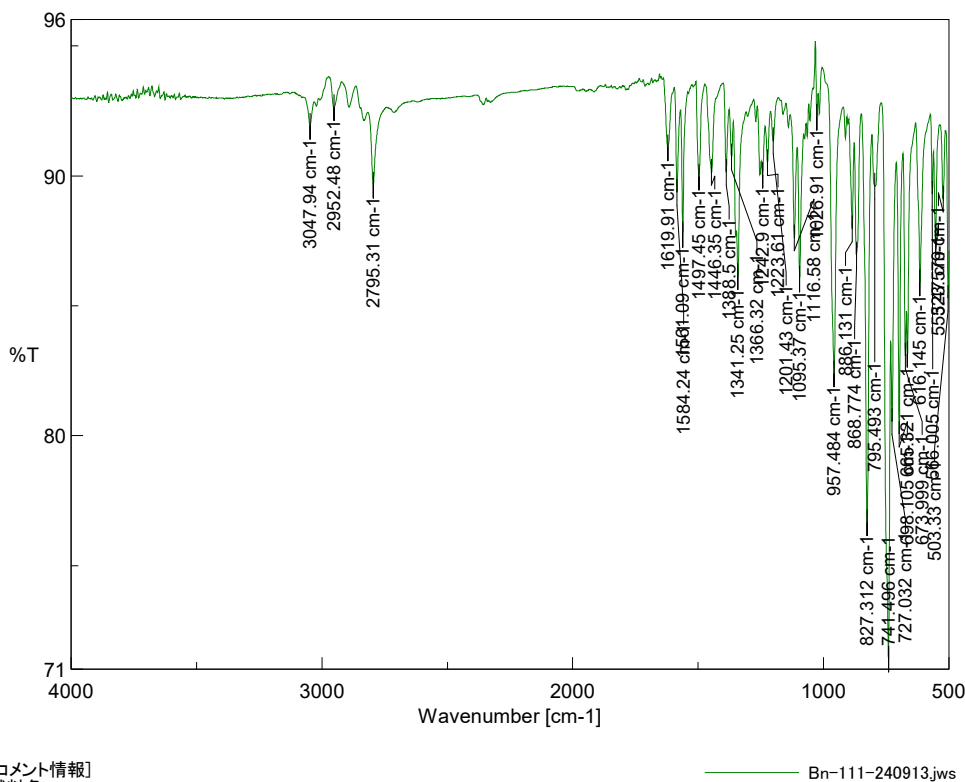


Fig. S37. IR spectrum of Bn-111.

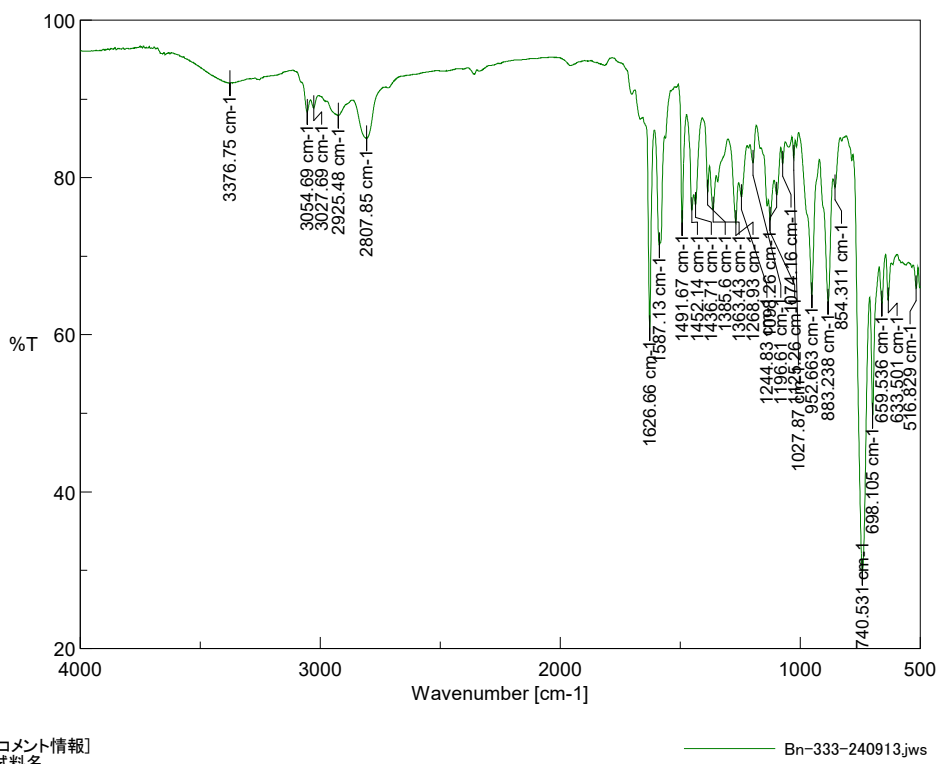


Fig. S38. IR spectrum of Bn-333.

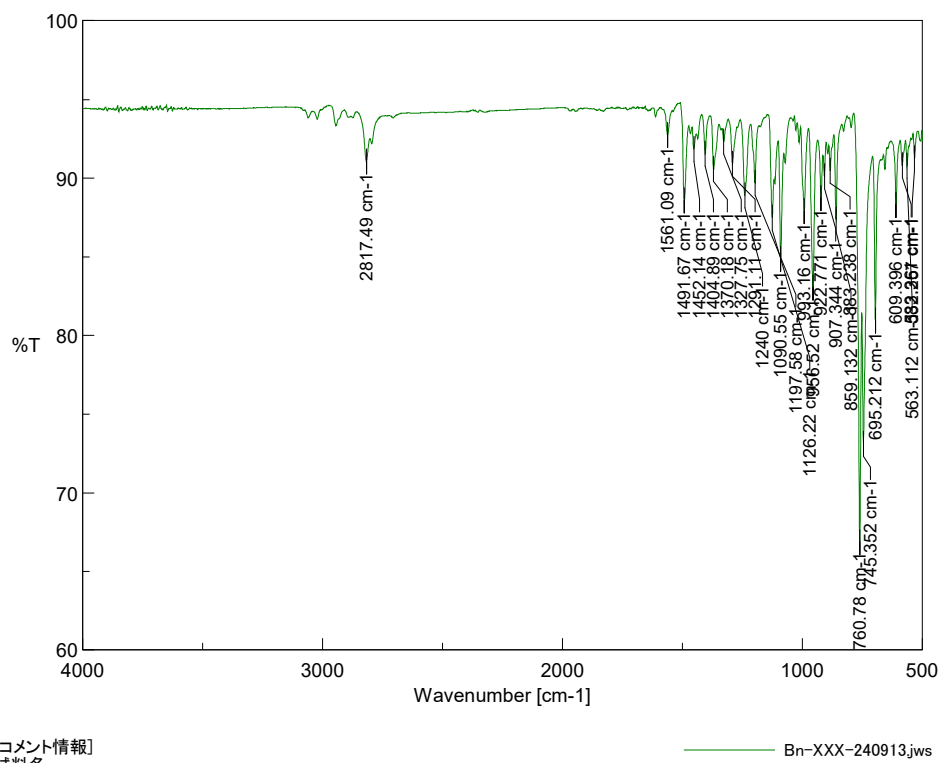


Fig. S39. IR spectrum of Bn-XXX.

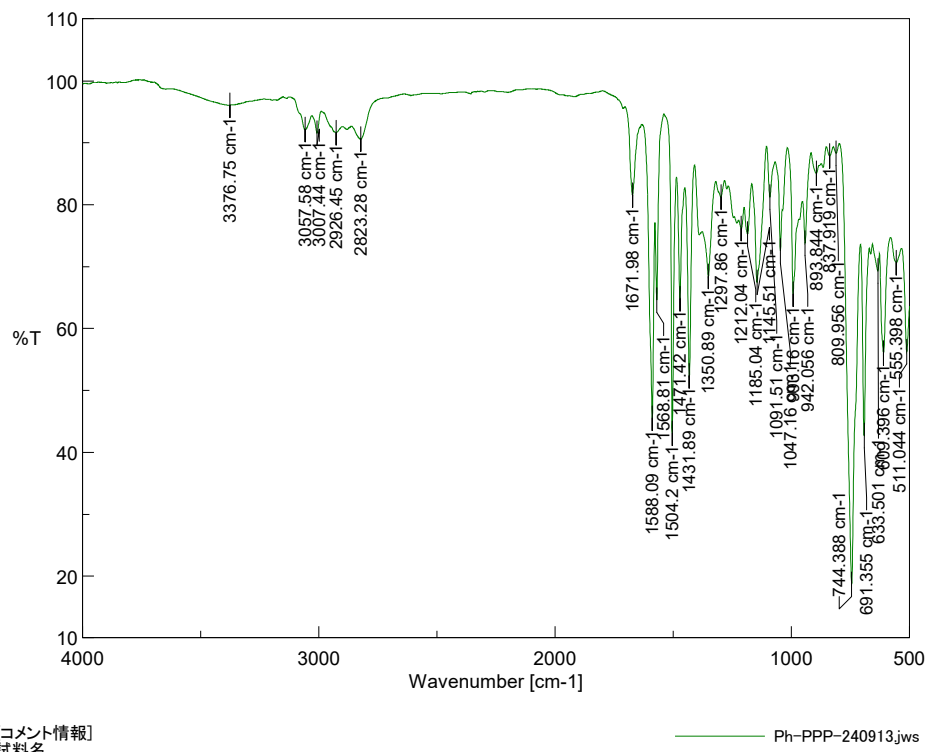


Fig. S40. IR spectrum of Ph-PPP.

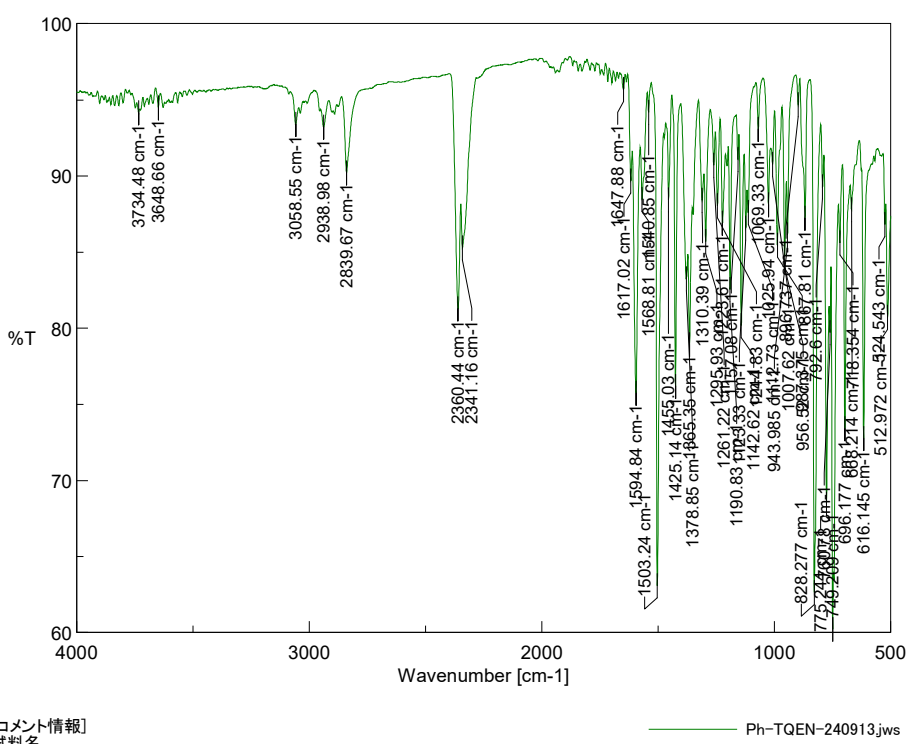


Fig. S41. IR spectrum of Ph-QQQ.

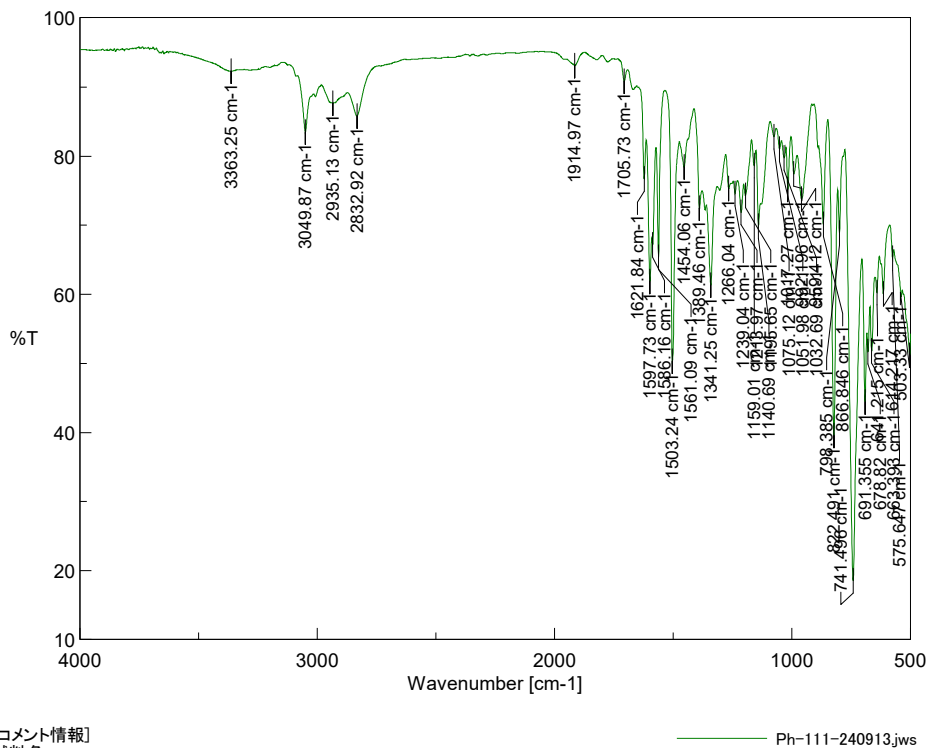


Fig. S42. IR spectrum of Ph-111.

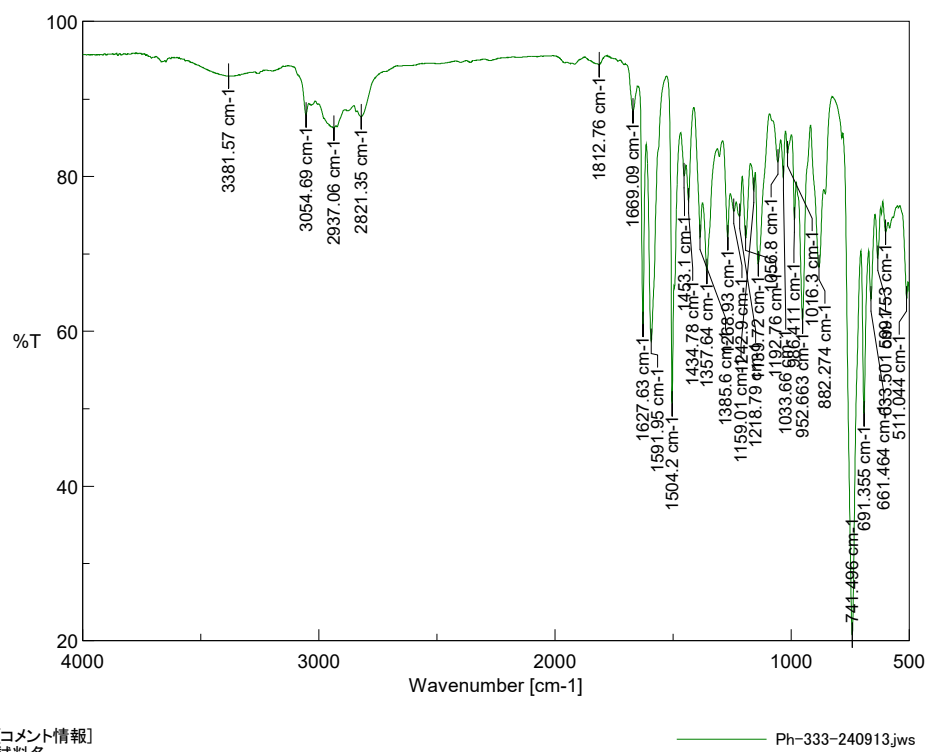


Fig. S43. IR spectrum of Ph-333.

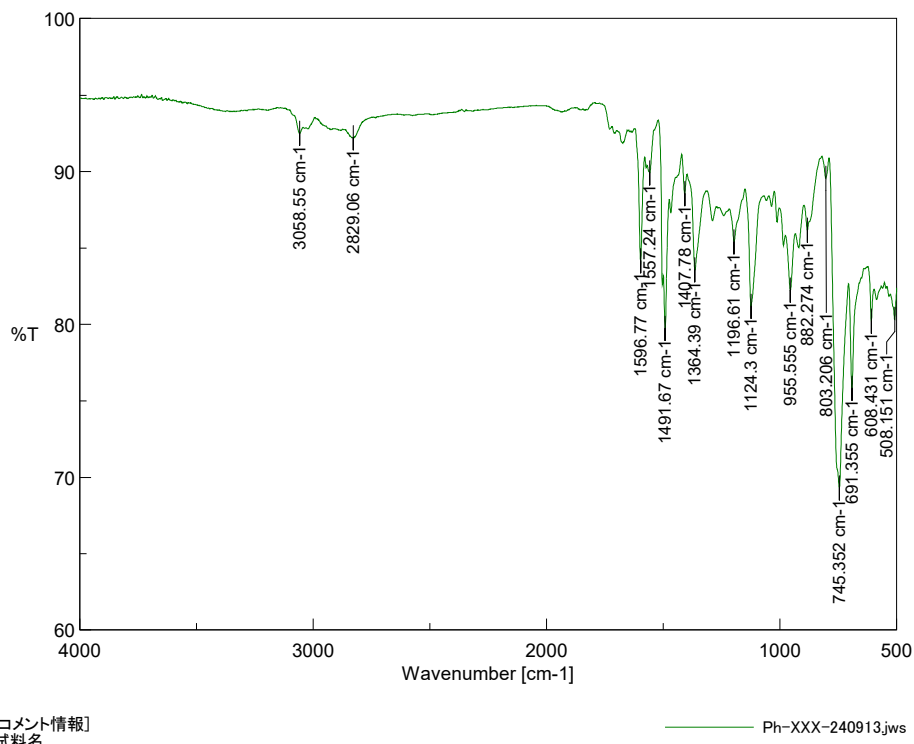


Fig. S44. IR spectrum of Ph-XXX.

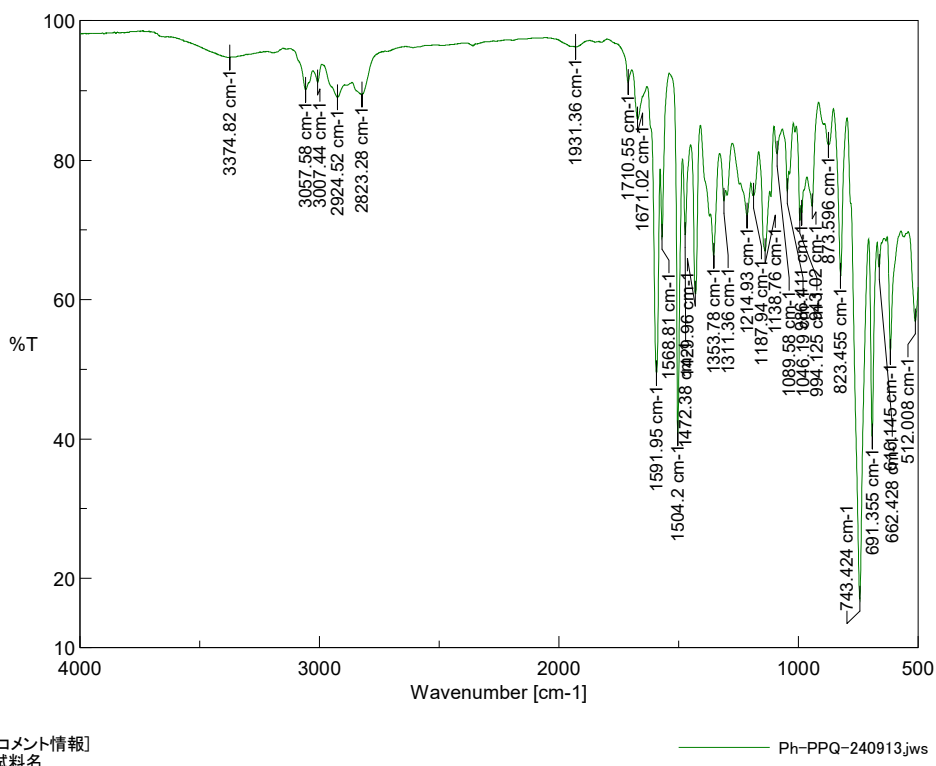


Fig. S45. IR spectrum of Ph-PPQ.

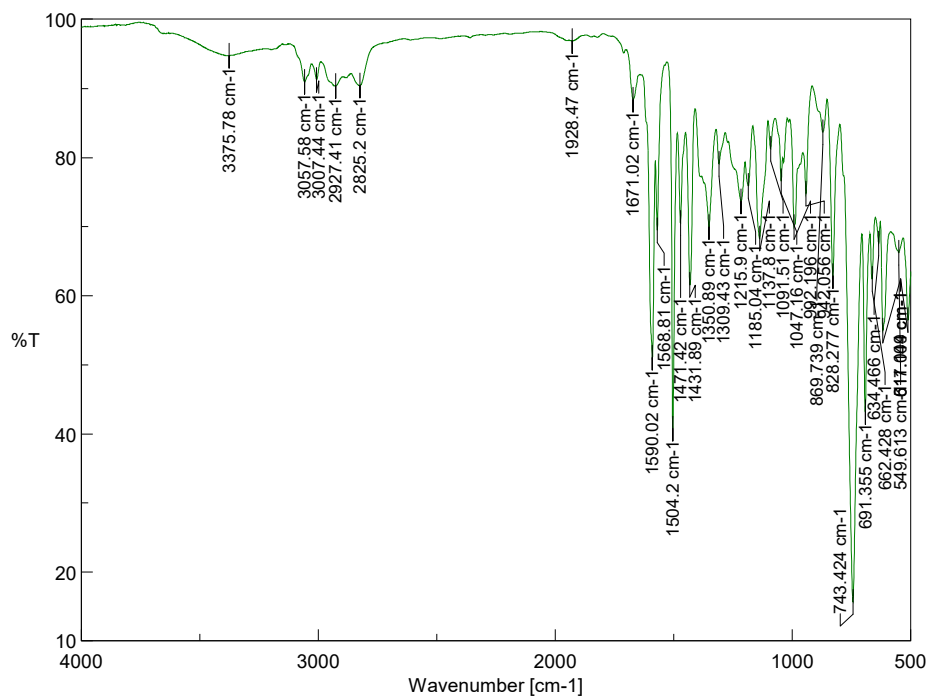


Fig. S46. IR spectrum of Ph-PQP.

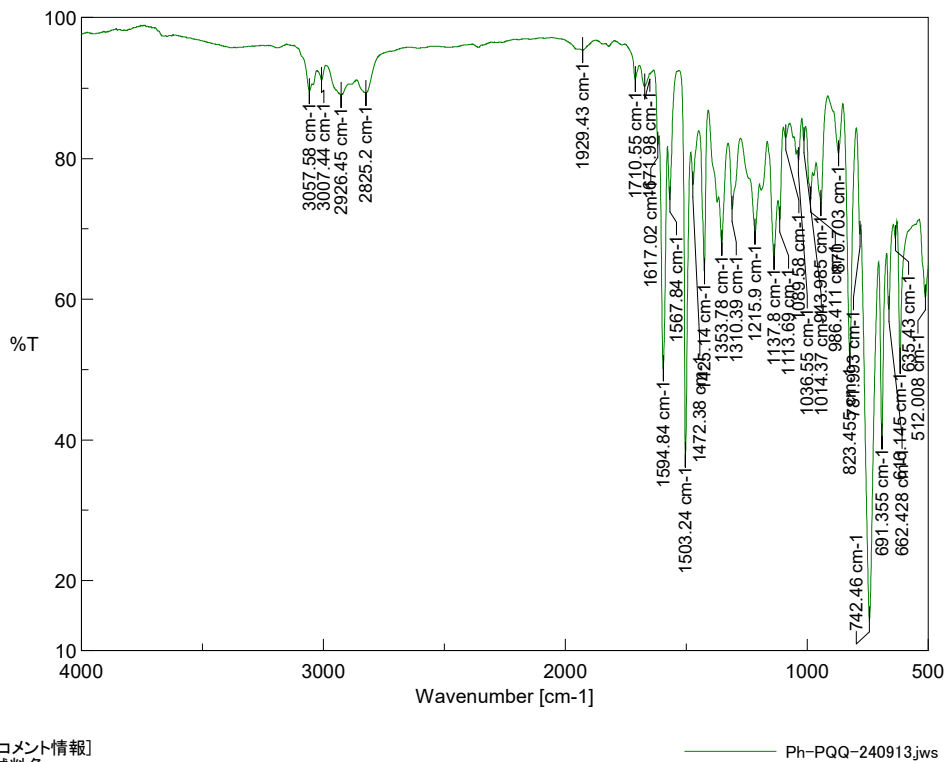


Fig. S47. IR spectrum of Ph-PQQ.

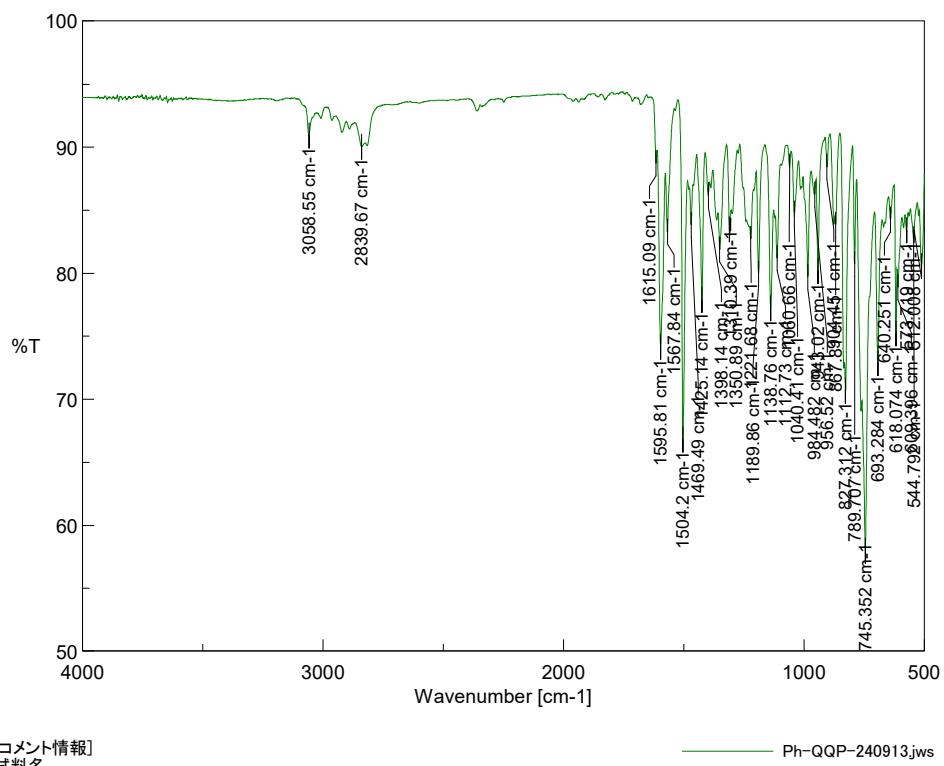


Fig. S48. IR spectrum of Ph-QQP.

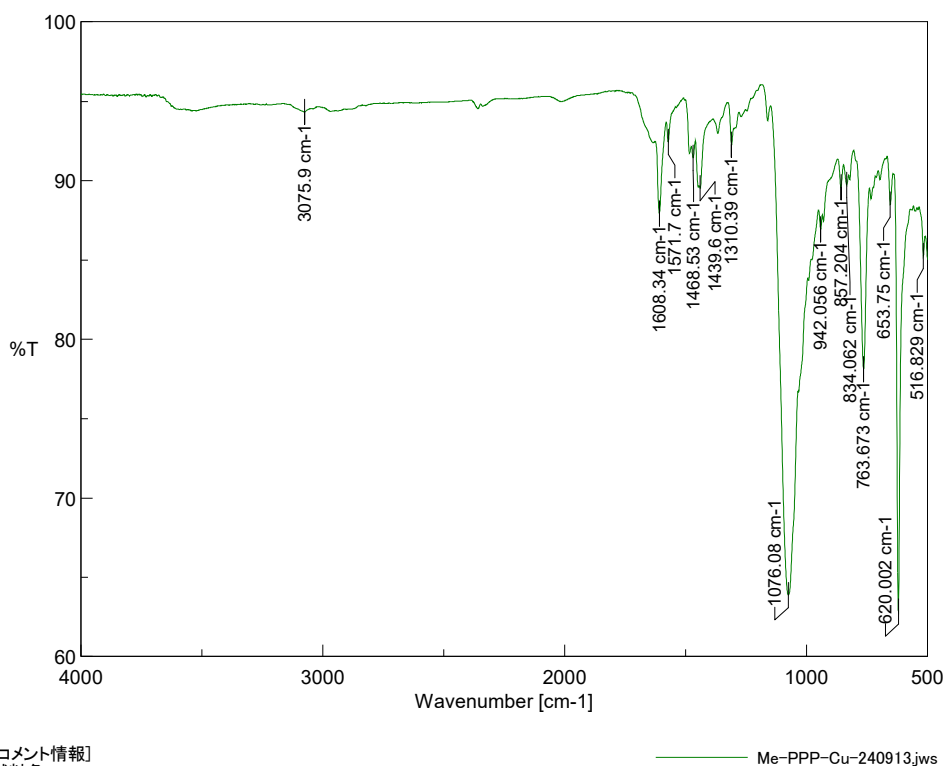


Fig. S49. IR spectrum of Me-PPP-Cu.

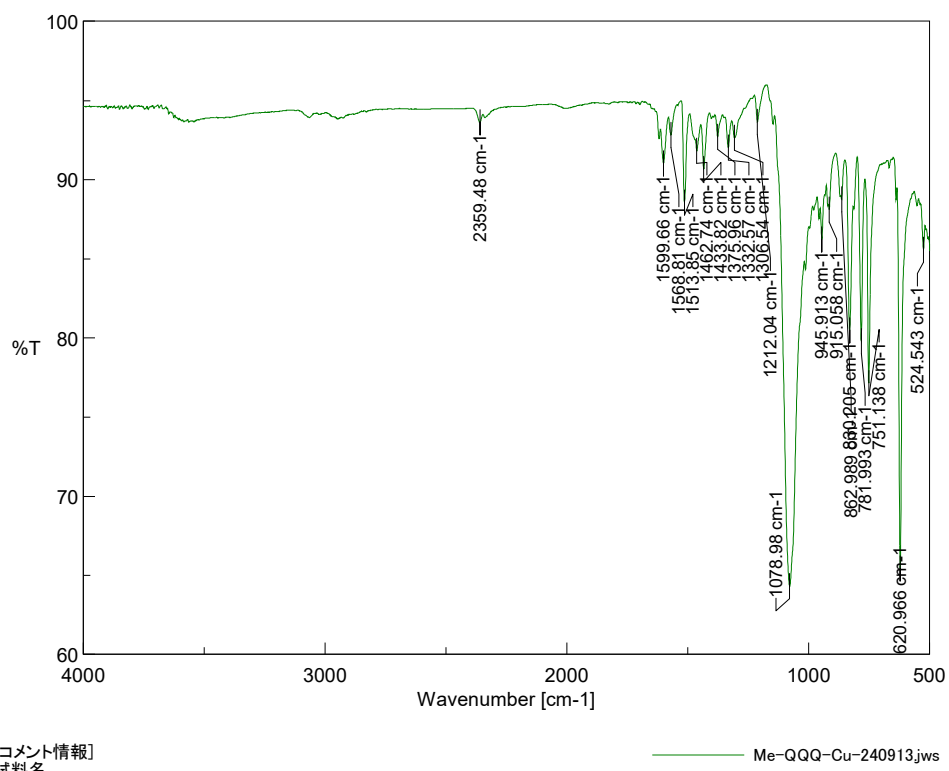


Fig. S50. IR spectrum of Me-QQQ-Cu.

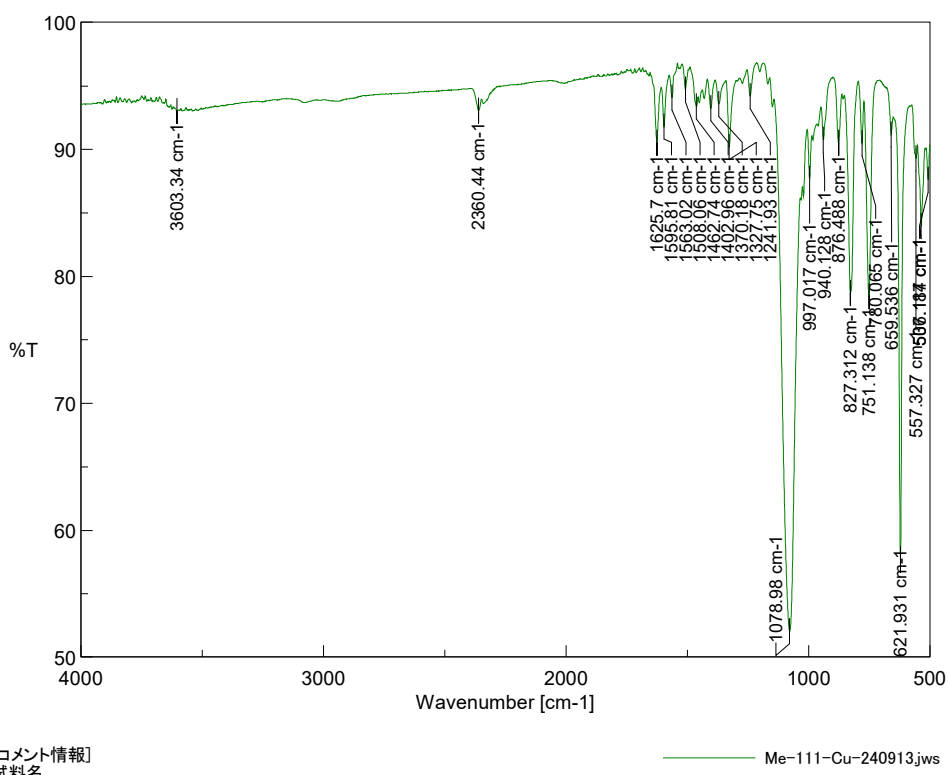
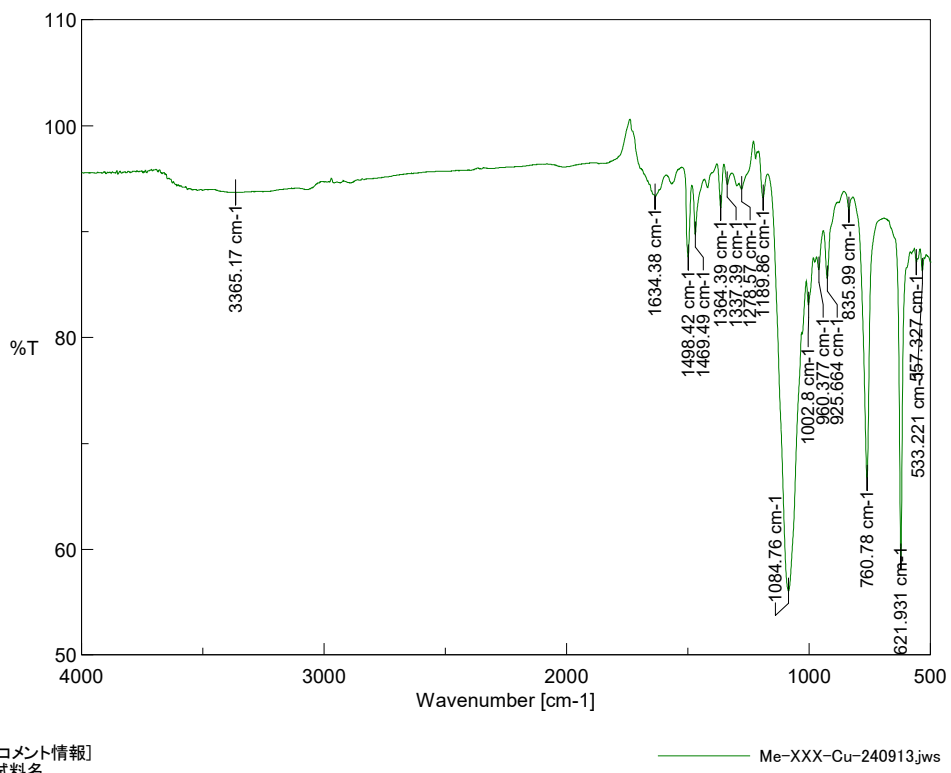
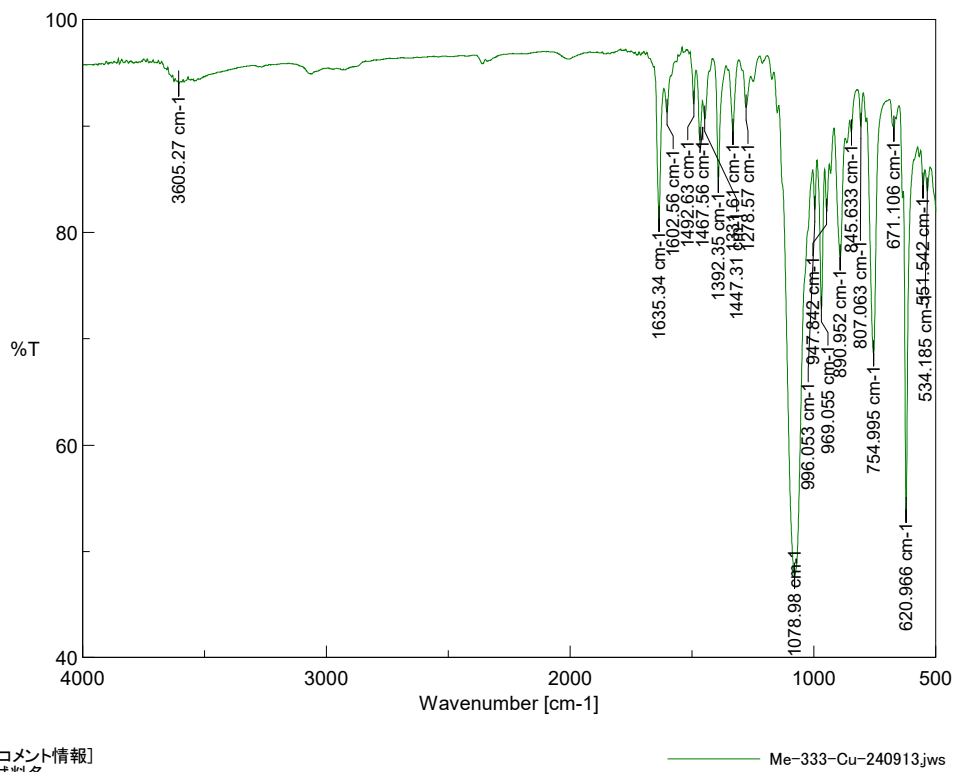


Fig. S51. IR spectrum of Me-111-Cu.



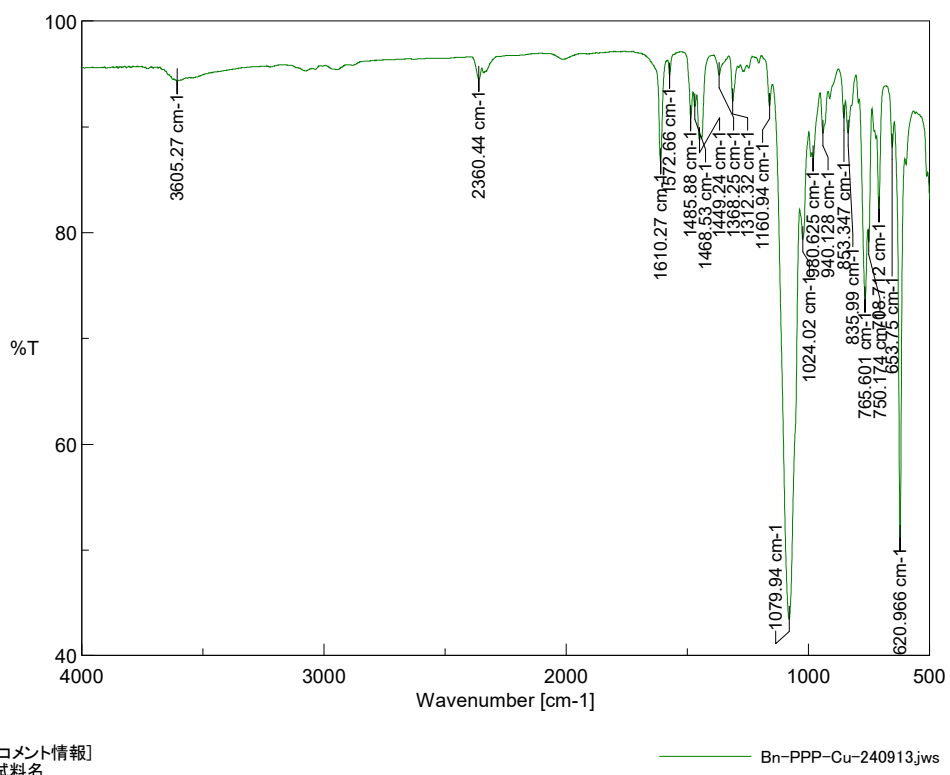


Fig. S54. IR spectrum of Bn-PPP-Cu.

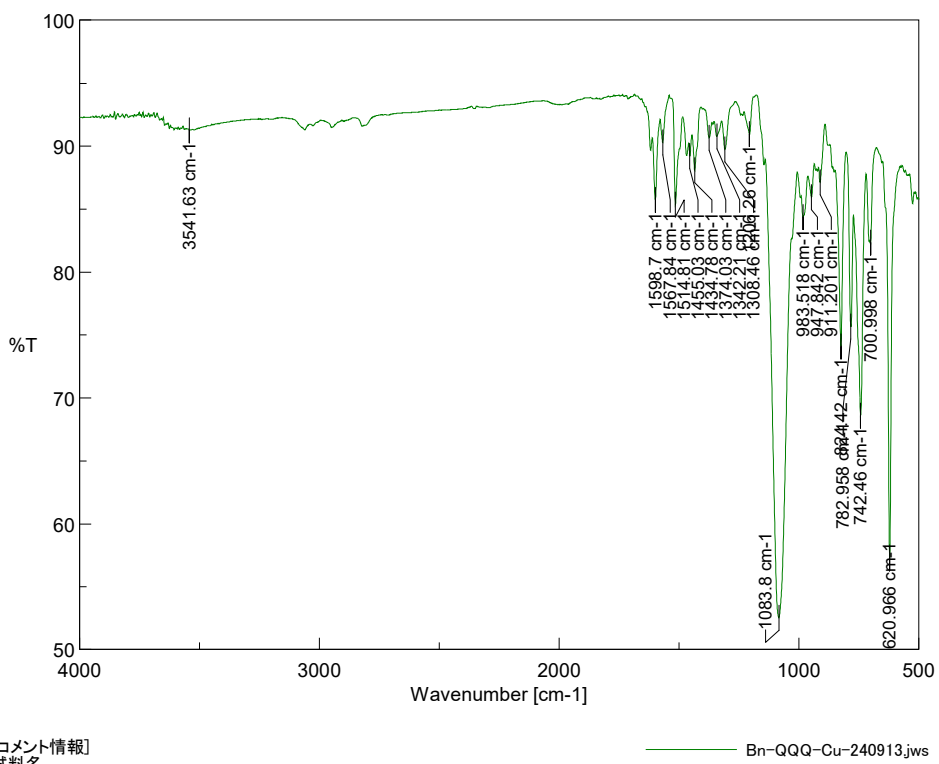


Fig. S55. IR spectrum of Bn-QQQ-Cu.

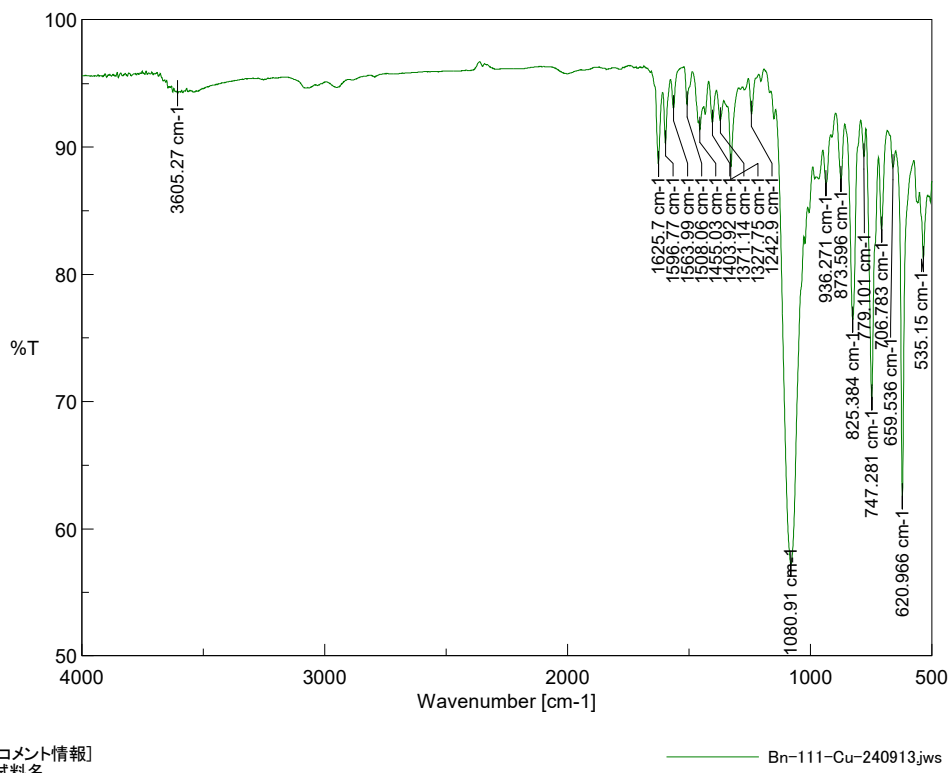


Fig. S56. IR spectrum of Bn-111-Cu.

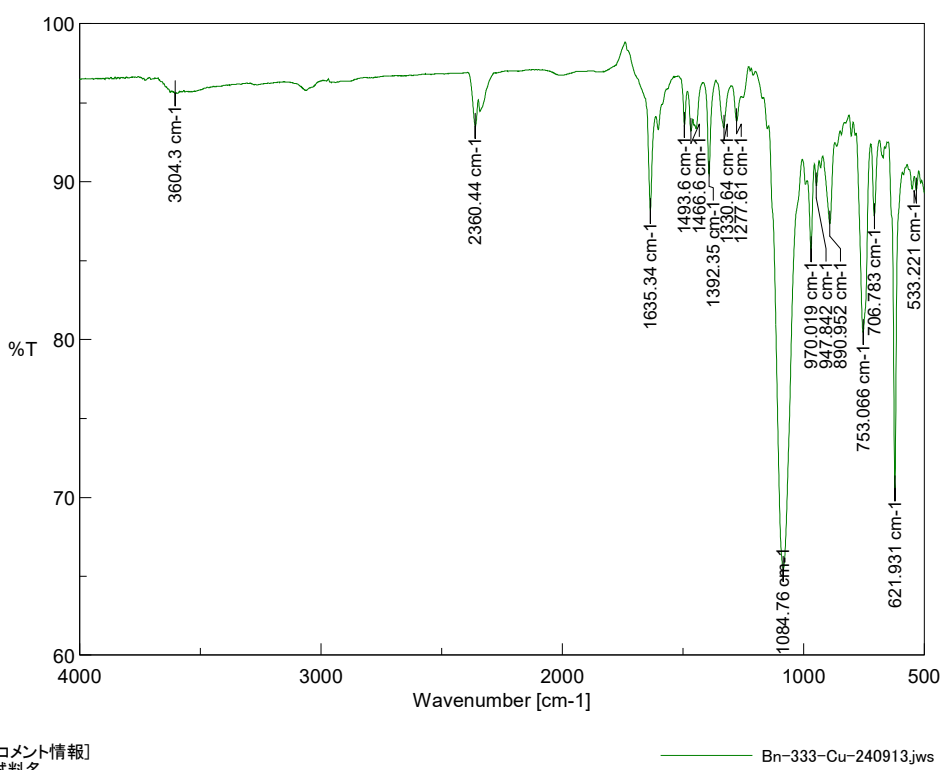


Fig. S57. IR spectrum of Bn-333-Cu.

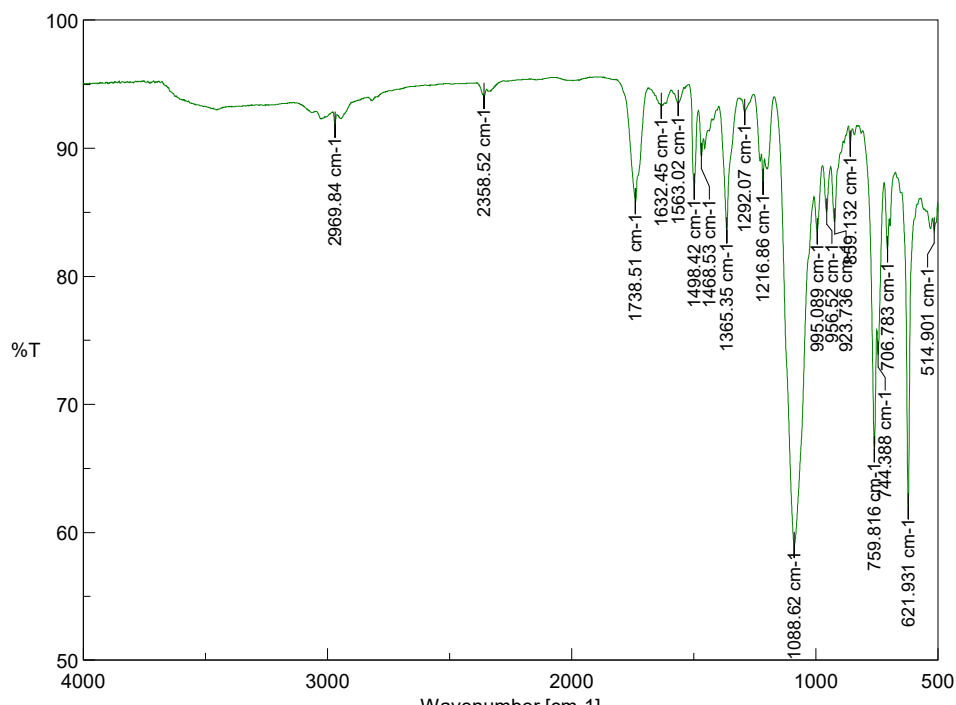


Fig. S58. IR spectrum of Bn-XXX-Cu.

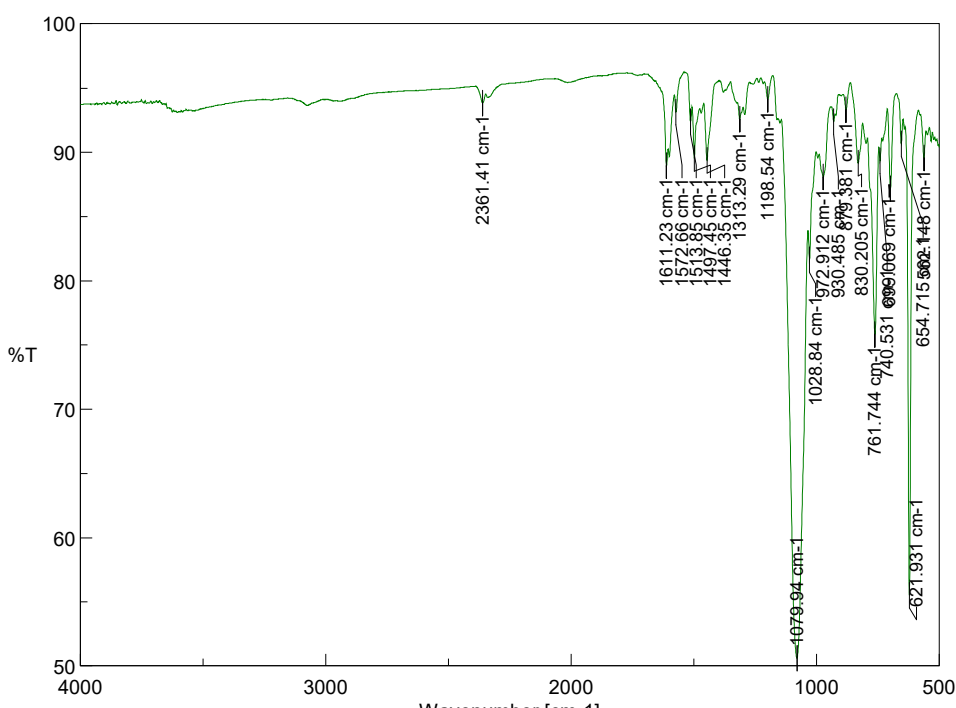


Fig. S59. IR spectrum of Ph-PPP-Cu.

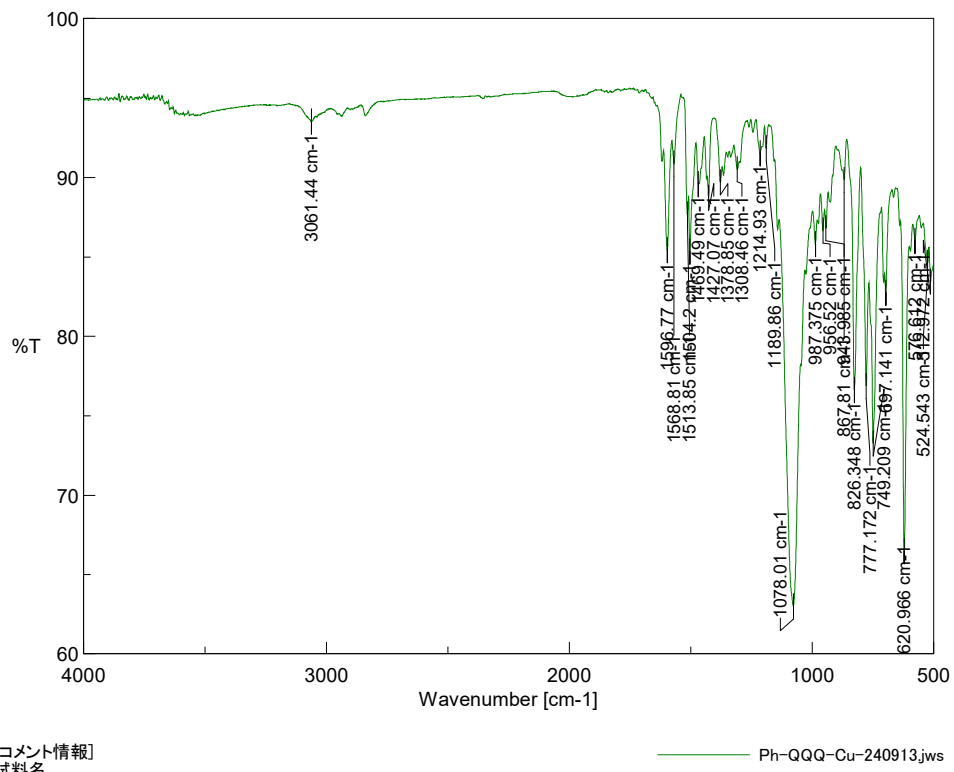


Fig. S60. IR spectrum of Ph-QQQ-Cu.

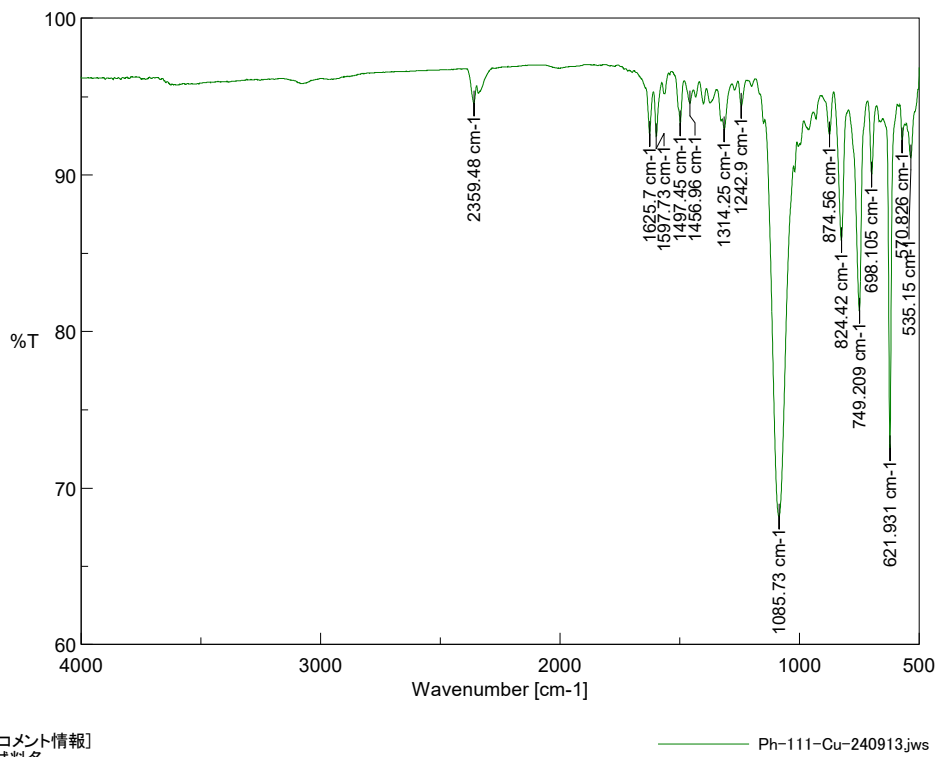


Fig. S61. IR spectrum of Ph-111-Cu.

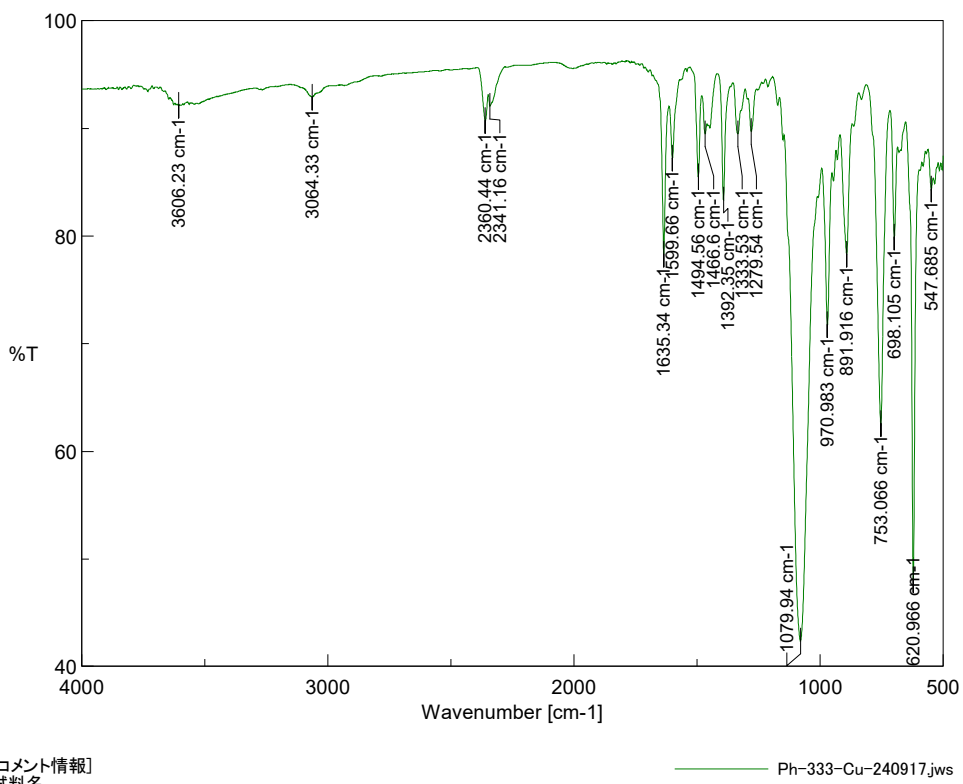


Fig. S62. IR spectrum of Ph-333-Cu.

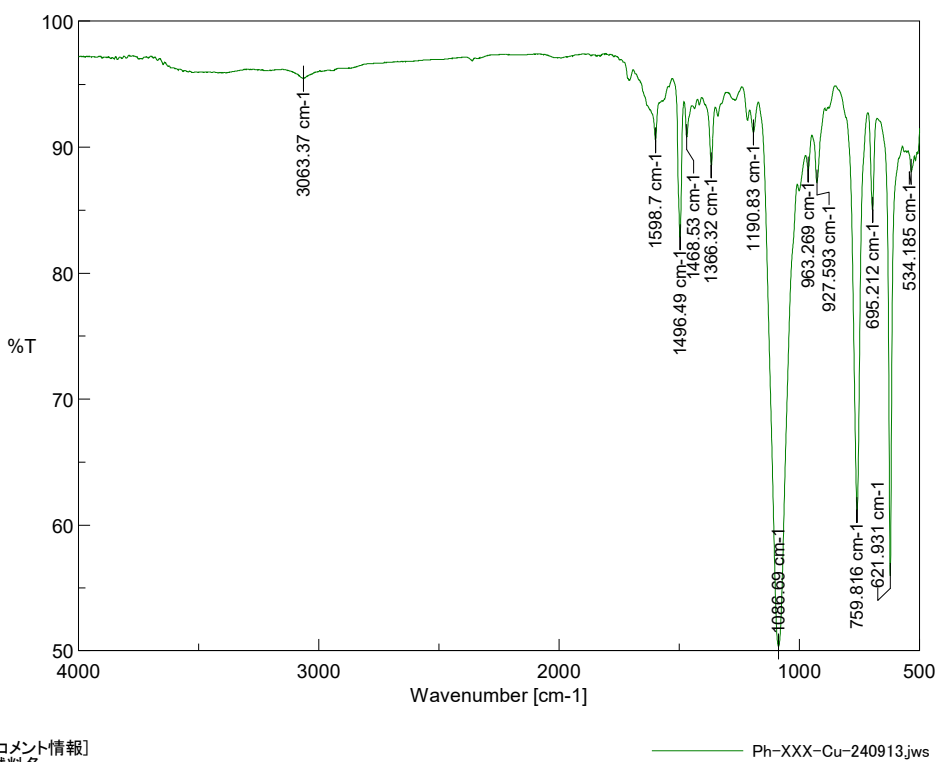


Fig. S63. IR spectrum of Ph-XXX-Cu.

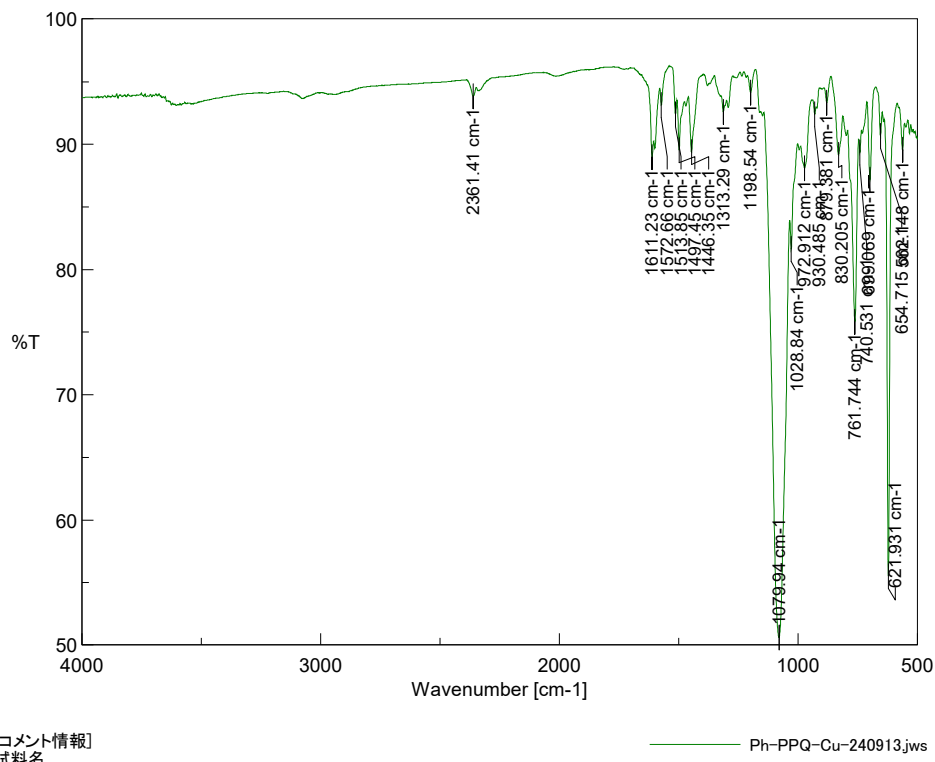


Fig. S64. IR spectrum of **Ph-PPQ-Cu**.

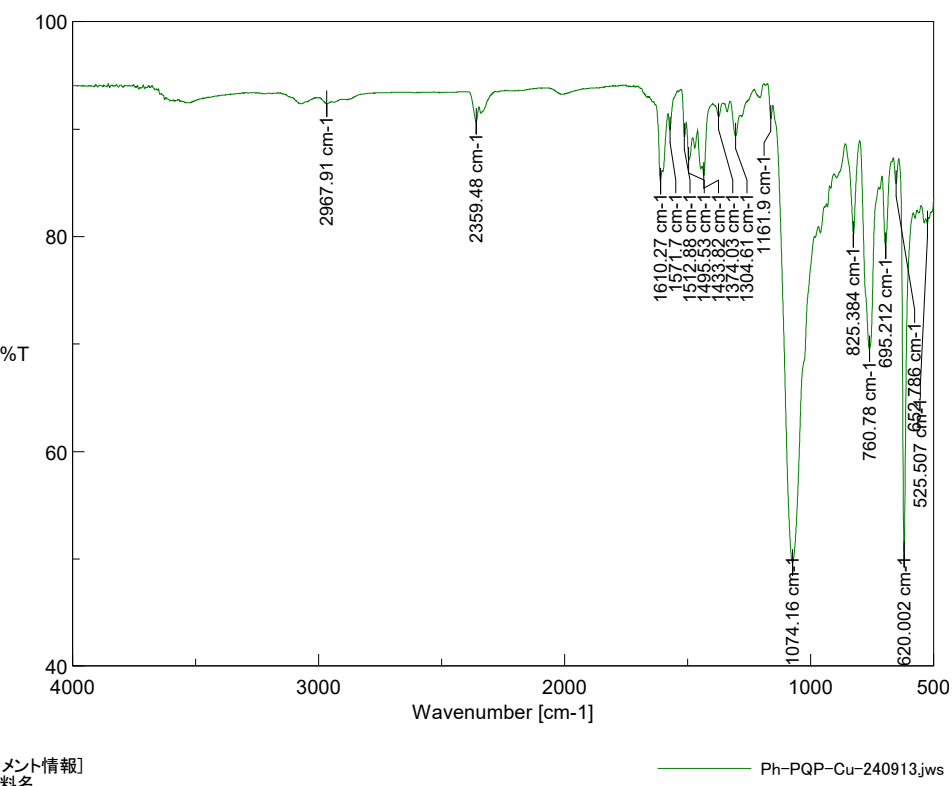


Fig. S65. IR spectrum of **Ph-PQP-Cu**.

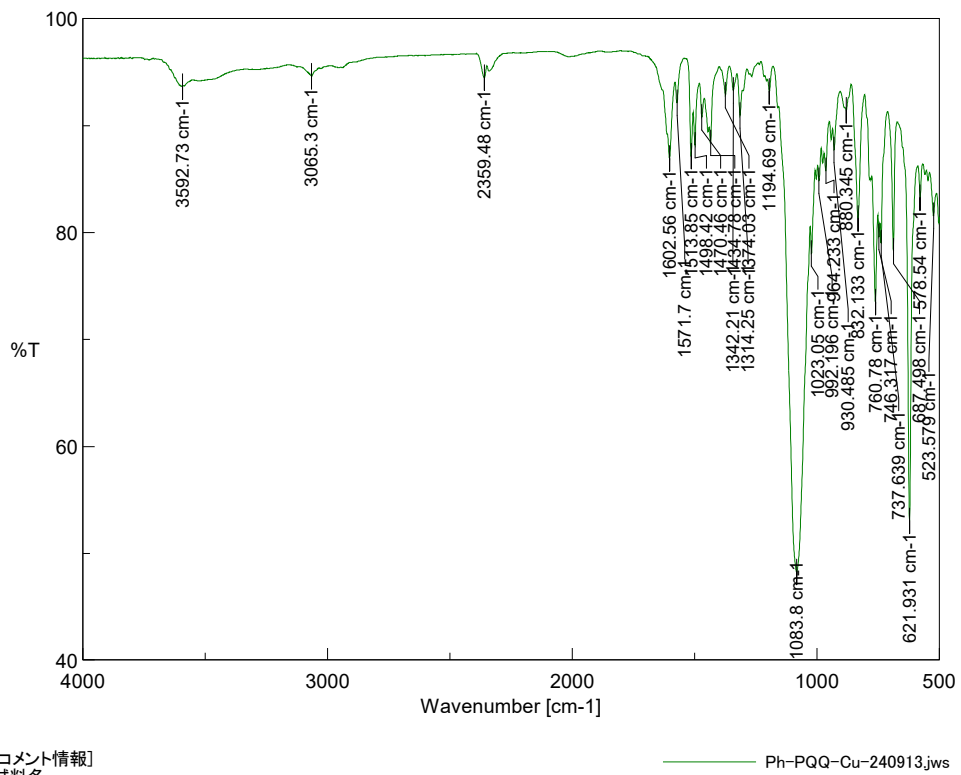


Fig. S66. IR spectrum of Ph-PQQ-Cu.

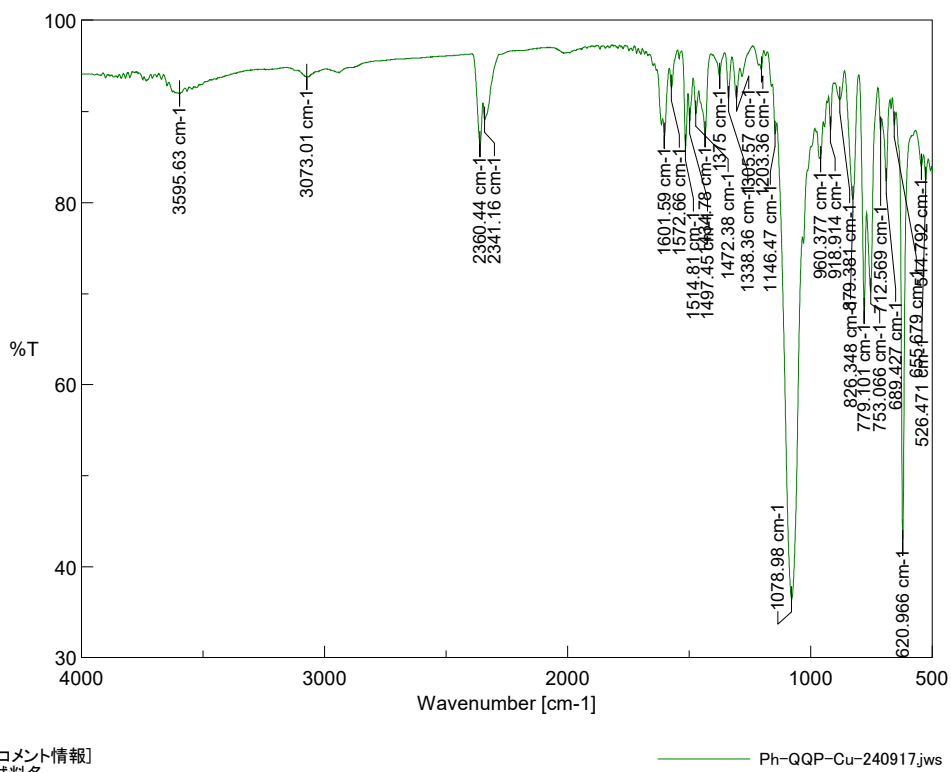


Fig. S67. IR spectrum of Ph-QQP-Cu.

References

1. X. Zhang, G.-S. Chen, H.-C. Liu, M.-J. Zhu, M.-Y. Xie, M.-S. Cen, Q.-J. Li, T.-S. Wang and H.-X. Zhang, *Electrochim. Acta*, 2023, **446**, 142099.
2. V. G. Snider, B. J. Pella and A. Mukherjee, *Inorg. Chim. Acta*, 2018, **469**, 447-452.